Universitat de Barcelona
Facultat de Física

# New Mechanisms in the Adsorption of Colloidal Suspensions

Ignacio Pagonabarraga Mora

Universitat de Barcelona
Facultat de Física

# New Mechanisms in the Adsorption of Colloidal Suspensions

Memòria presentada per Ignacio Pagonabarraga
per optar al Grau de Doctor en Ciències Físiques.

Barcelona, 25 de juny de 1995.

Universitat de Barcelona
Facultat de Física

# New Mechanisms in the Adsorption of Colloidal Suspensions

**Certifico** que la present tesi doctoral ha estat realitzada sota la meva direcció
Barcelona, 25 de maig de 1995.

Dr. J. M. Rubí Capaceti,
Catedràtic de Física
de la Matèria Condensada
de la Universitat de Barcelona

# Contents

# Resum de la tesi

## 1 Introducció

L'objecte d'aquesta tesi és l'estudi dels fenòmens d'adsorció en suspensions col.loidals. Aquests sistemes formen en moltes situacions una única capa de partícules adsorbides degut a l'existència d'interaccions atractives amb la paret i l'absència de tals interaccions entre les pròpies partícules, la qual cosa assegura l'estabilitat de la suspensió. A més, aquestes interaccions atractives entre els col.loids i la superfície fa que les parícules, un cop adsorbides, no es moguin. Es parla, per tant, d'adsorció localitzada. Degut a això, el procés d'arribada de les partíules a la superfície té una memòria llarga, en el sentit que la posició a la qual s'adsorbeix una partícula depèn de les posicions a les quals s'han adsorbit les anteriors. Així, aquest procés és intrínsecament de no equilibri, i nous mètodes, diferents dels usuals de la mecànica estadística d'equilibri han de ser desenvolupats. En aquest sentit, hom normalment dedueix equacions cinètiques que permeten predir el comportament de les partícules adsorbides. En el cas de col.loids, però, la forma específica per la qual arriben a la superfície, és a dir, els mecanismes de transport, juga un paper important que determina la forma en què les partícules poden adsorbir-se.Tanmateix, els estudis duts a terme s'han centrat, bé en una descripció detallada del moviments de la suspensió i la seva influència en l'arribada a la superfície, bé en el tractament acurat dels efectes de volum exclòs lligats a la fixació de les partícules a la paret. L'objectiu de la present tesi és comprendre la interrelació entre ambdós processos, i els seus efectes sobre la capa de partícules adsorbides.

# 2 Resultats

Al primer capítol hem introduït els models cinètics bàsics que han estat emprats a la literatura per descriure els efectes de volum exclòs a la superfície. Són el model "Random Sequential Adsorption" (RSA), que reprodueix algunes de les caraterístiques pròpies de l'adsorció de col.loids que es comporten com a partícules Brownianes, i el model "Ballistic Deposition" (BM), que ha estat proposat per descriure la deposició de col.loids pesants, quan el procés de transport està caracteritzat per un mombre de Péclet elevat.

Al segon capítol hem estudiat l'efecte de la inclusió d'una força externa paral.lela a la superfície en els models precedents. Encara que aquests models no incorporen el transport d'una forma acurada, l'objectiu ha estat veure la dependència del volum exclòs amb els efectes cinètics propis del transport, posant de manifest que no són deguts a efectes purament geomètrics, o que poguessin venir descrits per propietats d'equilibri del sistema. Dins d'aquesta descripció, un camp de forces paral.lel serveix també per descriure el comportament del sistema quan hom aplica un gradient de velocitat. La característica bàsica d'aquests models és que, a més del diàmetre de les partícules, apareix una nova longitud mínima a la qual dues partícules poden trobar-se a la superfície. Una partícula incident no pot adsorbir-se a una distància més petita que aquesta nova longitud a la dreta d'un col.loid prèviament adsorbit, amb la qual cosa la cinètica esdevé asimètrica. Associat a aquesta nova longitud mínima, que creix amb la magnitud força externa imposada, s'observa una disminució del recobriment màxim de la superfície , l'anomenat jamming limit. Aquesta dependència de les propietats dinàmiques amb la intensitat del camp extern no havia estat predit abans per cap model. Hem estudiat dos models unidimensionals, on es pot desenvolupar un estudi anàlitic força complet, que hem complementat amb simulacions numèriques. D'una banda, hem desenvolupat un model que segueix les idees del model RSA amb aquesta nova característica ja esmentada. En aquest cas, el model té solució analítica, la qual cosa ens ha permès fer un estudi de la cinètica, veient que té un comportament similar al model RSA pel que fa al règim assimptòtic, on l'amplitud depèn de $\sigma$, i a temps curts hem deduït que la desviació respecte de les prediccions d'equilibri apareix abans degut a que l'asimetria permet diferenciar configuracions que a l'equilibri són equivalents quan hi ha dues partícules adsorbides,

mentre que en RSA, és necessari esperar que n'hi hagi tres per començar a distingir configuracions equivalents a l'equilibri. D'altra banda, també hem estudiat un model que utilitza les idees de BM. En aquest cas, només és possible trobar una solució analítica quan la força aplicada és feble (quan $\sigma < -1 + 2/\sqrt{3}$). Per valors més grans, un nou fenomen apareix: una partícula pot rodar per sobre d'un cert nombre de partícules adsorbides abans d'arribar a adsorbir-se o ser refusada. Això implica que uuna esfera incindent interaccionarà amb un nombre indeterminat de partícules, tot i que l'adsorció és localitzada. En els models introduïts fins ara, la interacció de la partícula adsorbent amb les adsorbides ha estat considerada sempre local, en el sentit que l'acceptació o refús de la partícula incident només depèn de les posicions de les partícules veïes, mentres que ara depèn d'un nombre indeterminat de partícules, segons quina sigui la configuració a la superfície. A més, degut a l'atracció que existeix sempre entre les partícules i el substrat, quan $\sigma > 1$, un altre mecanisme apareix, pel qual les partícules incidents poden girar a l'esquerra de parells que estan separats una distància $1 + \sigma$. Això provoca un salt en el recobriment màxim, perquè posicions que estaven prohibides, ara queden permeses. La funció de distribucióí radial presenta més pics que la usual degut a les noves distàncies mínimes que apareixen, que implica que són possibles nous mecanismes de rodament. En particular, quan la distancia $\sigma$ esdevé múltiple del diametre, aleshores apareix una ressonància entre els mecanismes de gir associats a les dues distàncies mínimes presents al model, i un substrat amb una forta ordenació local apareix.

Al tercer capítol hem estudiat l'efecte del transport en adsorcions col.loidals en les quals l'adsorció té lloc en presència d'un camp gravitatori, a un nombre de Péclet elevat, la qual cosa implica que la difusió pot ser menyspreada. Com a nou mecanisme respecte dels tractaments anteriors de l'adsorció tenint en compte el transport, hem incorporat les interaccions hidrodinàmiques (HI), que existeixen sempre entre partícules que es mouen en el si d'un fluid. En el nostre cas hem considerat que la suspensió és diluïda, i que per tant, aquestes interaccions fan que el moviment de la partícula incident depengui només de les posicions de les partícules adsorbides. Primer hem estudiat configuracions molt simples de partícules adsorbides. En el cas més senzill hem pogut dur a terme un estudi analític, encara que la resta del treball ha estat fet amb l'ajut de simulacions numèriques. Aquestes situacions simplificades han permès posar de manifest i quantificar l'efecte de les HI a l'adsorpció

de col.loids pesants. Hom a trobat que les HI introdueixen una repulsió efectiva entre la partícula incident i l'adsorbida, que pot arribar a donar resultats quantitativament diferents respecte a les prediccions de BM, i que té un llarg abast. Un cop establertes les característiques bàsiques, hem estudiat la cinètica d'emplenament d'un substracte unidimensional. L'estudi ha estat fet mitjançant simulacions, on es resolen numèricament les trajectòries de les partícules, on les HI apareixen de forma implícita perquè afecten l'expressió dels coeficients de fricció, i expressions aproximades d'aquests són introduïts dins del que hom anomena *hipòtesi d'aditivitat*, ja que no existeixen expressions analítiques d'aquests coeficients per configuracions generals de partícules. Per aquest model unidimensional, la geometria és senzilla, així que la hipòtesi que la partícula incident només interactua amb els primers veïns és raonable, fet que alleuja el temps necessari per dur a terme les simulacions. Hem trobat que, malgrat que les magnituds globals com el recubriment com a funció del temps, el recobriment màxim o la fracció de línea accessible, no depenen fortament de les HI, l'estructura local difereix de la predita per BM. Tot i que la funció de distribució de parells ve caracteritzada per uns pics a distàncies múltiples del diàmetre, el decaïment després d'aquests pics és sustancialment més lent en el model amb HI, la qual cosa indica que degut a la repulsió efectiva, la distància entre partcícules tendeix a ser més gran. També hem estudiat la deposició sobre un substrat bidimensional. En aquest cas, la descripció ha de fer-se amb més detall perquè la repulsió efectiva fa que la trajectòria de la partícula incident canviï de direcció. En particular, aquesta repulsió efectiva tendeix a crear triplets allargats a la superfície, allà on el model BM prediu l'aparició de "clusters" isòtrops. Novament, la funció de distribució radial de parelles mostra un decaïment més suau de la funció després dels pics. Per aquest model més realista hem estat capaços de comparar les prediccions del nostre model amb resultats experimentals recents sobre l'adsorció de partícules de melamina. Comparant les corbes per la funció de ditribució radial obtingudes experimentalment, amb HI i amb BM, hom observa que l'acorde entre els experiments i HI és notablement millor que amb BM. En particular, el decaïment més suau després del primer pic és observat experimentalment. Així, hom ha provat que el model BM, que havia estat introduït com un bon model per descriure l'adsorció de partícules pesades, només és vàlid a la regió on el transport al fluid ve dominant pels termes inercials, en lloc dels viscosos (que és on les HI són importants). Tanmateix, el transport de partícules col.loidals ve controlat pels termes de dissipació viscosa, ja que el nombre de Reynolds és molt

petit. D'altra banda, hi ha magnituds físiques de la capa adsorbida, com ara la permeabilitat elèctrica, que depenen de la distribució relativa de partícules. Per tant, el mecanisme d'adsorció influirà en general en les propietats físiques de la superfície que es crea.

Finalment, al capítol quatre, hem desenvolupat una teoria termodinàmica del procés d'adsorció. Ens hem centrat en l'anàlisi de les situacions en les quals l'adsorció ve controlada per una barrera d'energia a la superfície. Una descripció termodinàmica acurada exigeix tenir en compte que la difusió a través d'una barrera de potencial és un fenomen que indueix relacions no lineals entre el nombre de partícules que poden atravessar la barrera i la força termodinàmica que origina el traspàs de partícules. Per això, hem introduït una nova variable a la superfície, anomenada *variable interna*, i que està relacionada amb les diferents configuracions internes de les partícules a la superfície. En aquest cas en què el transport des del volum ve controlat pel pas de la barrera, hem estat capaços de deduir una equació de Langmuir generalitzada que és vàlida localment. En els models del tipus RSA, hom ha obtingut equacions de Langmuir globals, per l'evolució del recubriment mig de la superfície. L'obtenció d'equacions formalment equivalents al nivell local resulta d'interès, ja que dóna generalitat a aquest comportament, alhora que el desenvolupament de la teoria termodinàmica permet entendre l'origen d'un tal comportament. Si el transport a la superfície no ve controlat per una barrera d'energia, hem mostrat la plaussibilitat d'una equació de Langmuir generalitzada global per descriure la cinètica del recubriment global, encara que a hores d'ara encara no és clara la relació entre aquest comportament global i la termodinàmica local del sistema. El comportament global és produït en aquest cas per l'aparició de barreres entròpiques degut a la dificultat, per les partícules incidents, de trobar una posició accessible a la superfície. L'única limitació dels resultats obtinguts amb una teoria termodinàmica és que hom introdueix la hipòtesi d'equilibri local en un procés de no equilibri. De tota manera, la pròpia teoria no pot predir la seva limitació, i no deixa de ser remarcable que una equació de tipus Langmuir sigui trobada per tot el procés. D'altra banda, la formulació termodinàmica presenta l'avantatge que, degut a la seva estructura estàndar, permet introduir de forma sistemàtica les fluctuacions en les equacions de les magnituds físiques. D'aquesta manera, hom pot estudiar l'evolució de les fluctuacions al voltants d'estats de referència. Hem deduït els teoremes de fluctuació-dissipació pertinents quan existeix un grau de llibertat in-

tern, i hem aplicat els resultats a l'estudi de les fluctuacions de densitat en un model on hom permet la difusió superficial. Degut a l'intercanvi de massa entre el volum i la superfície, un decaïment més lent de les correlacions, respecte l'esperat en sistemes purament difusius, es observat.

# 3 Conclusions

En aquesta tesi hem dut a terme una sèrie d'estudis per entendre la relació que existeix entre els processos de transport i els efectes geomètrics de volum exclòs en l'adsorció de suspensions col.loidals. La motivació ha estat que, degut a la seva complexitat, hom ha tendit a valorar només la importància d'un del elements. Mitjançant l'estudi detallat de dos casos diferents, hem mostrat la interrelació entre ambdós elements, i la necessitat de procedir a un estudi global de l'adsorció, malgrat resulti costós. En aquest sentit, la utilització de simulacions numèriques esdevé un mètode indispensable. També hem mostrat que el transport introdueix nous mecanismes a l'adsorció, que poden resultar qualitativament diferents dels considerats fins al moment, i que tenen una forta influència tant en les magnituds globals, com en l'estructura de la capa adsorbida. D'altra banda, hem desenvolupat un formalisme termodinàmic per descriure apropiadament l'adsorció. El marc natural ha estat la termodinàmica de processos irreversibles, i hem discutit com incorporar les no-linealitats pròpies del procés mitjançant una descripció acurada de la difusió prop de la superfície. La formulació termodinàmica ha permès poder obtenir les equacions d'evolució apropiades també per les fluctuacions al voltant d'estats de referència.

# Introduction

The study of the dynamics of model colloidal suspensions in the presence of solid surfaces is of great fundamental and applied interest. It provides an understanding of the basic principles which control the behavior of the colloids such as macromolecules, latex particles, ferromagnetic particles, etc., and bioparticles such as proteins, enzymes, viruses or bacteria, near interfaces and their interaction with them. Of special importance is the understanding of mass exchange between the suspension, in particular the adsorption process, which has applications ranging from biophysics (for example, the study of the dental enamel as affected by suspensions of bacteria) to filtration techniques, besides its general interest in polymer-colloid science. A quantitative analysis of adsorption phenomena is also relevant in biophysics, polymer-colloid science and medicine since it enables a better understanding and controlling of protein and cell separation processes, enzyme immobilization, biofulding of transplants and artificial organs, etc.

Model colloidal systems are particularly important because their well defined surface properties and monodispersity allow their use also for predicting molecular adsorption phenomena, as well as for testing various aspects of statistical-mechanics theories[1]. Nonetheless, colloidal adsorption also involves more complex processes taking place during their adsorption compared to molecular adsorption. On the one hand colloids are more sensitive to external force fields and hydrodynamic flows than molecules, and on the other, at the surface they can either deform or recombine, and there may exist short-range attractive forces related either to the reconstruction of the electrical double layer when the colloids are polarizable, to van der Waals attrac-

tive forces, or even to chemical reactions with the substrate occuring at the contact point. All these different phenomena at the surface lead to localization of the particles at the interface because they create effective attractive particle-surface interactions. Then, colloids are partially or totally immobilize at the interface. Moreover, except in the case that adsorption occurs from unstable or marginally stable suspensions[51] or that the colloidal suspension be unstable, colloids form a monolayer adsorbed on the solid surface. The immobilization of colloids upon adsorption implies that adsorption becomes an irreversible process which has a finite memory because the arrival of one particle will depend on the positions at which previous colloids have been adsorbed, and since the particles are not allowed to fluctuate at the surface, non-equilibrium configurations of adsorbed colloidal particles are then generated[19]. As a consequence, the theoretical treatment of colloidal adsorption has been based on non-equilibrium methods, basically consisting on the appropriate formulation of kinetic evolution equations.

Langmuir was the first who introduced a kinetic equation in order to describe the adsorption process when only one layer of particles adsorb on a surface[21]. He studied the molecular adsorption of gases on solid surfaces hydrogen on platinum and, therefore, he did not had to consider those complications characteristic of colloidal adsorption. He considered that determining factor of the adsorption kinetics was that the incoming particles could not adsorb on regions already occupied by adsorbed molecules. Then, if we call $\theta$ the fraction of the surface covered by particles, he assumed that the rate of adsorbing particles should be proportional to the fraction of the surface not yet covered by adsorbed molecules, while the desorbing rate, if adsorption is not completely irreversible, was assumed to be proportional to the amount of adsorbed particles. Therefore,

$$\frac{d\theta}{dt} = k_a c_b (1 - \theta) - k_d \theta \tag{1}$$

where $k_a$ and $k_d$ are the adsorption and desorption constants, respectively, and $c_b$ is the concentration of atoms in the vicinity of the surface. This equation has also been used to describe the adsorption kinetics of colloids. However, its extension to these systems should be done with care, because in its derivation none of the peculiarities of colloidal adsorption have been taken into account. Two major features have to

be incorporated to study the temporal evolution of the surface covered by colloidal particles:

- Eq.(1) assumes that the surface not covered by particles equals the area accessible to new incoming ones. This is true if the adsorbing particles are small enough, as is the case of molecular adsorption. When the size of the adsorbing particles becomes relevant, the, the geometrical surface excluded by adsorbed particles becomes more complex, as shown in fig.0.1 for the case of disks.
- In the derivation of eq.(1) the specific transport of particles from the bulk to the surface has been neglected. In general, different forces act on colloids, and they are more sensitive to the external conditions under which adsorption takes place. In particular, the transport mechanism can also influence the available surface area for incoming particles.

At low coverages, the Langmuir equation can provide reasonable results in colloidal adsorption because particles will not influence each other. The Langmuir equation has been generalized to take into account phenomenologically the new features which affect colloidal suspension. A new function $\Phi(\theta)$ is introduced, which accounts for the fraction of the surface at which the center of an incoming particle can adsorb as a result from the particle interactions, either due to their finite size or to the existence of attractive or repulsive forces between them. In general, it is a non-linear function of the coverage, although at low coverages it coincides with the free surface fraction area, $1-\theta$. One can then write down the generalized Langmuir equation

$$\frac{d\theta}{dt} = k_a c_b \Phi(\theta) - k_d \theta \tag{2}$$

which can be understood as an evolution equation for a surface concentration $\theta$. In general, the combined action of transport and geometric effects at the surface determine the specific form of both the constant $k_a$ and the available function $\phi$. However, this fact has only been recently recognized, and in fact, most of the studies carried out to describe properly the bulk transport phenomena have concentrated on the obtention of $k_a$ or its equivalent, as a function of the different relevant parameters of the adsorption process, while the the detailed description of the volume exclusion effects

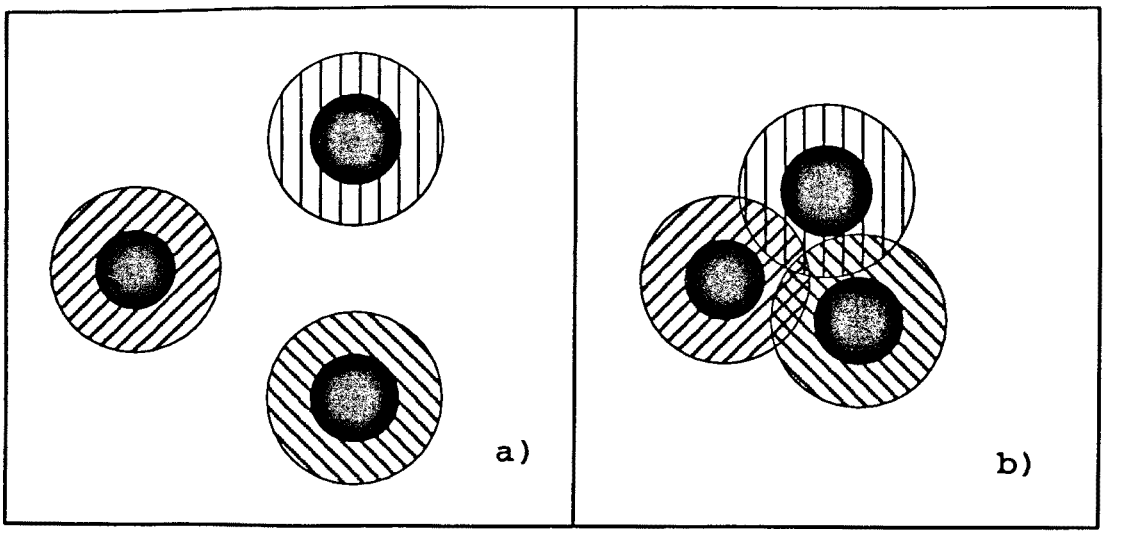


Figure 0.1: Surface exclusion effects in adsorption of spherical colloidal particles. Top view of the surface. *a)* If the adsorbed particles are far apart, the area excluded to the center of an incoming one (*stripped and black regions*) is proportional to the area of each particle (*black region*). *b)* When some adsorbed particles are close enough (the center-to-center distance is smaller than two diameters), then excluded areas overlap (*double and triple striped areas*). Then, the excluded area to the center of an incoming sphere (*total stripped and black regions*) is no longer proportional to the areas of the adsorbed particles.

controlling the arrival of particles at the surface have been based on the geometry, neglecting the way in which particles arrive from the bulk.

# 1 Transport and adsorption

## 1.1 Macroscopic description

At a *macroscopic* level of description, the colloidal suspension is regarded as a continuum, characterized through the corresponding fields, which satisfy appropriate balance equations. The specific transport coefficients may, in principle, be functions of the colloidal concentration, keepig track of their interactions, as well as on the distance of the colloids to the surface. However, most of the studies performed at the macroscopic level disregard the spatial dependence of the transport coefficients. Smoluchowski[5] was the first to study the adsorption from a suspension in order to describe fast coagulation of colloids. He simplified the boundary condition assuming the so-called *"Smoluchowski-Levich"* boundary condition or *"perfect sink"*, according to which all particles arriving at a small distance of the surface are irreversibly captured in an infinite energy sink, allowing further particles to be adsorbed at the same position. Much work on the study of collectors in a variety of hydrodynamic conditions have been carried out using this assumption[6][24], incorporating different kinds of interactions. When this boundary condition constitutes a good approximation, such a procedure has allowed to have a good idea about the effects of electric and hydrodynamic interactions, dispersive forces, gravity field and shear flows on the adsorption rates[8]-[12].

The formulation of a general expression for the boundary condition describing the behavior of the system at the surface is difficult due to the existence of short range interactions and dependence on hydrodynamic conditions, besides the ignorance of the specific properties of the surface. It seems to suggest that the specific behavior of the solution in the neighboehood of the surface may depend on many factors, therefore being difficult to derive general functional relations between the different hydrodynamic fields being present at the interface. The theoretical studies oriented to rigurously derive more general boundary conditions within this *macroscopic* descrip-

tion have relied upon the fact, on the one hand, that short range forces have often proved to be the determining factor of the rate of particle transfer and adsorption on collector surfaces and, on the other, that such forces are confined to a very small region close to the collector surface, in comparison to the extension of the diffusion boundary layer thickness. Taking into account that then two different length scales appear, convective transport can be decoupled from surface force effects, the latter arising either from dispersive van der Waals forces or double layer forces. When the combined action of the different surface forces create an energy barrier[22][14], it can be shown that the effective boundary condition for the convective region outside this thin layer around the surface corresponds to a first order chemical reaction which, in the absence of diffusion, is equivalent to eq.(1) if desorption is allowed. Furthermore, the different parameters characterizing electric, dispersive and hydrodynamic forces modify the different multiplicative constants without modifying the functional dependence at the small coverage at which these theoretical analysis have been carried out. The existence of reaction-like boundary conditions have also been introduced in the adsorption on a fluid interface[15]. Subsequently, Dabroś *et al.*[16] have studied both theoretically and numerically the global transport equations in the presence of a surface energy barrier together with the perfect sink boundary condition as a function of the different dimensionless relevant parameters and in particular, they have shown when the energy barrier is large compared to $k_BT$ that the results of Refs.[22] and [14] are recovered. More recently, in order to take into account more realistic surface kinetics, boundary conditions of the type of a chemical reaction have been phenomenologically introduced, and its effect on the adsorption kinetics has been taken as a first order chemical reaction[17]. Although in this last reference the mass distribution close to the surface is studied, basically all the theoretical efforts have been devoted to the analysis of the adsorption kinetics. Moreover, since they are only valid at low surface coverages, the distribution of mass at the surface is always assumed to be homogeneous. A number of studies have also been performed in order to analyze the evolution of the bulk mass concentration when the surface kinetics is given by a Langmuir equation (1) and the coupling between the bulk and the surface is taken into account[25].

At this macoscopic level of description, however, the formulation is based on intuitive arguments, and therefore it is difficult to devise general mechanisms to derive

general boundary conditions which take into account all the different mechanisms which take place at the surface. Moreover, it cannot give a foundation to the phenomenological boundary conditions which are proposed to describe different kinds of interfacial behavior.

## 1.2 Mesoscopic description

In order to obtain a general expression for the surface kinetics keeping track of all possible couplings between the bulk and the surface properties, a *mesoscopic* description of the system should be performed. The starting point for such a mesoscopic description consists of the evolution equations for the colloidal particles, taking into account the friction forces with the solven. Then, by performing the appropriate averages, one can deduce balance equations describing the evolution of the hydrodynamic fields, in the same spirit in which the hydrodynamic equations for simple fluids can be obtained from its microscopic dynamics[18]. The intuitive approximation on the separation between convection and adsorption can be avoided and expressions for the different constants appearing in Langmuir-like boundary conditions can be expressed in terms of microscopic parameters. The dynamics of the colloids is given by the Kramers equation[19] and, from it, the adsorption dynamics can be studied as done by Peters[20] who also includes hydrodynamic interactions between particles[21]. He but always assumes, however, that the perfect sink boundary condition applies at this level of description. Such an approximation has enabled him to study the effects of the particle-particle interactions in the diffusivity of the bulk suspension and its effect in the rates of adsorption and he is able to compare with the predictions of the macroscopic theory, obtained by solving the appropriate convection-diffusion equation (see Levich[6]), but a detailed study of the appropriate boundary condition is lacking. In order to carry out a detailed analysis of the transport processes at the solid surface at the *mesoscopic* level, it is necessary to consider two basic features of the process:

- The existence of surface forces in the vicinity of the surface makes it necessary to distinguish a new length scale $l$, in general much smaller than the length $L$ associated with the length scale of change at the bulk phase[22];

- Sufficiently close to the surface there will exist Born-type repulsive forces, which prevent the particles from entering into the surface. Therefore, the appropriate boundary condition to be imposed upon the colloidal concentration at the wall is one of particle impermeability, that is, a vanishing component of the mass flux normal to the surface.

This second condition implies that the mass is conserved in the system, while the perfect sink condition assumed that mass was disappearing from the system. In particular, it means that the particles will eventually attain an equilibrium Boltzmann distribution close to the wall. On the other hand, due to this conservation law, the accumulation of mass towards the surface will be an essentially unsteady process[8].

Then, in order to properly derive the macroscopic boundary conditions from this *mesoscopic* dynamics, it is crucial to take into account the length scale separations, $l << L$. Shapiro *et al.*[8] have shown, using singular perturbation techniques[24], that by appropriate describing the concentration of particles at distances smaller than $l$ from the surface and at distances of order $L$, it is possible to derive balance equations for the bulk phase and for the adsorbed phase. Moreover, they can derive the relation between both phases depending on the specific surface potential. In particular, if this last quantity is characterized by a deep minimum compared to the thermal energy, then this boundary condition is equivalent to the one derived by Ruckenstein*et al.*[22]. In this case, the steady state is quickly achieved in the bulk phase, recovering the description obtained from the *macroscopic* description. As shown in ref.[8] this situation describes the adsorption of aerosols. For a shallow minimum there exists a coupling between the diffusion close to the wall and the flux coming from the bulk, leading to a global unsteady process. If the surface potential exhibits a maximum besides the energy minimum, the previous results are also derived, although in this case the conditions upon which the perfect sink boundary condition is recovered also depends on the height of the energy barrier.

In order to avoid the simplifications involved in the theoretical analysis both at the macroscopic and mesoscopic level, numerical simulations have been performed. In particular these techniques have alloed to study the trajectories of individual particles in the host fluid, and it has been useful for predicting collector efficiencies[24][26][27] as a function of its geometry and of the different forces acting on the colloids.

New simulation techniques have been used to study the dynamics of Brownian particles in the presence of a wall, accounting for hydrodynamic effects, such as Brownian dynamics[20]. More recently, the Stokesian Dynamics[18] has also been applied to study the dynamics of suspended spheres close to a wall. However, all these methods have focused more on the surface effects on the bulk dynamics, rather than in the adsorption process itself[30][31].

All these transport studies have been limited to study the low surface coverage regime of the adsorption process. However, although the bulk suspension is diliute, large concentrations can be achieved at the surface. In this regime, then geometric exclusion effects become dominant. We will next summarize the main approches which have been followed to describe these effects.

# 2 Volume Exclusion Effects and Adsorption

When the adsorption is irreversible, in the sense that particles, once adsorbed at the surface can no longer move, as particles arrive at the surface, they start to exclude part of the surface for the arrival of other particles. If the coverage is small, this excluded area is proportional to the number of particles on the surface. If the number increases, then the excluded area of the different particles will interact, as shown in fig.0.1. If only one layer of particles is formed on the surface, this process will end at the *jamming* limit, beyond which no more colloids can be adsorbed at the surface.

The experimental observation that the jamming coverage obtained adsorbing ferritin proteins on a glass surface[1] coincided with the one predicted by a simple kinetic model called Random Sequential Adsorption (RSA), together with the subsequent study of the structure of the adsorbed layer[2], suggested that excluded surface effects, which have to play a major role at large coverages, could be described in terms of some simple kinetic models. More recent experiments on the jamming obtained from the adsorption of latex spheres[3] have further confirmed this idea.

Radom Sequential Adsorption models were introduced for the first time by Flory[8][7] in order to describe cyclation processes in polymers. Cohen *et al.*[9] noticed that Flory's problem is equivalent to the random sequential filling of a lattice line by

dimers. Subsequently, the continuum limit of this lattice problem was studied (the so-called *car parking problem*)[13][13], which is the version of relevance for colloid, because colloidal particles are large compared with the sites at which they can adsorb on the surface. This model is irreversible, because after a particle has been placed on the line, it does not move, and it has an infinite memory because the place at which one particle can adsorb depends on the places at which the previous ones have arrived. Moreover, it also describes the excluded volume effect, because it takes into account the size of the particles on the line. Feder compare his results wih this model[2], and more recent experimental results on the adsorption of proteins[1] also show a good agreement on the jamming coverage with the two dimensional RSA prediction[11].

Generalizations of RSA have been introduced to take into account the different forces which may act on the colloids. In this sense, electric double layer forces for charged colloids have been considered in this context[42]-[44] and it has also been argued whether a Boltzmann distribution of the particles on the surface can be observed or not. The gravity field has also been introduced in an approximate way by appropriately modifying the kinetic rules, giving rise to the monolayer version of the Ballistic Model (BM)[34]. Experimental results on the adsorption of melamine particles[26] have made possible to compare both the jamming limit and the pair distribution functions obtained experimentally with the predictions of BM. While the jamming was seen to agree with BM's result, discrepancies in the pair distribution functions were observed. In fact, similar results have been reported later on with respect to RSA, as discussed in the next paragraph. This fact shows that when comparing experiments with kinetic results care should be taken, since there are physical quantities which are not very sensitive to the different forces acting on the adsorbing particles, while in others, the specific conditions upon which adsorption takes place can introduce significant modifications.

# 3 Transport and Volume Excluded Effects in Adsorption

Although the generalizations presented at the end of the previous section introduce in an approximate way the effects of particle-particle interactions and transport in a specific regime, more recently it has been clear that a detailed treatment of both transport mechanisms and volume excluded effects were necessary.

To this end, computer simulations have been performed under different conditions considering both the memory and surface exclusion effects, characteristic of the adsorption kinetic models, in order to elucidate the effects of transport of the colloids in the adsorption process, together with its interplay with the different colloidal and/or external forces. The first attempt to incorporate the diffusion of the particles from the bulk to the surface was performed by Senger *et al.*[32], with the so-called Diffusion Random Sequential Adsorption model (DRSA), being able to show that the same jamming limit as the one predicted by RSA was obtained. The pair distribution function, however, always differed with respect to the RSA ones, except at the jamming. On the other hand, the asymptotic kinetics towards the jamming was different from the one predicted by RSA[31]. They considered a scalar constant diffusion coefficient, although it should be taken as a position-dependent tensor due to hydrodynamic interactions[24]. The effect of these interactions on the adsorption kinetics has been studied using the ideas of Brownian Dynamics [20] considering the effects of other external fields by Adamczyk *et al.*[1]. A Brownian Dynamics simulation describing hydrodynamic interactions in a more precise way has been performed by Bafaluy *et al.*[24], with the aim of studying its effect on the relative distribution of adsorbing spheres. It was shown that, at least at low coverages, the differences in the pair distribution function between RSA and DRSA disappear when hydrodynamic interactions are considered, due to a cancellation of effects. Thus, this result explains why a simple kinetic model was able to compare so well with experimental results.

# 4 Purpose and Objectives of this Thesis

Our objective in this thesis is to study the effects of transport and external fields on the kinetics of the adsorption process as well as the structure of the adsorption aggregates, pointing out the new mechanisms which appear as a result of the differnt condition under which adsorption takes place. We will take appropriately into account both the irreversible character of the adsorption process associated to its infinite memory and the surface exclusion effects due to the finite size of the particles. We have subdived this work in four chapters:

- In the first chapter we present a summary of the RSA and BM models in order to stablish clearly their basic properties and predictions. They will be used in the next chapters to elucidate the effects on adsorption of external fields and interactions;
- We then study in the second chapter the modifications in surface exclusion effects of the kinetic models when an external field parallel to the adsorbing surface is applied. A physical example constitutes the case in which an external shear flow is applied. Up to now, the kinetic adsorption models have been studied for quiescent fluids, although experiments on the adsorption of colloids in the presence of applied shears have been performed[50].
- In the third chapter we will concentrate on the effects of hydrodynamic interactions in the adsorbed layer when diffusion is irrelevant. We will include these interactions in a more detailed description than that used in the standard Brownian dynamics method. Results are obtained both on the adsorption on a 1-d and 2-d solid substrate. In this last situation, we have compared with experimental results on the adsorption of colloidal particles[26] and we are able to understand some discrepancies observed when those experimental data are compared with BM results.
- We present in the fourth chapter a deduction of a generalized Langmuir equation within the framework of non-equilibrium thermodynamics in the presence of interfaces[2], which serves to understand the coupling between surface kinetics and bulk transport processes. This formalism makes it easy to incorporate

fluctuations to the different hydrodynamic fields. We introduce a simple adsorption model with diffusion to study the effect of the coupling between bulk and surface transport processes on the fluctuation dynamics, and therefore on the scattering functions of the surface.

Finally, we conclude making clear the principal results of the thesis, and discuss new perspectives opened by the present work

# References


[1] Z. Adamczyk, B. Siwek, M. Zembala and P. Belouschek, Adv. Colloid Interface Sci. **48**, 151 (*1994*).

[2] M.C. Bartelt and V. Privman, Int. J. Mod. Phys. B **5**, 2883 (*1991*).

[3] B. Widom, J. Chem. Phys **44**, 3888 (*1966*)

[4] I. Langmuir, J. Amer. Chem. Soc. **38**, 221 (*1916*); **40**, 1361 (*1918*).

[5] M. Smoluchowski, Phys. Z. **17**, 585 (*1916*); Z. Phys. Chem. **92**, 129 (*1917*).

[6] V.G. Levich, *Physicochemical Hydrodynamics*, Prentice Hall, Englewood Cliffs, New York, *1962*.

[7] T.G.M. Van de Ven, *Colloidal Hydrodynamics*, Academic Press, London, *1989*.

[8] G.E. Clint, J.H. Clint, J.M. Corkill and T. Walker, J. Colloid Interface Sci. **44**, 121 (*1973*).

[9] Z. Adamczyk and T.M.G. Van de Ven, J. Colloid Interface Sci. **80**, 340 (*1981*).

[10] Z. Adamczyk and T.M.G. Van de Ven, J. Colloid Interface Sci. **82**, 497 (*1981*).

[11] Z. Adamczyk, T. Dabroś, J. Czarnecki and T.G.M. Van de Ven, J. Colloid Interface Sci. **97**, 91 (*1984*).

[12] K. Chari and R. Rajagolapan, J. Chem. Soc., Faraday Transactions **81**, 1345 (*1985*).

[13] E. Ruckenstein and D.C. Prieve, J. Chem. Soc. Faraday II **69**, 1522 (*1973*)

[14] L.A. Spielman and S.K. Frienlander, J. Colloid Interface Sci. **46**, 22 (*1974*).

[15] R.P. Borwankar and D.T. Wasan, Chem. Eng. Sci. **38**, 1637 (*1983*).

[16] T. Dabroś and Z. Adamczyk, Chem. Eng. Sci. **34**, 1041 (*1979*).

[17] Z. Adamczyk and T.G.M. Van de Ven, J. Colloid Interface Sci. **97**, 68 (*1984*).

[18] J.H. Irving and J.G. Kirkwood, J. Chem. Phys. **18**,817 (*1950*).

[19] T.J. Murphy and J.L. Aguirre, J. Chem. Phys. **57**, 2098 (*1972*).

[20] M.H. Peters, J. Colloid Interface Sci. bf 121, 179 (*1988*).

[21] M.H. Peters, J. Colloid Interface Sci. bf 138, 451 (*1990*).

[22] H. Brenner and L.G. Leal, J. Colloid Interface Sci. **62**, 238 (*1977*).

[23] M. Shapiro, H. Brenner and D.C. Guell, J. Colloid Interface Sci. **136**, 552 (*1990*).

[24] D.A. Edwards, H. Brenner and D.T. Wasan, *Interfacial Transport Processes and Rheology*, Butterworth-Heinemann, Boston, *1991*.

[25] R. Varoqui and E. Pefferkorn, J. Coll.Int.Sci. **109**, 520 (*1986*).

[26] L.A. Spielman and J.A. Fitzpatrick, J. Colloid Interface Sci. **42**, 607 (*1973*).

[27] L.A. Spielman and P. Cukor, J. Colloid Interface Sci. **43**, 51 (*1973*).

[28] D.L. Ermak and J.A. McCammon, J. Chem. Phys. **69**, 1352 (*1978*).

[29] J.F. Brady and G. Bossis, Ann. Rev. Fluid Mech. **20**, 111 (*1988*).

[30] G.S. Ansell and E. Dickinson, J. Chem. Phys. **85**, 4079 (*1986*).

[31] G. Bossis, A. Meunier and J.D: Sherwood, Chem. Eng. Sci. **47**, 981 (*1992*).

[32] J. Feder and I. Giaever, J. Colloid Interface Sci. **78**, 144 (*1980*).

[33] J. Feder, J. Theor. Biol. **80**, 237 (*1980*).

[34] G.Y. Onoda and E.G. Liniger, Phys. Rev. A **33**, 715 (*1986*).

[35] J.P. Flory, J. Am. Chem. Soc. **61**, 1518 (*1939*).

[36] E.R. Cohen, H. and Reiss, J. Chem. Phys. **38**, 680 (*1963*).

[37] A. Rényi, Publ. Math. Inst. Hung. Acad. Sci., **3**, 109 (*1958*) (translated in Selected Transl. Math. Stat. Prob. **4**, 203 (*1963*)).

[38] J.J. González, P.C. Hemmer and J.S. Hoye, J. Chem. Phys. **3**, 228 (*1974*).

[39] J.W. Evans, Rev. Mod. Phys. **65**, 1281 (*1993*).

[40] J.J. Ramsden, Phys. Rev. Lett. **71**, 295 (*1993*).

[41] E.L. Hinrichsen, J. Feder and T. Jossang, J. Stat. Phys. **44**, 793 (*1986*).

[42] Z. Adamczyk, M. Zembala, B. Siwek and P. Warszyński, J. Colloid Interface Sci. **140**, 123 (*1990*).

[43] Z. Adamczyk, B. Siwek and M. Zembala, J. Colloid Interface Sci. **151**, 351 (*1992*).

[44] Z. Adamczyk, B. Siwek, M. Zembala and P. Weroński, Langmuir **8**, 2605 (*1992*).

[45] R. Jullien and P. Meakin, J. Phys. A **25**, L189 (*1992*).

[46] P. Wojtaszczyk, P. Schaaf, B. Senger, M. Zembala and J.C. Voegel, J. Chem. Phys. **99**, 7198 (*1993*).

[47] B. Senger, P. Schaaf, J.C. Voegel, A. Johner, A. Schmitt and J. Talbot, J. Chem. Phys **97**, 3813 (*1992*).

[48] P. Schaaf, A. Johner and J. Talbot, Phys. Rev. Lett. **66**, 1603 (*1991*).

[49] F.J. Bafaluy, B. Senger, J.C. Voegel and P. Schaaf, Phys. Rev. Lett. **70**, 623 (*1993*).

[50] J. Sjollema and H.J. Busscher, Colloids Surfaces **47**, 337 (*1990*).

[51] D. Bedeaux, A. M. Albano and P. Mazur, Physica **82A**, 438 (*1976*).

# Chapter 1

# Basic Kinetic Models

Feder and Giaever[1] and Feder[2] were the first who pointed out that the irreversible adsorption of proteins on solid surfaces, when neither desorption nor surface diffusion were observed, could be described in terms of a sequential kinetic model. This model took into account the excluded volume effects related to the irreversibility of the process, although neglected the fact that particles arrive from a suspension. Therefore, this analogy seemed to indicate that these geometric effects where the dominant in the adsorption process, and that the specific conditions of arrival from the suspension affected only the rules of the kinetic model.

We present in this chapter the properties of the two basic kinetic models which have been used to describe the adsorption of Brownian particles, the random sequential adsorption model (RSA), and for heavy particles, the ballistic deposition model (BM). They constitute the basic theoretical decription which is assumde to describe colloidal adsorption. Therefore, in chapters 2 and 3 we will have to compare our results with these basic models.

## 1.1 The Random Sequential Adsorption Model

RSA is a model in which objects are placed in a d-dimensional volume. Sequentially, a position for a trial object is chosen uniformly random within the volume. If the object overlaps either totally or partially with a previously placed one, the trial particle is rejected and a new position is randomly chosen for a new object. If it does not overlap with any previously placed object, the trial particle is irreversibly fixed at that position, without any further movement, and the process continues with a new trial object. This sequential filling process usually starts with an empty volume, and ends when no more objects can be placed in the given volume, reaching the so-called *jamming limit*. Although some studies exist on the RSA of spheres in a cube[6], most of the studies have been performed on the adsorption of two or three dimensional objects on a 2-d substrate, essentially a planar surface, and of one or two dimensional objects on a one dimensional substrate, basically a linear segment, both for simplicity in the analysis and for its physical applications[7]. For the same reasons, much work has been performed on the study of the adsorption on a lattice, although we will be interested on the adsorption on a continuum substrate.

The first RSA model was introduced by Flory[8] to study ciclation processes on a polymer. In fact, the reacting parts of the linear polymer chain were considered as sites of a one dimensional lattice. The polymer was considered as a line along which reactants were pendant. Flory studied the particular process in which adjacent groups randomly link, leaving a few isolated unreacted ones. The role of exclusion volume is introduced in these problems since, given a certain reaction rules, not all the pendant groups are able to react, and the aim is to determine both the kinetics and the structure of the polymer chain (the distribution of reacted and unreacted units). The process has an infinite memory because once linked, the groups cannot separate. The irreversibility and infinite memory which characterizes this kinetic process makes that the final state cannot be described by a Gibbs measure, making clear the difference between these lattice models and standard lattice-gases. Flory's problem is equivalent to the random sequential coverage of a lattice line by dimers[9]. The empty sites in this latter case are equivalent to the unreacted groups in the former, and the jamming consists of a set of isolated vacant sites. More complex reaction rules are given, for example by González *et al.*[13]. This kind of models, in

its lattice version, has also been applied extensively to the study of chemisorption and reaction on crystal surfaces[7]. In this case, the surface structure of the crystal forms a lattice upon which adatoms can deposit. In general, however, the basic RSA rules are modified to account for the possibility that the adsorption rates depend on the neighbors. These generalize models are called cooperative sequential adsorption models (CSA), especially in their lattice version. These sequential adsorption models have been typically applied, besides to chemical reactions, to model chemisorption and two dimensional single-crystal surfaces, ecological and sociological systems, deposition of particles, and multilayer and grain growth[7]. All these RSA and CSA are kinetic models, in which one is interested in the evolution of the number of objects in the volume as a function of time, as well as on the distribution of objects on the volume, which may also be a function of time. Then, one usually focuses on physical quantities such as the jamming limit, the asymptotic and short time kinetics related to the global evolution of the adsorbed particles, and the spatial and temporal correlations, as well as the structure of the aggregates at different coverages to study the short-scale and structural properties of the process.

Initially, it was thought that RSA configurations could be used as equilibrium realizations of hard sphere systems. However, the absence of fluctuations associated to the irreversible character of the process leads to intrinsically different configurations respect to those of equilibrium[10]. In particular, in RSA not all the configurations are equally likely, and the jamming coverage is always smaller than close packing, which the maximum density accessible in equilibrium[11] (see fig.1.1). Nonetheless, at low coverages RSA configurations are equivalent to the equilibrium ones. As Widom showed[19], the thermodynamic properties of RSA are equivalent to the equilibrium ones untile terms squared in the coverage.

Analytic solution for the evolution of the coverage of RSA exists for its 1-d version. Both the lattice and the continuum model make use of the *shielding* property, according to which the evolution of an unoccupied segment of the line limited by two adsorbed particles, hereafter referred to as a *gap*, is independent of the evolution of the neighbouring ones, since it only depends on the probability that a new incoming particle destroys it, and the incoming probability is uniform[11][7]. In higher dimensions the shielding property is lost, and no exact solutions are known. However, in difference with respect to many other parts of statistical mechanics, the 1-d models

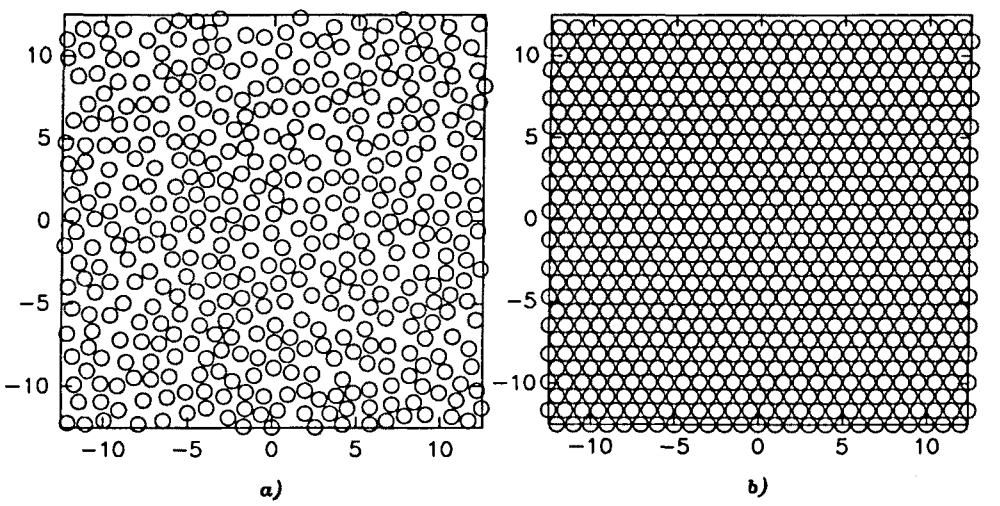


Figure 1.1: Maximum coverage of disks on a surface. a) RSA configuration; b) Equilibrium hard disk configuration.

already exhibit many of the non-trivial features of the higher dimensional versions of the model.

Regarding the continuum RSA 1-dimensional model, which is also referred to as the *car-parking problem*, although it can be obtained from the corresponding lattice version by appropriately rescaling the size of the incoming particles respect to the lattice separation[10][13][11][14] , it was solved the first time by Renyi[13], who found the time evolution of the coverage as a function of time, and expressed the jamming limit as a quadrature. We will solve now the 1-d continuum RSA model, writing evolution equations for the number density of gaps[25]. This formalism will be useful to study BM afterwards, and will be used in chapter 2.

Let us consider the adsorption of rods of length $a$ on an infinite 1-d line. Rods arrive uniformly random at the line at a rate $k_a$ per unit length and per unit time. Let $\tilde{G}(\tilde{l},\tilde{t})d\tilde{l}$ denote the number density of gaps with length between $\tilde{l}$ and $\tilde{l}+d\tilde{l}$ at time $\tilde{t}$. The natural time, $\tau$ and length $\lambda$ units are $\tau=(ak_a)^{-1}$ and $\lambda=a$, respectively. Therefore, we can define dimensionless length $l$ and time $t$ variables, as $l=\tilde{l}/a$ and $t=ak_a\tilde{t}$, and a dimensionless gap density function as $G(l,t)=a\tilde{G}(\tilde{l},\tilde{t})$.

We can derive the evolution equations for the gap density functions making use of the *shielding* property, according to which the gaps evolve independently from each other. Therefore, we should determine how gaps are created and destroyed. To this end, one should take into account that in RSA, particles are adsorbed if the trial position for their center does not produce an overlap of the incoming particle with a preadsorbed one. In terms of the kinetics of the gaps, this means that if one tries to locate the center of a particle on a gap of length smaller than one, it will overlap with one of the limiting rods. Therefore, gaps smaller than one cannot be destroyed. On the other hand, gaps larger than one are destroyed at a rate proportional to the fraction of the gap in which the center of an incoming particle does not lead to overlap with any of the rods which delimit the gap, which is $l-1$ for a gap of length $l$. When a gap of length $l>1$ is destroyed, two new gaps appear, one of length $l'$, with $l'\epsilon[0,l-1]$, and another one of length $l-l'-1$. The new created gaps can be either greater or smaller than one. According to these creation and destruction mechanisms, we can write the evolution equations

$$\frac{\partial G(l,t)}{\partial t} = -(l-1)G(l,t) + 2\int_{l+1}^{\infty} G(l',t)\,dl' \qquad l > 1 \tag{1.1.1}$$

$$\frac{\partial G(l,t)}{\partial t} = 2\int_{l+1}^{\infty} G(l',t)\,dl' \qquad l < 1 \tag{1.1.2}$$

The first term at the right hand side of eq.(1.1.1) indicates that gaps of length $l$ are destroyed proportionally to its number, $G(l,t)$, and to the length available for the adsorption of an incoming particle in such gaps, which is $l-1$ as indicated above. The second term of the first equation accounts for the fact that gaps of length $l$ are created by destruction of any larger gap, proportionally to the number of such larger gaps, $G(l',t)$. The factor 2 in front of it indicates that there are two symmetrical ways to create a gap of a given length from a larger one. The second equation indicates that gaps of length smaller than one cannot be destroyed, but they are appear through the same mechanism as the large ones. Note that the function $G$ in the integrals take values of $l'$ which are always greater than one. Then, eq.(1.1.1) is an integro-differential equation for $G$ in the range $l > 1$, while eq.(1.1.2) is a differential equation for $G$ in the range $l < 1$, once eq.(1.1.1) has been solved. In order to solve the system of eqs.(1.1.1)-(1.1.2) we should take into account that initially the line is empty, which implies that initially there density of gaps is zero. According with this initial conditions, we introduce the "ansatz" for the gap distribution function

$$G(l,t) = t^2 e^{-(l-1)t} F_{rsa}(l,t) \tag{1.1.3}$$

where $F_{rsa}(l,t)$ satisfies

$$\frac{\partial F_{rsa}(l,t)}{\partial t} = 2\int_0^{\infty} dx e^{-(x-1)t} F(x+l+1,t) \tag{1.1.4}$$

Since initially, $F_{rsa}$ cannot depend on $l$ because the line is empty, the structure of eq.(1.1.4) implies that none of its derivatives will depend on $l$ either. Then, if $F_{rsa}$ is analytic, it will not depend on $l$ afterwards. In this case, eq.(1.1.4) reduces to the ordinary differential equation

$$\frac{dF_{rsa}(t)}{dt} = 2\frac{e^{-t}-1}{t} F_{rsa}(t) \tag{1.1.5}$$

which has as solution

$$F_{rsa}(t) = \exp\left[-2\int_0^t \left(\frac{1-e^{-u}}{u}\right) du\right] = \frac{e^{-2\gamma}}{t^2} e^{-2E_1(t)} \tag{1.1.6}$$

compatible with the initial condition, where $\gamma = 0.57721...$ is the Euler constant, and $E_1(x)$ the exponential-integral function[28]. Once the solution for $l > 1$ is known, substitution of expression (1.1.3) in the integral of eq.(1.1.2) gives

$$G(l,t) = \int_0^t 2\tau e^{-l\tau} F_{rsa}(\tau)\, d\tau \qquad\qquad l < 1 \tag{1.1.7}$$

Eqs.(1.1.3) and (1.1.7) completely define the gap distribution function. They give a regular function at any time, except at jamming, where there exists no gaps of length larger than 1, as can be easily seen from eq.(1.1.3), and there exists a logarithmic divergent concentration of gaps of vanishing length. If we look at the gap distribution function at jamming, eq.(1.1.7) reads

$$\begin{aligned} G^\infty(l) &= 2e^{-2\gamma}\int_0^\infty \frac{dt}{t} e^{-lt} e^{-2E_1(t)} = 2e^{-2\gamma}\left(\int_0^1 \frac{dt}{t} e^{-lt} e^{-2E_1(t)}\right. \\ &+ \left.\int_1^\infty \frac{dt}{t} e^{-lt}(e^{-2E_1(t)} - 1) + \int_1^\infty \frac{dt}{t} e^{-lt}\right) \end{aligned} \tag{1.1.8}$$

where we have singled out the divergent contribution in the limit $l \to 0$. The first and second terms at the right hand side do not diverge, although in the first one the integrand can be expanded in a power series of $l$, the second should be worked out with care. Then, the leading behavior when $l \to 0$ is determined by the third integral, and therefore[18][11]

$$G^\infty(l) \sim -2e^{-2\gamma}\log(l) + \gamma + \mathcal{O}(l), \quad l < 1 \tag{1.1.9}$$

Once the gap distribution is known, it is possible to calculate the number density of gaps per unit length during the filling process. Since there is only one adsorbed

particle for each gap, then we can also know the fraction of line covered by particles, also referred to as the density of adsorbed particles $\theta(t)$, as the process evolves. We can write

$$\theta(t) = \int_0^\infty G(l,t)dl = \int_0^t F_{rsa}(t')\,dt' \tag{1.1.10}$$

where we have used the properties of the function $G(l,t)$ to arrive at a simpler expression in the second equality. If we let the time go to infinity, we obtain the jamming coverage of the line, $\theta_{rsa}(\infty) = 0.74759...$[13].

From the expression for the coverage as a function of time it is possible to determine the line available function $\phi$, because it gives the rate of increase of the coverage,

$$\phi(t) = \int_1^\infty (l-1)G(l-1,t)dl = \frac{d\theta}{dt} \tag{1.1.11}$$

and using both eqs.(1.1.10) and (1.1.11), one can derive the available line fraction as a function of the coverage, $\phi(\theta)$, leading to an equation for the covergae evolution equivalent to eq.(2) in the absence of desorption.

Although some analytic results have been obtained for the density on RSA of dimers in a square lattice[20], no exact results are known for the coverage in continuum RSA in two or higher dimensions, and most of the results, as for example the jamming coverage of disks in a two dimensional substrate, are determined from computer simulations[11]. However, a general theory has been developed making use of the distribution function theories of liquid theory, and hierarchies of Kirkwood-Salsburg type have been derived[21], and also a geometrical analysis of the structure at jamming based on Voronoi tesselations has been performed[11]. More generally, perturbative schemes have been carried out to obtain quantitative predictions of the process. Using scaled particle theory ideas[22], perturbative expressions for the available surface function as shown in eq.(2) are derived[20], showing that until the third power in the coverage, the same behavior that equilibrium configurations is recovered[19] . Similar expansions follows by analogy with lattice perturbative methods[24], and also introducing an operator formalism[25]. There also exist a number of asymptotic expansions to determine the way in which coverage approaches its jamming value. While

in the lattice models this approach is exponential[7], in continuum RSA a power-law approach is observed. The first experiments[2] and analytical calculations[10] on the adsorption of disks predicted a power-law behavior, with exponent $-1/d$, $d$ being the dimension of the system. Swendsen[18] conjectured that the same behavior should be obtained for continuum RSA of objects of any shape. More detailed studies for RSA of non spherical particles[27][28][29] showed that the general law was

$$\theta_{rsa}^{\infty} - \theta_{rsa}(t) \sim \frac{1}{t^{1/p}} \tag{1.1.12}$$

with $p$ being the number of degrees of freedom per adsorbed object. When the objects do not have a proper area, such as needles, more complex irrational powers are obtained[30]. The analytic solution for the 1-d case, eq.(1.1.10), makes it possible to verify this power law, as shown in Appendix A and obtain the corresctions to the leading asymptotic behavior.

Besides the study of the kinetics of global physical quantities, in order to characterize RSA in more detail, it is also important to study local properties during the coverage of the substrate. The basic quantity of interest here is the pair correlation function, which has been studied basically through computer simulations even in the 1-d model[31], although there exist recent calculations[37] based on the relationship between the pair correlation function and the gap distribution function[18]. According to this relationship, both functions coincide for distances smaller than one, because only one particle can be closer than two to a given particle. This fact leads to the result that at jamming, the pair distribution function has to exhibit a logarithmic divergence upon contact, as shown in eq.(1.1.9)[2]. A characteristic feature of the pair correlation function of RSA is its faster decay compared to the equilibrium ones and exhibit less oscillations after the first peak, which indicates a faster decay of correlations (see fig.1.2) and that a less structured system is formed on the surface. In particular, when calculated on a lattice, it exhibits a faster-than-exponential decay at all times[7], and the results for the continuum model exhibit a decay faster than the one obtained in the lattice models[37]. Closely related to the pair correlation function, there has also been pursued a study of the global fluctuations of the process as a way to characterize it[37][34].

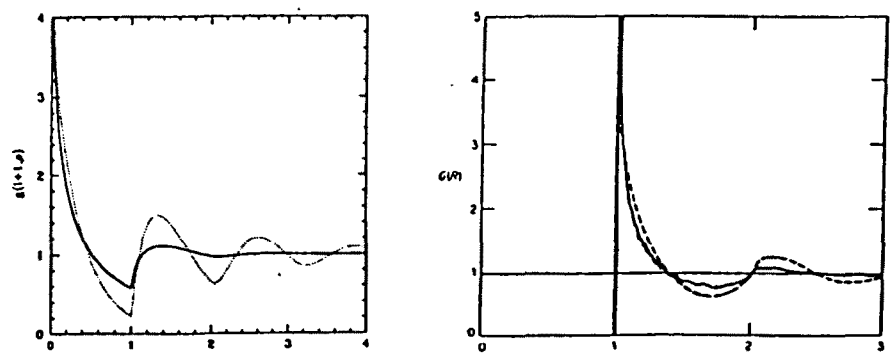

Figure 1.2: Pair correlation function for a system of hard disks obeying: (—) RSA kinetics at jamming, (- - -) equilibrium at the same coverage at a) 1-D, b) 2-D.

## 1.2 Ballistic Deposition Model

BM was introduced as a new kinetic model which solved some of the deficiencies of RSA with respect to real systems. In particular, the strict rejection when the incoming particle overlaps a preadsorbed one, does not correspond to a realistic situation. In principle, this model should take into account the effects of an attracting force towards the substrate besides the geometrical blocking effects characteristic of RSA, and can be thought as the monolayer version of the more general rain model for random deposition[35].

As in RSA,this is a sequential model, but it has been introduced for spherical objects adsorbing on a continuum 2-d or 1-d surface. The position for an incoming particle is chosen uniformly random over the substrate. A particle arrives along a linear trajectory. If it does not overlap with a preadsorbed object, it remains fixed at the same initial position on the surface. Otherwise, it rolls over the preadsorbed sphere it has touched, trying to reach the surface following the steepest descent path. Only if the incoming particle gets trapped before reaching the substrate, it is rejected. The process continues with a new trial object. This sequential filling process usually starts with an empty surface, and, again, a jamming state is attained when no more particles can reach the substrate[34]. BM can be defined entirely in terms of motion of the incoming particles along the substrate; if a particle overlaps a preadsorbed one it will move one diameter apart along their line of centers, and if it overlaps again, then it is rejected (in 1-D). The corresponding rules for the 2-D case are shown in app.?? of chapter 3. In this way, this model can also be extended to three dimensions[34].

The one dimensional version of BM can be solved analytically using the same techniques we have developed in the previous section for RSA, since here also there exists a shielding property implying that the evolution of each the gap is independent of its neighbors[25].

We will use the same notation as in the previous section, and will derive the appropriate evolution equations for the dimensionless gap distribution functions. If one tries to locate the center of a disk in a gap of length smaller than 1, the incoming particle will be trapped by the two particles limiting the gap before reaching the surface (see fig.1.3a). Therefore, gaps smaller than one can only be created. None of

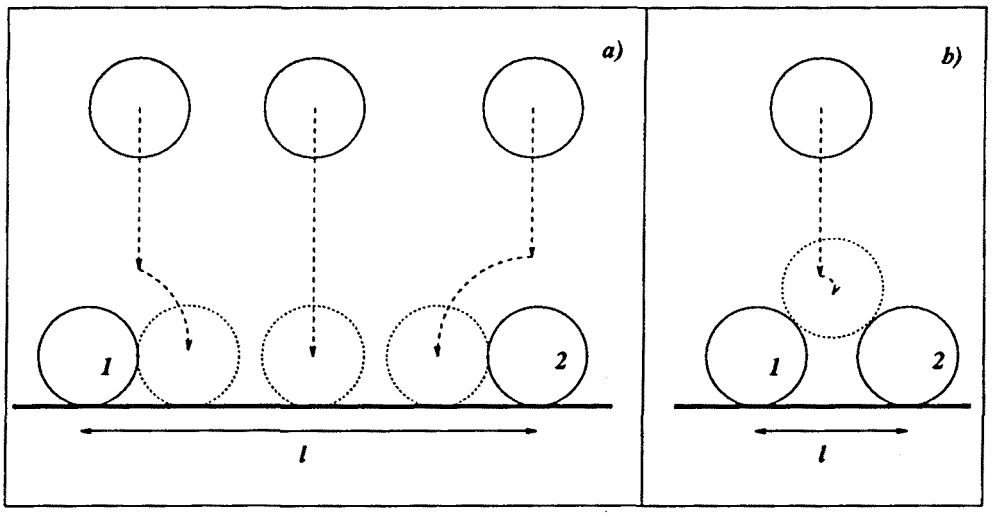


Figure 1.3: Illustration of the 1-d ballistic deposition process for disks of diameter 1. a) gap $l > 1$, b) gap $l < 1$.

the particles whose center arrives at a gap of length $l > 1$ will be rejected. Therefore, these gaps are destroyed at a rate proportional to their number and to $l + 1$ since the incoming sphere can roll over the ones which delimit the gap (see fig.1.3b). What regards the creation of gaps, we should distinguish those particles which arrive directly at the line and those which arrive after rolling over a preadsorbed particle. The first ones lead to the same rate of gap creation as we have already discussed in RSA, that is, two new gaps are created, one of length $l' \epsilon [0, l-1]$ and another of length $l - l' - 1$, and this may happen for two equivalent positions in each gap. The second one is related to the fact that a finite fraction of the adsorbing particles will roll over preadsorbed disks, and arrive at the surface in contact with them, forming clusters, the simplest of which is a pair. Then, only one gap is created, of length $l - 1$. Therefore, there will exist a finite fraction of pairs in the adsorbed layer during the filling of the substrate. According to these creation and destruction mechanisms, the evolution equations are

$$\frac{\partial G(l,t)}{\partial t} = -(l+1)G(l,t) + 2G(l+1,t) + 2\int_{l+1}^{\infty} G(l',t)\, dl' \quad , l \geq 1 \quad (1.2.13)$$

$$\frac{\partial G(l,t)}{\partial t} = 2G(l+1,t) + 2\int_{l+1}^{\infty} G(l',t)\, dl' \quad , l \leq 1 \quad (1.2.14)$$

The first term at the right hand side of eq.(1.2.13) indicates that gaps of length $l$ are destroyed proportionally to its number, $G(l,t)$, and to the length available for the adsorption of an incoming particle in such gaps. The second term incorporates the new singular mechanism according to which a gap of length $l + 1$ can originate one of length $l$ by rolling, with a rate equal to the diameter of the spheres. Finally, the third term of the first equation tells that gaps of length $l$ are created by direct adsorption of any gap larger than $l + 1$, proportionally to the number of such larger gaps, $G(l', t)$. The factor 2 in front of the last two terms indicates that, due to the symmetry, there are two postions at which a gap of length $l$ can be created. The second equation indicates that gaps of length smaller than one can only be created, and that there exist no new creation mechanisms for them. Note that the function $G$ in the integrals take values of $l'$ which are always greater than one. As before, once we solve the integro-differential equation (1.2.13), eq.(1.2.14) becomes a differential equation for $G$ in the range $l < 1$. We will consider the same initial condition as used in RSA, i.e. that initially there are no gaps. In order to solve eq.(1.2.13) we introduce

an "ansatz" equivalent to eq.(1.1.3),

$$G(l,t) = t^2 e^{-(l+1)t} H(t) \tag{1.2.15}$$

Substituting it in eq.(1.2.13), leads to an ordinary differential equation for $H(t)$ which can be solved, giving

$$G(l,t) = t^2 e^{-(l+1)t} e^{2(1-e^{-t})} F_{rsa}(t) \quad l \geq 1 \tag{1.2.16}$$

where $F_{rsa}(t)$ is given in eq.(1.1.6). Substituting this expression for the gap distribution function in eq.(1.2.14), and solving the differential equation leads to

$$G(l,t) = \int_0^t d\tau 2\tau(1+\tau) e^{-(l+2)\tau} e^{2(1-e^{-\tau})} F_{rsa}(\tau) \qquad , l \leq 1 \tag{1.2.17}$$

In the jamming limit it is easy to verify that there are no gaps of length larger than one, and that there is a finite fraction of gaps at contact, although with no logarithmic behavior. The function $G(l,t)$ does not take into account the formation of pairs, and therefore, cannot describe the evolution of the gaps of length zero. These gaps exhibit a singular behavior because a finite fraction of adsorbed disks are forming pairs. In chapter 2, we will describe the evolution of both the regular and singular part of the gap distribution function, along the lines of Ref.[37].

Once we know the gap density function, we can determine the coverage of the line as a function of time. We should take into account, however, that since now pairs of particles are formed, one gap does not necessarily corresponds to one particle. Then, we have to use the fact that the fraction of covered surface is one minus the fraction of uncovered surface, which is directly related to $G(l,t)$. We have then

$$\theta_{bm}(t) = 1 - \int_0^\infty l G(l,t)\, dl \tag{1.2.18}$$

Upon substituting the expression for $G$, eqs.(1.2.16) and (1.2.17), in eq.(1.2.18)

and simplifying it, one arrives at

$$\theta_{bm}(t) = \int_0^t (1+2\tau)e^{2(1-\tau-e^{-\tau})} F_{rsa}(\tau)\, d\tau \tag{1.2.19}$$

Letting the time going to infinity, we obtain the jamming coverage, $\theta_{bm}^{\infty} = 0.80865...$[25], which is larger than the RSA value, due to the appearance of clusters of connected patricles. An analysis of the asymptotic kinetics in eq.(1.2.19) gives

$$\theta_{bm}^{\infty} - \theta_{bm}(t) \sim 2e^{2(1-\gamma)} \frac{e^{-2t}}{t} \tag{1.2.20}$$

which is faster than the power-law approach characteristic of RSA. This is due to the fact that, because of the rolling mechanism, the fraction of the area which leads to adsorption does not go to zero in the jamming for BM, while it vanishes for RSA[34].

As for the RSA model, there exist no analytic solutions of BM for a two dimensional substrate. In this case, basically numerical simulations have been performed[34][38][33] to study the coverage and its asymptotic behavior, the pair correlation function and the cluster formation and evolution, as well as its percolation properties[40]. One finds the same qualitative behavior showed in the 1-d model. Perturbative expansions at low coverage for the pair correlation function and the available surface function[38] have been performed, and also the distribution function approach has been applied to find general hierarchies of equations generalizing methods used in equilibrium statistical mechanics[52]. At the end of chapter 3 we present in detail the rolling mechanisms for the 2-d BM. What regards the radial pair distribution function, the singular adsorption mechanism related to the rolling leads to the appearance of a delta function at distances multiples of the diameter, producing a local structure quite different from the RSA one. Moreover, in 2-d more peaks in the radial pair correlation function appear, due to rolling on connected clusters with different geometries[33].

## 1.3 Generalized RSA and BM Models

A series of generalizations of these standard kinetic models have been performed to try to accommodate some of the mechanisms which are relevant in the adsorption of colloids and which have been neglected in their formulation. For example, the effect of diffusion has been incorporated to study the asymptotic kinetics[31] and a model has been developed in which the adsorption rate depends on the length of the gap[32], taking into account in an effective way the results of simulations on the adsorption with constant diffusion which showed that adsorption rate is not homogeneous[43]. More recent studies have also been performed to incorporate the possibility of a non-homogeneous adsorption rates, which enables one to compare more realistically with the diffusion-adsorption process[7]. Since in experimental situations polydispersity cannot in general be avoided, generalization of RSA to deal with adsorption of mixtures has been considered[45][46][47].

The effect of desorption has also been introduced, giving then a rate equation for the coverage closer to those proposed in the generalized Langmuir equation, (2). In this case, an equilibrium state is finally reached. Both the low-to-intermediate coverage regime, through the development of equations for the distribution functions[48], and the asymptotic behavior[49] have been studied, basically using one dimensional models. Surface diffusion and its interplay with adsorption kinetics has also been addressed[50]. The restriction that there exists only one adsorbed layer has also been removed, and the blocking effects of RSA incorporating multilayering have been considered[51].

From a formal point of view, a generalized adsorption model has also been studied in which a new parameter is introduced, which is a quotient between the probability of arriving after rolling over one preadsorbed sphere relative to that of arriving at the surface directly[37]. This model contains as special cases RSA (when the parameter is zero) and BM (when it is one). Again, an analytic solution exists in 1-d[37], and in 2-d a distribution function theory has been developed[52].

In order to describe the adsorption of proteins, generalizations of RSA have also been considered. On one hand, some models have been developed for adsorption on non-uniform substrates[53][54]. On the other hand, more detailed kinetic models have

been carried out to include the fact that upon adsorption, the protein change their structure even in a completely irreversible adsorption process. Both a lattice[55] and a continuum 1-d[57], where an analytic solution exists, and 2-d models[58] have been developed.

# Appendices

## 1.A Asymptotic behavior of 1-d RSA

In this appendix we will derive the asymptotic behavior of the density in 1-d RSA, using the exact expression for the fraction of covered line given in eq.(1.1.10), which we express

$$\theta_{rsa}(t) = \theta_{rsa}^{\infty} - e^{-2\gamma} \int_t^{\infty} \frac{d\tau}{\tau^2} e^{-2E_1(\tau)} \qquad (1.A.21)$$

where we have used eq.(1.1.6). In order to obtain the leading behavior of the previous equation, we rewrite it as

$$\theta(t)_{rsa} = \theta_{rsa}^{\infty} - e^{-2\gamma} \int_t^{\infty} \frac{d\tau}{\tau^2} \left( e^{-2E_1(\tau)} - 1 \right) - \frac{e^{-2\gamma}}{t} \qquad (1.A.22)$$

where we have taken into account that the exponential-integral vanishes at infinity. Since $2E_1(t) < 1$ for $t > 1$, we can expand the integrand in powers of $E_1$, leading to

$$\theta_{rsa}^{\infty} - \theta_{rsa}(t) = \frac{e^{-2\gamma}}{t} + \sum_{n=1}^{\infty} \frac{(-2)^n e^{-2\gamma}}{n!} \int_t^{\infty} \frac{d\tau}{\tau^2} E_1^n(\tau) \qquad (1.A.23)$$

and, for the same reason, the inequality

$$\frac{2^n}{n!} \int_t^{\infty} \frac{d\tau}{\tau^2} E_1^n(\tau) < \frac{2^{n-1}}{(n-1)!} \int_t^{\infty} \frac{d\tau}{\tau^2} E_1^{n-1}(\tau) \qquad (1.A.24)$$

is fulfilled, which ensures that the series in eq.(1.A.23 ) is convergent. This means that $1/t$ is the leading asymptotic behavior, in agreement with the result (1.1.12), and that corrections to this behavior can be calculated systematically. In particular, the first correction gives

$$\theta^{\infty}_{rsa} - \theta_{rsa}(t) = \frac{e^{-2\gamma}}{t} - 2e^{-2\gamma}\left\{\left(1+\frac{1}{t}\right)E_1(t) - \frac{e^{-t}}{t}\right\} + \mathcal{O}\left(\frac{e^{-2t}}{t}\right) \quad (1.A.25)$$

Now, using the asymptotic expansion of $E_1(t)$[28], we can derive the first correction to the power-law behavior,

$$\theta^{\infty}_{rsa} - \theta_{rsa}(t) = \frac{e^{-2\gamma}}{t}\left(1 - 2\frac{e^{-t}}{t^2} + \mathcal{O}\left(\frac{e^{-t}}{t^3}\right)\right) \quad (1.A.26)$$

whereas Pomeau obtained as the first correction to the powar-law leading behavior, a function $\log(t)e^{-t}/t^2$[10]. In fact, it can be verified that this term does not correspond to the next term in the asymptotic expansion performing the limit

$$\frac{\int_t^{\infty}\frac{dt'}{t'^2}\left(e^{-2E_1(t')}-1\right)}{\frac{\log(t)e^{-t}}{t^2}} \xrightarrow{t\to\infty} 0 \quad (1.A.27)$$

# References


[1] J. Feder and I. Giaever, J. Colloid Interface Sci. **78**, 144 (*1980*).

[2] J. Feder, J. Theor. Biol. **80**, 237 (*1980*).

[3] G.Y. Onoda, and E.G. Liniger, Phys. Rev. A **33**, 715 (*1986*).

[4] P. Wojtaszczyk, P. Schaaf, B. Senger, M. Zembala, and J.C. Voegel, J. Chem. Phys. **99**, 7198 (*1993*).

[5] J.J. Ramsden, Phys. Rev. Lett. **71**, 295 (*1993*).

[6] D.W. Cooper, J. Colloid Interface Sci. **119**, 442 (*1987*); Phys. Rev. A **38**, 522 (*1988*).

[7] J.W. Evans, Rev. Mod. Phys. **65**, 1281 (*1993*).

[8] J.P. Flory, J. Am. Chem. Soc. **61**, 1518 (*1939*).

[9] E.R. Cohen and H. Reiss, J. Chem. Phys. **38**, 680 (*1963*).

[10] J.K. Mackenzie, J. Chem. Phys. **37**, 723 (*1962*).

[11] P.C. Hemmer, J. Stat. Phys. **57**, 865 (*1989*).

[12] B. Widom, J. Chem. Phys. **44**, 3888 (*1966*); **58**, 4043 (*1973*).

[13] J.J. González, P.C. Hemmer and J.S. Hoye, J. Chem. Phys. **3**, 228 (*1974*).

[14] M.C. Bartelt, J.W. Evans and M.L. Glasser, J. Chem. Phys **99**, 1438 (*1993*).

[15] A. Rényi, Publ. Math. Inst. Hung. Acad. Sci., **3**, 109 (*1958*) (translated in Selected Transl. Math. Stat. Prob. **4**, 203 (*1963*)).

[16] J. Talbot and S.M. Ricci, Phys. Rev. Lett. **68**, 958 (*1992*).

[17] M. Abramowitz and I.A. Stegun, *Handbook of Mathematical Functions*, Dover Publishers, New York, (*1972*).

[18] R.H. Swendsen, Phys. Rev. A **1981**, 504 (*1981*).

[19] E.L. Hinrichsen, J. Feder and T. Jossang, J. Stat. Phys. **44**, 793 (*1986*).

[20] J.W. Evans and R.S. Nord, J. Chem. Phys. **79**, 2380 (*1983*).

[21] G. Tarjus, P. Schaaf and J. Talbot, J. Stat. Phys. **63**, 167 (*1991*).

[22] H. Reiss and P. Schaaf, J. Chem. Phys. **91**, 2514 (*1989*).

[23] P. Schaaf and J. Talbot, Phys. Rev. Lett. **62**, 175 (*1989*).

[24] J.W. Evans, Phys. Rev. Lett. **62**, 2642 (*1989*).

[25] R. Dickman, J.S. Wang and I. Jensen, J. Chem. Phys. **94**, 8252 (*1991*).

[26] Y. Pomeau, J. Phys. A **13**, L193 (*1980*).

[27] J. Talbot, G. Tarjus and P. Schaaf, Phys. Rev. A **40**, 4808 (*1989*).

[28] R.D. Vigil and R.M. Ziff, J. Chem. Phys. **91**, 2599 (*1989*).

[29] P. Viot and G. Tarjus, Eurphys. Lett. **13**, 295 (*1990*).

[30] G. Tarjus and P. Viot, Phys. Rev. Lett **67**, 1875 (*1991*).

[31] E. Burgos and H. Bonadeo, J. Phys. A **20**, 1193 (*1987*).

[32] B. Bonnier, D. Boyer and P. Viot, J. Phys. A **27**, 3671 (*1994*).

[33] F.B. Pedersen and P.C. Hemmer, J. Chem. Phys. **98**, 2279 (*1993*).

[34] B. Senger, P. Schaaf, J.C. Voegel, P. Wojtaszczyk and H. Reiss, Proc. Natl. Acad. Sci. USA , (in press) (*1995*).

[35] P. Meakin and R. Jullien, J. Physique **48**, 1651 (*1987*).

[36] R. Jullien and P. Meakin, J. Phys. A **25**, L189 (*1992*).

[37] P. Viot, G. Tarjus and J. Talbot, Phys. Rev. E **48**, 480 (*1993*).

[38] A.P. Thompson and E.D. Glandt, Phys. Rev. A **46**, 4639 (*1992*).

[39] H.S. Choi, J. Talbot, G. Tarjus and P. Viot, J. Chem. Phys. **99**, 9296 (*1993*).

[40] H.S. Choi, J. Talbot, G. Tarjus and P. Viot, Phys. Rev. E **51**, 1353 (*1995*).

[41] P. Schaaf, A. Johner and J. Talbot, Phys. Rev. Lett. **66**, 1603 (*1991*).

[42] G. Tarjus and P. Viot, Phys. Rev. Lett. **68**, 2354 (*1992*).

[43] B. Senger, J.C. Voegel, P. Schaaf, A. Johner, A. Schmitt and J. Talbot, Phys. Rev. A **44**, 6926 (*1991*).

[44] F.J. Bafaluy, H.S. Choi, B. Senger and J. Talbot, Phys. Rev. E (in press).

[45] J. Talbot and P. Schaaf, Phys. Rev. A **40**, 422 (*1989*).

[46] G. Tarjus and J. Talbot, J. Phys. A **24**, L913 (*1991*).

[47] P. Meakin and R. Jullien, Physica A **187**, 475 (*1992*).

[48] G. Tarjus, P. Schaaf and J. Talbot, J. Chem. Phys. **93**, 8352 (*1990*).

[49] X. Jin, G. Tarjus and J. Talbot, J. Phys. A **27**, L195 (*1994*).

[50] V. Privman and M. Barma, J. Chem. Phys. **97**, 6714 (*1992*).

[51] M.C. Bartelt and V. Privman, Int. J. Mod. Phys. B **18**, 2883 (*1991*).

[52] G. Tarjus, P. Viot, H.S. Choi and J. Talbot, Phys. Rev. E **49**, 3239 (*1994*).

[53] X. Jin, N.H.L. Wang, G. Tarjus and J. Talbot, J. Chem. Phys. **97**, 4256 (*1993*).

[54] B. Bonnier, Y. Leroyer and E. Pommiers, preprint

[55] S.M. Ricci, J. Talbot, P. Schaaf, B. Senger and J.C. Voegel, J. Phys. Chem. **98**, 4906 (*1994*).

[56] D. Boyer, J. Talbot, G. Tarjus, P.R. Van Tassel and P. Viot, Phys. Rev. E **49**, 5525 (*1994*).

[57] P.R. Van Tassel, P. Viot, G. Tarjus and J. Talbot, J. Chem. Phys. **101**, 7064 (*1994*).

[58] P.R. Van Tassel, P. Viot, G. Tarjus and J. Talbot, Phys. Rev. E **49**, 5307 (*1994*).

# Chapter 2

# Adsorption in the Presence of External Fields

In the previous chapter we have introduced the kinetic models which are considered representative to model the essentials of colloid adsorption. However, in them the transport from the bulk is incorporated in a simplified way. If Brownian motion of colloids is dominant, then RSA is used to predict the kinetics of the process, while if adsorption takes place at large Péclet numbers, and then the external force drives the particles to the surface, then BM is used. However, the effect of more genral transport situations has not been addressed, and, for example, RSA is still used to explain the kinetics [1] and stricture[2] of the adsorption of suspensions under shear. In this case, if the diffusion boundary layer is large RSA can be expected to give a reasonable description of the process, but if convective terms become important close to the surface, then it is not clear whether RSA is still a good model o not. The objective of the present chapter is to understand whatare the implications of an external field in the standard kinetic models introduced previously, in particular how excluded volume effects will be modified by these external constraints. Though the gravity field can be considered as an external field, it acts as a driving force which allows the adsorption process to take place, since otherwise particles would

not come to the surface in the absence of diffusion. Hence, it seems interesting to address the effect of external forces which modify the bulk transport processes of the colloidal suspensions, but which is not directly related to the adsorption. An example of practical interest would then be the case of polarizable particles in the presence of an electric field parallel to the surface. This situation would correspond to the experimental study of capillary electrophoresis, in which adsorption on the walls of a capillary is studied. The electric field will introduce a new kinetic mechanism, e.g. the possibility for adsorbed particles to desorb, which will compete with the usual adsorption kinetics mechanisms.

We will focus on how surface exclusion effects are modified by the presence of an additional force. The first part will be devoted to generalize the kinetic models introduced in chapter 1 to account for the new external field, although we will not take into account the possibility of an enhanced desorption, despite its potential experimental interest[3]. We will concentrate on the changes which will introduce the additional applied force on the adsorption probabilities and in the kinetics of the process, and will consider the appropriate generalizations of RSA and BM. As already noted, while the first one seems to reproduce appropriately the adsorption of colloids when diffusion is important, and its generalization could be of interest to describe the experiments on protein adsorption[1], the second constitutes a first step to understand the effects of external fields on the adsorption of heavy particles. In this last case, however, in order to have a more detailed description of the layer structure, a more realistic description of the bulk transport is needed, as discussed in chapter 3.

In the previous paragraphs, we have referred to different physical situations. In principle, the existence of an external field acting parallel to the substrate, or the shearing of the solvent are quite different situations which cannot be expected to be described by the same model. However, the essential common feature of both situations from the point of view of adsorption is that incoming particles cannot adsorb at any available position on the surface. Rather, they are drifted along the direction of the force, before reaching the wall. Then, in the absence of a detailed description of the transport, both a shear and an applied force parallel to the substrate produce the same behavior. It is also worth noting that the adsorption from a quiescent liquid in the presence of gravity field on a substrate which is not horizontal will be also described within the same framework.

We will concentrate on the one-dimensional version of these models. Although a 2-D model will be necessary to perform comparisons with experimental results, the 1-D version is simpler to deal with and, as we will see, analytic solutions can be obtained. Moreover, as it is usual in these kinetic models, their 1-D versions already contain the basic features of the process at higher dimensions, and therefore, no new qualitative properties are expected. In particular, a new rolling mechanism in the generalized BM model already appears in 1-D.

## 2.1 One-Dimensional Generalized Deposition Models

We will consider the one dimensional version of a kinetic adsorption model in which particles do not arrive perpendicularly to the substrate. Rather, as shown in fig. 2.1a), disks of radius one arrive at the line forming an angle $\alpha$ with the normal to the wall. This angle will be the only free parameter of the model. If a constant external field, $F_e$, parallel to the surface is applied besides the usual gravitational force $F_g$, and neglecting hydrodynamic effects, then $\alpha$ is related to the physical parameters of interest by $\tan\alpha = \frac{F_e}{F_g}$. An equivalent relation is satisfied if the host fluid is subject to a plug flow. If instead, a Couette flow is applied, then more care should be taken, because in this case the incoming particle will describe a parabola. A relationship with the case of straight trajectories can be found if one takes into account that there is a minimum distance at which an incoming particle following a parabola can land in the nearby of a preadsorbed disk. Suppose an adsorbed disk is at the center of a coordinate system. If the motion takes place in a shear $\beta$, the trajectory of the incoming particle can be written as $x = x_0 - \frac{\beta}{2}z^2$, with x being the horizontal distance away from the sphere at the center, while $z$ represents the height from its center. Finally $x_0$ will be the distance at which the incoming sphere will land. One can calculate the minimum allowed value for $x_0$ at the right hand side of the preadsorbed particle, giving $x_0 = (\beta + \beta^{-1})/2$. Then, one can calculate which angle $\alpha$ gives incoming straight trajectories which end at a minimum separation at the right of a preadsorbed sphere of value $x_0$. Such an angle satisfies $\cos\alpha = 4\beta/(1+\beta^2)$. Finally, if adsorption takes place in a quiescent fluid, in the presence of a gravity field, on a

substrate which is inclined an angle $\gamma$ with respect to the horizontal, then, obviously $\alpha = \gamma$. The three different physical situations are described by a single parameter $\alpha$, which gives an idea of the distance from the standard kinetic models. For simplicity's sake, in the rest of the chapter we will use the image corresponding to the last physical situation introduced.

We will analyze separately the situations in which incoming particles are not allowed to roll over preadsorbed ones, corresponding to RSA type rules, and when they are allowed, within the framework of BM rules.

## 2.2 Inclined Random Sequential Adsorption Model

As shown in fig.2.1a), for disks arriving along inclined straight lines to the surface, there is a minimum distance of approaching to the right hand side of a preadsorbed particle, $\sigma$, which is related to $\alpha$ through $1 + \sigma = 1/\cos(\alpha)$. We will not consider the actual mechanisms which control the transport of the particles to the surface. Rather, we will determine the position of the incoming particle on the surface on the basis of the corresponding geometric rules, according to the basic method of RSA to accommodate adsorbing particles. Though the rules are general for any dimension, we will focus on its 1-D version, since we will only deal with this case, and we will consider all spheres being of the same size. Positions for the center of trial particles are chosen uniformly random along the line. In usual RSA, the particle sticks irreversibly at that position if no *overlap* exists with a preadsorbed sphere, with *overlap* meaning that the distance from the center of the incoming particle to any of the preadsorbed ones is smaller than the diameter of the spheres; otherwise the trial particle is rejected and a new position is tried. In this model, we should change the concept of *overlap* according to fig.2.1a). Now, a particle is irreversibly located at the position if the distance from its center to the center of any of the preadsorbed spheres at its right hand side is longer than unity, and larger than $1+\sigma$ to any of the preadsorbed spheres at its left hand side; otherwise, the incoming particle is rejected. It is worth noting that this description of the model in terms of the excluded length makes it possible to consider the system as if we had incoming particles of length one which, upon arrival at the surface, deformed a length $1 + \sigma$ towards the right. This asymmetry

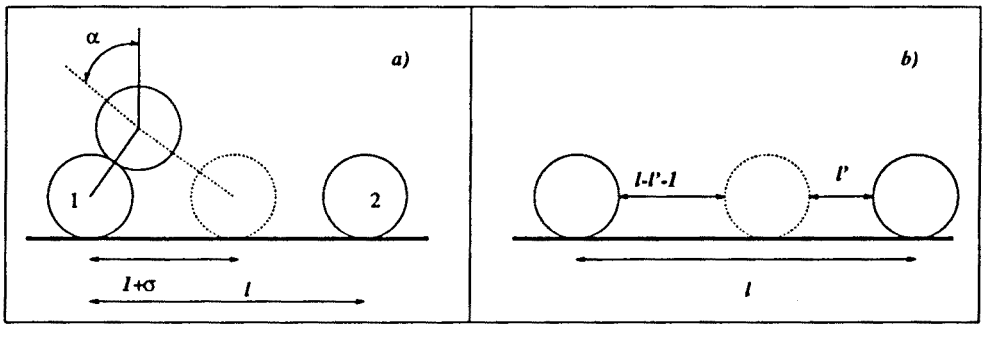


Figure 2.1: a) Trajectory of an incoming particle of diameter unity forming an angle $\alpha$ with the normal to the adsorbing line, in the presence of two adsorbed disks,1 and 2, at a distance $l$. $1+\sigma$ represents the minimum distance between a preadsorbed disk and the incoming particle on the line to its right. b) New gaps appearing when an incoming particle lands at distance $h'$ from the preadsorbed disk at right.

in the deformation makes these models different from the restructuring-particle RSA proposed in the literature to study the adsorption of certain proteins which undergo structural changes at the surface[8].

### 2.2.1 Analytic Study

It is possible to obtain an analytic expression for the gap density functions, using the methods developed in chapter 1, since here, again, the evolution of a given gap

is independent of its neighbors, which enables one to derive a closed equation for the one gap distribution function. Such evolution equations can be deduced once we know the different mechanisms by which particles can arrive at the line, creating and destroying gaps. We will use the same dimensionless unities and notation introduced in chapter 1.

Let us consider a gap of length $l$. According to the rules introduced in the previous section, an incoming particle should be at a minimum distance $\sigma$ at the rigth of the particle which delimits the gap at its left hand side. Then, if $l < 1+\sigma$, any incoming particle in this gap will overlap with the sphere which delimits the gap at its right, and will therefore be rejected. Then, gaps of length smaller than $1+\sigma$ can only be created. Otherwise, it can be destroyed by direct adsorption of an incoming particle. Since initial positions are chosen uniformly along the substrate, the previous fact means that a gap of length $l > 1+\sigma$ will be destroyed at a rate proportional to $l-\sigma-1$, which is the length of the available part of the gap where the center of an incoming particle can arrive without overlapping with the disks which delimit it. When a gap of length $l$ is destroyed, two new gaps are created, one of length $l'$ at the right of the incoming particle, which can have any value smaller than $l-\sigma-1$, and another one of length $l-l'-1$ at its left, which can have a minimum value of $\sigma$ and a maximum one of $l-1$, as shown in fig.2.1 b). Note that the new gaps may be either larger or smaller than $1+\sigma$.

We can now derive the appropriate evolution equations for the gaps. Let us consider first the case $l > 1+\sigma$. These intervals are destroyed at rate proportional to the available fraction of the length at which an incoming particle can arrive, $l-\sigma-1$, and to the number of such gaps. On the other hand, a gap of length $l$ may be created by destruction of a gap of length $l' > l$. Such creation rate will be proportional to the number of gaps of length $l'$, and one should take into account that if the gap of length $l$ is created at the left hand side of the incoming particle, the length of the initial gap should be at least $l+1$, while if it created at the right of an incoming disk, then the minimum possible length is $l+\sigma+1$. Therefore, the evolution equation for the one gap distribution function, $G(l,t)$ when $l > 1+\sigma$ corresponds to the integro-differential

equation

$$\frac{\partial G(l,t)}{\partial t} = -(l-\sigma-1)G(l,t)+\int_{l+1}^{\infty} G(l',t)dl'+\int_{l+\sigma+1}^{\infty} G(l',t)dl' \quad , l \geq 1+\sigma \tag{2.2.1}$$

On the other hand, if we consider the behavior of a gap of length $l < 1+\sigma$, we should take into account that it can only be created. In principle, the creation mechanisms are the same that originate the gaps in the previous regime. However, when a particle arrives, it should be at a minimum distance $\sigma$ at the left of a preadsorbed particle. This implies that gaps smaller than $\sigma$ will only be created at the right hand side of the incoming disks. Therefore, the appropriate kinetic equations read

$$\frac{\partial G(l,t)}{\partial t} = \int_{l+1}^{\infty} G(l',t)dl' + \int_{l+\sigma+1}^{\infty} G(l',t)dl' \quad , 1+\sigma \geq l \geq \sigma \tag{2.2.2}$$

$$\frac{\partial G(l,t)}{\partial t} = \int_{l+\sigma+1}^{\infty} G(l',t)dl' \quad , \sigma \geq l \tag{2.2.3}$$

Eqs.(2.2.1)-(2.2.3) constitute a set of integro-differential equations which completely determine the function $G(l,t)$, once the appropriate initial conditions are prescribed. To avoid confusion in the notation, we will write down $G_1(l,t)$ when we refer to the gap distribution function for $l \geq 1+\sigma$, $G_2(l,t)$ when $\sigma \leq l \leq 1+\sigma$, and $G_3(l,t)$ when $l \leq \sigma$.

We will again consider that initially the line is empty, which implies that $G(l,0) = 0$. Then, we try the same "ansatz" for the gap distribution function already proposed to solve the RSA model, eq.(1.1.3). Therefore,

$$G_1(l,t) = t^2 e^{-(l-\sigma-1)t} F(t) \tag{2.2.4}$$

where the factor $t^2$ has been introduced for convenience. This leads us to an ordinary differential equation for the new function $F(t)$,

$$\frac{dF(t)}{dt} = \frac{e^{-t}+e^{-(1+\sigma)t}-2}{t} F(t) \tag{2.2.5}$$

which has as solution,

$$F(t) = \exp\left\{-\int_0^t \frac{1-e^{-u}}{u}du - \int_0^t \frac{1-e^{-(1+\sigma)u}}{u}du\right\} \tag{2.2.6}$$

Here the lower limit in the integral has been taken to satisfy the appropriate initial condition. It can also be written in terms of exponential integral functions, $E_1$, as

$$F(t) = \frac{e^{-2\gamma}}{(1+\sigma)t^2} e^{-E_1(t)-E_1((1+\sigma)t)} \tag{2.2.7}$$

Once the function $G_1(l,t)$ has been determined, eqs. (2.2.2) and (2.2.3) become differential equations for $G_2(l,t)$ and $G_3(l,t)$ which can be expressed as quadratures,

$$G_2(l,t) = \int_0^t \tau F(\tau) e^{-l\tau} \left\{1 + e^{\sigma\tau}\right\} d\tau \tag{2.2.8}$$

$$G_3(l,t) = \int_0^t \tau F(\tau) e^{-l\tau} d\tau \tag{2.2.9}$$

where, again, the lower limit of the integrals has been chosen according to the condition that initially there are no gaps of length smaller than $1+\sigma$. It is worth noting that $G_2(l,t)$ can be expressed in terms of $G_3(l,t)$, giving

$$G_2(l,t) = G_3(l,t) + G_3(l-\sigma,t) \tag{2.2.10}$$

which can be understood as an additivity property. It tells that gaps larger than $\sigma$ originating at the left of an incoming particle follow the same kinetic that the gaps smaller than $\sigma$, because in fact, there exists an exclusion length $\sigma$. Gaps created at the right of the incoming particles are created through the same mechanism which contrlls the appearence of smaller gaps, but taking into account that we are now interested in larger gaps. Eqs.(2.2.4), (2.2.8) (or its equivalent eq.(2.2.10)) and (2.2.9) completely define the one-gap number density at any time.

Moreover, we have used to normalization property, at any time

$$\int_0^\infty (1+l)\, G(l,t)\, dt = 1 \tag{2.2.11}$$

associated to the fact that the total length of the substrate does not change during the filling process.

At jamming, the distribution of gaps is gives

$$G_1^\infty(l) = 0 \qquad , l \geq 1+\sigma \tag{2.2.12}$$

$$G_2^\infty(l) = G_3^\infty(l) + G_3^\infty(l-\sigma) \qquad , 1+\sigma \geq l \geq \sigma \tag{2.2.13}$$

$$G_3^\infty(l) = \frac{e^{-2\gamma}}{1+\sigma} \int_0^\infty dt \frac{e^{-lt}}{t} e^{-E_1(t)-E_1((1+\sigma)t)} \quad l \leq \sigma \tag{2.2.14}$$

showing that only those gaps which cannot be destroyed can survive in the jamming.

We can now study if in this modified RSA model there exists also a logarithmic divergence of the gaps of vanishing length at jamming, as the one observed in RSA, eq.(1.1.9). To this end, we have to study the asymptotic behavior of $G_3^\infty(l)$ for $l \to 0$. We rewrite eq.(2.2.14) in order to explicitely separate the divergent contribution of the integral, which appears due to the slow decay of the integrand when $l \to 0$

$$\begin{aligned} G_3^\infty(l) &= \frac{e^{-2\gamma}}{1+\sigma} \left\{ \int_0^1 \frac{e^{-tl}}{t} e^{-E_1(t)-E_1((1+\sigma)t)}\, dt + E_1(l) \right. \\ &+ \left. \int_1^\infty \frac{e^{-tl}}{t} \left( e^{-E_1(t)-E_1((1+\sigma)t)} - 1 \right) dt \right\} \end{aligned} \tag{2.2.15}$$

and, to first order in $l$

$$\begin{aligned} G_3^\infty(l) &\sim \frac{e^{-2\gamma}}{1+\sigma} \left\{ -\log(l) - \gamma + \int_0^1 \frac{1}{t} e^{-E_1((1+\sigma)t)-E_1(t)}\, dt \right. \\ &+ \left. \int_1^\infty \frac{e^{-E_1((1+\sigma)t)-E_1(t)} - 1}{t}\, dt \right\} + O(l) \end{aligned} \tag{2.2.16}$$

showing the existence of the same logarithmic of divergence as in usual RSA. In order to compare in more detail with RSA, it is more convenient to write the previous equation as

$$G_3^{\infty}(l) \sim \frac{1}{2(1+\sigma)}\left[G_{rsa}^{\infty}(l) + \int_0^{\infty} \frac{e^{-2E_1(t)}}{t}\left(e^{-E_1((1+\sigma)t)+E_1(t)} - 1\right)\, dt\right] + O(l) \quad (2.2.17)$$

with $G_{rsa}^{\infty}$ given through eq.(1.1.9). This behavior shows that the divergence's amplitude is modulated by a factor $1+\sigma$. Moreover, it is half the RSA value even in the limit of small $\sigma$ due to the fact that gaps of length smaller than $\sigma$ can only be created at the right of an incoming disk, instead of being created at both sides. In fact, if we make $\sigma \longrightarrow 0$ before studying the behavior of the one-gap distribution function, then the form of this function for gaps of vanishing length is controlled by $G_2(l,t)$ because $G_3(l,t)$ disappears, and, as can be seen in eq.(2.2.2), gaps in this region can be created at both sides of the incoming disk. On the other hand, for a finite value of $\sigma$, the function $G_2(l,t)$ also exhibits a logarithmic divergence at jamming for $l=\sigma$, as can be deduced from eq.(2.2.10), which shows that $G_2(l,t)$ behaves as $G_3(l,t)$. This means that, unlike standard RSA, two logarithmic divergences appear related to the fact that now there are two minimum distances at which disks can approach. Moreover, the divergence associated to the two minimum distances 1 and $1+\sigma$ exhibit the same divergent behavior, being both half the value of the one corresponding to RSA. In the limit $\sigma \longrightarrow 0$ the two peaks coalesce into a single one, which becomes the one obtained in RSA.

Once we know the gap density function, we can derive the coverage of the line as a function of time. We will make use of eq.(1.1.11), according to which the rate of incoming particles is proportional to the fraction of the line at which incoming particles are accepted. Then, we can construct the available line fraction function $\phi(t)$, which in this case has the form

$$\frac{d\theta}{dt}\phi(t) = \int_{1+\sigma}^{\infty} (l-1-\sigma)G_1(l,t)dl = F(t) \quad (2.2.18)$$

where we have inserted eq.(2.2.4) which gives the corresponding one-gap distribution function. In fig.2.2a), we show the available line fraction as a function of time for

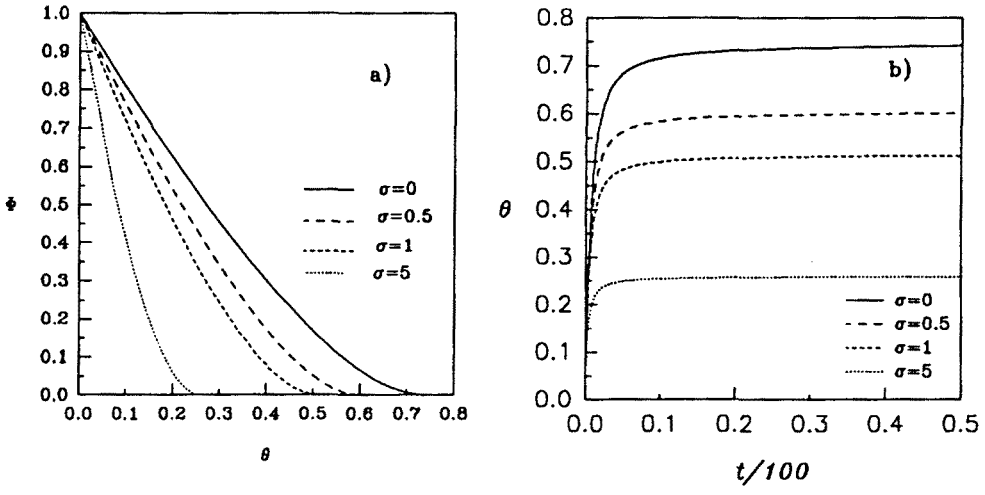


Figure 2.2: a) Available line fraction function as a function of the coverage for different inclination angles. b) Time evolution of the fraction of covered line for different values of the exclusion length $\sigma$.

different values of the parameter $\sigma$, recovering the standard RSA function for $\sigma = 0$. The last term of eq.(2.2.18) allows us to identify the function $F(t)$, introduced so far as a way to find the gap distribution function, with the available line fraction. It is curious to note that eq.(2.2.18) has the same form that the one obtained in standard RSA, as shown in eq.(1.1.11). In respect to the global coverage, the differences between the two models lies on the fact that the function $F(t)$ is different. Eq.(2.2.18) enables one also to express the coverage as a function of time as a quadrature,

$$\theta(t) = \int_0^t F(\tau)d\tau \tag{2.2.19}$$

and in fig.2.2b) we show the time evolution of the coverage for different values of $\sigma$.

The jamming coverage, $\theta^{\infty}(\sigma)$ as a function of $\sigma$ is then obtained from eq.(2.2.19) letting the time go to infinity. In fig.2.3 we show the jamming coverage as a function of the angle of incidence $\alpha$ normalized with respect to $\pi/2$. It is seen that as this parameter increases, a drastic decrease in the maximum number of particles that can be accommodated on the line is observed, since only gaps larger than $1+\sigma$ are destroyed. We will use eq.(2.2.19) to study the dependence of the maximum coverage on $\sigma$ perturbatively. If $\sigma << 1$, the jamming limit is found to be

$$\theta^{\infty}(\sigma) = \frac{e^{-2\gamma}}{1+\sigma}\int_0^{\infty} \frac{e^{-2E_1(t)}}{t^2} e^{-E_1((1+\sigma)t)+E_1(t)}\, dt \tag{2.2.20}$$

Then, we may expand the second factor in the integral in powers of $\sigma$, leading to

$$\theta^{\infty} = \theta^{\infty}_{rsa} - \frac{\theta^{\infty}_{rsa}}{2}\sigma + \left(\frac{3}{2}\theta^{\infty}_{rsa} - e^{-2\gamma}\right)\frac{\sigma^2}{4} - \left(\theta^{\infty}_{rsa} - \frac{7}{3}e^{-2\gamma}\right)\frac{\sigma^3}{4} + \mathrm{O}(\sigma^4) \tag{2.2.21}$$

In fig.2.3 one can see that this expansion, when expressed appropriately in terms of the incident angle $\alpha$, up to third order in powers of the angle agrees reasonably well with the exact results up to angles of the order of $30^{o}$. In order to have an idea of the behavior for incident trajectories almost parallel to the substrate, we should expand the appropriate limit of eq.(2.2.19).

Although it is not possible to express the integral as a combination of known functions, eq.(2.2.19) is of great help when trying to understand the filling kinetics. For example, we can analyze both the short time and the asymptotic behavior of $\theta$ in time. For short times the integral can be developed in powers of the time because $F(t)$ is a regular function. One obtains

$$\theta(t) = t - (1+\frac{\sigma}{2})t^2 + (5+5\sigma+\frac{3}{2}\sigma^2)\frac{t^3}{6} + O(t^4) \tag{2.2.22}$$

indicating that at short times $\theta$ evolves as a power law, and differences with respect to standard RSA start in the second power of time. This is reasonable, because one should wait to have at least to particles adsorbed in the line to start to detect the effects of the new restrictions on the deposition of particles.

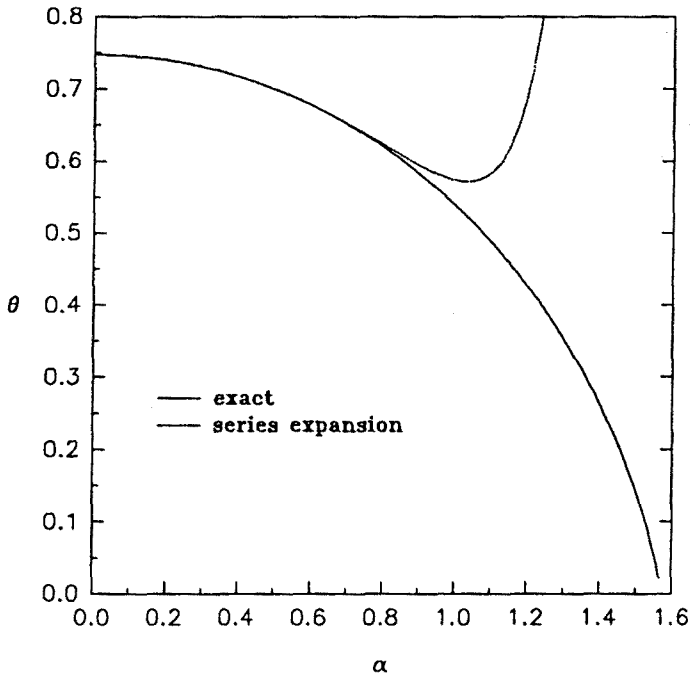


Figure 2.3: The maximum coverage of the line as a function of the incident angle, normalized by a factor $\pi/2$. Dashed line corresponds to the expansion for small values of $\sigma$, up to third order.

The asymptotic approach to the jamming can be studied using the technique introduced in the Apendix A of chapter3. One obtains

$$\theta_\infty - \theta(t) \sim \frac{e^{-2\gamma}}{(1+\sigma)t}\left(1 - \frac{e^{-t}}{t}\right) + O\left(\frac{e^{-t}}{t^3}\right) \tag{2.2.23}$$

which exhibits a power-law decay to leading order due to the fact that the target areas for incoming particles in the neighborhood of the jamming limit go to zero, and again, there appears a prefactor $1+\sigma$. Due to the asymetric deposition of disks, the correction to the asymptotic behavior is half the one obtained in RSA, as shown in eq.(1.A.26 ).

As a final point regarding global quantities, from the knowledge of the fraction of the line covered as a function of time, eq.(2.2.22), and the available line fraction as a function of time, it is possible to contruct,by a perturbative analysis, the available line fraction as a function of the coverage, which is of interest, since it is more directly related to the properties of the filling process[19]. One arrives at

$$\phi(\theta) = 1 - (2+\sigma)\theta + (1 + \sigma + \frac{\sigma^2}{2})\frac{\theta^2}{2} + \mathcal{O}(\theta^3) \tag{2.2.24}$$

Note that at zero coverage this quantity is equal to one since initially the line is empty, and then any incoming particle is adsorbed. The second term simply shows that one adsorbed disk excludes an area equal to its diameter plus the additional exclusion length $\sigma$, as shown in fig.2.1a. The next term is the first which takes into account that the total exclusion length produced when two disks are adsorbed becomes more complex since their exclusion lengths overlap. In fact, the available fraction of the line up to order $\theta^n$ can be constructed by looking at the different ways in which $n$ disks overlap, as has been done for RSA[20][6]. Widom showed that the functions $\phi$ for RSA and equilibrium coincided up to the third power in $\theta$. We can also compare eq.(2.2.24) with the equilibrium available line fraction. However, in our model one particle excludes a length $2 + sigma$, instead of 2 in the usual equilibrium situation for the same kind of particles. In order to compare our results with the equilibrium ones, we should rescale the length of the disks by a factor $(2+\sigma)/2$ in the equilibrium

result, which implies that the concentration used by Widom[19] for rods of length one should be multiplied by a fcator $2/(2+\sigma)$. One than obtains

$$\phi_{eq}(\theta) = 1 - (2+\sigma)\theta + \frac{21}{(2+\sigma)}\theta^2 + \mathcal{O}(\theta^3) \tag{2.2.25}$$

which shows that the available function in the inclined RSA model deviates from the equilibrium one already in the second power in $\theta$, while in standard RSA differences appear in the third power of $\theta$. This is due to the asymetry introduced in the kinetics by the inclined direction of arrival. In standard RSA, the configurations generated by two particles are equivalent to the equilibrium ones, in the sense that one cannot discern which one has been adsorbed first. In inclined RSA, however, the appearence of a new minimum length at which two particles can adsorb, imply that even with two adsorbed particles, not all the configurations are equivalent to the equilibrium ones. If the distance between them is smaller than $1+\sigma$, the one at the right has to have arrived before. Then, this asymetry in the kinetics induce faster deviations from equilibrium.

### 2.2.2 Structure of the adsorbed layer

In the previous section we have studied the behavior related to global quantities of the adsorption process. Now, we will focus on the analysis of the local structure of the adsorbed disks, which will be described by the pair distribution function. To this end, we have carried out numerical simulations for the deposition of disks of diameter one on a line of length 1000, using periodic boundary conditions in order that finite size effects become less important. We start the simulations with an empty line, which will be filled according to the rules introduced in this chapter until the jamming coverage is reached. In fig.2.4 we show the pair distribution functions at jamming obtained for four different values of $\sigma$, $\sigma = 0., 0.16, 0.43, 1.015$, and 2.86, which correspond approximately to values of the incident angles $\alpha = 0^o, 31^o, 45.5^o, 60^o$, and $75^o$.

As shown in chapter1 (see fig.1.2), in RSA the pair distribution function is characterized by a fast decrease of correlations after a peak at a distance of about one diameter,the peak appearing because disks cannot adsorb closer than one diameter.

This peak becomes a logarithmic singularity at jamming. The most characteristic feature in the pair correlation functions for this new model is the appearance of a second peak. It is induced by the adsorption mechanism, which forbids that an incoming particle get closer than $1+\sigma$ at the right hand side of a preadsorbed disk. In fig. 2.4a, the second peak for $1+\sigma$, is hardly recognizable due to resolution of the plot. For $\sigma = 1$, this new peak should appear at a distance $r = 2$ from the reference disk, and then it coincides with the second rounded peak which exists in RSA. The interference of both peaks leads to a slower deay of the global peak in this region. On the other hand, the irreversible character of the deposition process leads to a decay of the correlations faster than in equilibrium, as already discussed for RSA)[37].

The behavior of the peaks in the pair distribution function, $g(r)$, at jamming can be understood from the analytic solution of the previous section. We will use the fact that, due to the new kinetics rules, if a particle is at a distance $r \leq 1+\sigma$ from the reference one, there can not be a second one in between. We have shown in chapter1 that in this case $g(r)$ coincides with the one-gap distribution function $G(r+1)$, which implies that the peaks originate from the distribution of nearest neighbors of the reference disk. The divergence of the peak at distance 1 has the form given in eq.(??), until $r = 1+\sigma$. Eq. (2.2.16) indicates that it diverges logarithmically, as in RSA[10][11], although with half its height (see eq.(1.1.9). The new peak at a distance $2+\sigma$ is given by the limiting value of $G_2(r)$. We have shown that it can be expressed in terms of the one-gap distribution function corresponding to smaller gaps, as shown in eq.(2.2.10). This implies that the second peak will exhibit the same divergent behavior as the peak at contact. On the other hand, this last equation shows that the peak is shifted by the density of gaps of length $1+\sigma$. This explains why the second peak is always higher than the one at $r = 1$. If $\sigma > 11$ then the pair distribution function is not equal to the one gap distribution function, but the singularity of $g(r)$ in the second peak has to be described by it, since the rest of the function is analytic.

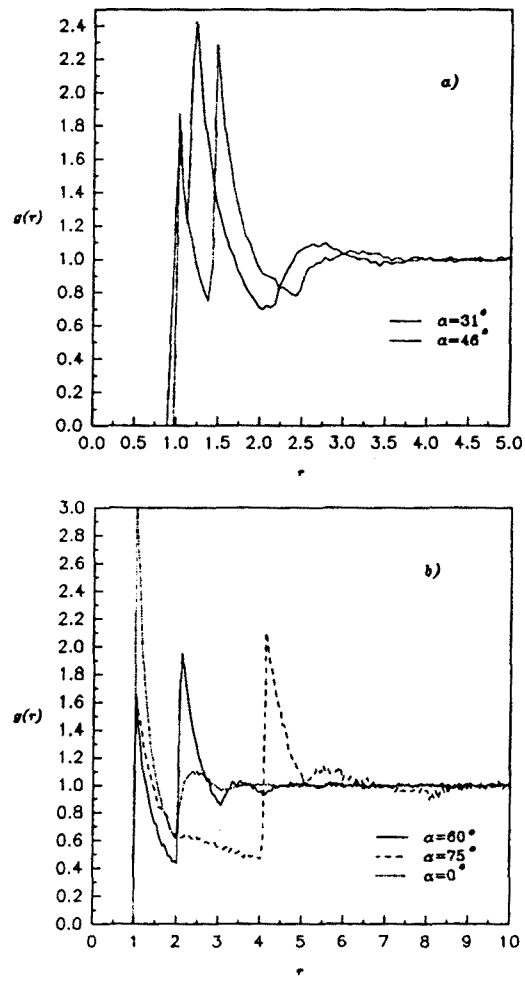


Figure 2.4: Pair distribution functions at jamming, for different values of the incident angle. a) 31° (—) and 45.5° (- - -),b) 0° ( ), 60° (—) and 70° (- - -).

## 2.3 Inclined Ballistic Deposition Model

As a second case, we will proceed to analyze an analogous model to the one introduced in the previous subsections (see fig.2.1a), in which adsorption obeys BM's rules[7]. As in BM, disks arrive sequentially to the line following straight trajectories. If they touch a preadsorbed particle, they are allowed to roll over it trying to reach the substrate, instead of being directly rejected. The difference of the model we will introduce in this section with respect to BM lies on the fact that now the trajectories of the incoming particles will not be perpendicular to the substrate. Rather, they will form an angle $\alpha$ with the normal, as shown in fig.2.5.a). BM is intended to describe the adsorption of heavy colloids in he presence of gravity fields[7], at leat in respect to its kinetics. Analogously, this model can describe the adsorption of the same suspension when an additional force parallel to the surface acts on the suspended particles.

Disks are sequentially launched at a certain height alomg an inclined trajectory. They move ballistically towards the substrate. If during its motion, the incoming disk does not overlap any preadsorbed particle, then it is irreversibly located at the corresponding position on the line. Otherwise, it will roll over the preadsorbed disk trying to reach the substrate along the steepest descent path. Only if it gets trapped during this motion and is unable to reach the line, it will be rejected.

In order to understand how particles will roll, let us focus on an incoming particle as the one depicted in fig.2.5a). We will consider that through the center of each adsorbed disk passes a straight line forming an angle $\alpha$ with the normal. In fig.2.5a, we call $\Gamma$ the line associated to the adsorbed disk 1. If the trajectory of the incoming particle is at the left of line $\Gamma$ upon touching disk 1, then the particle will roll towards the left hand side of particle 1, trying to reach the line keeping at contact with disk 1. If overlap is detected with a second adsorbed particle at the left of disk 1, the adsorbing particle cannot reach the substrate and is rejected. If the center of the incoming disk is at the right hand side of $\Gamma$ when touching disk 1, it will roll towards the right hand side of particle 1, until its trajectory becomes tangent to the adsorbed disk. At that point, it will continue its motion towards the line along the straight line $\Gamma'$ trying to reach the line. Note that $\Gamma'$ is parallel to $\Gamma$, and is the first line at the right of disk 1 such that an incoming disk with its center moving along it will not be

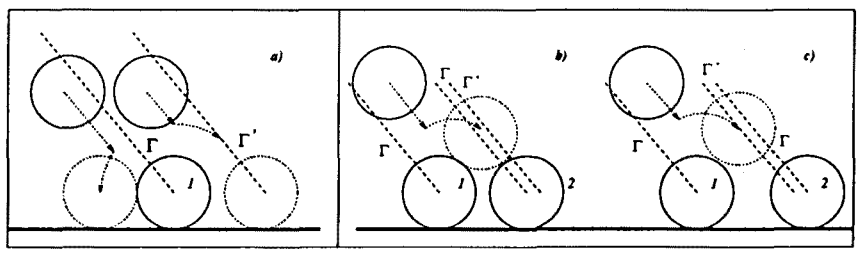


Figure 2.5: a)Disk arriving at the line in the presence of an adsorbed particle. b) and c) Different rolling mechanisms when two a particle arrives at the line in the presence of two preadsorbed disks separated a distance $l$.

modified by disk 1. In standard BM, a particle rolls to the rigth over the preadsorbed one until it reaches the line, while here, at some point the incoming disk leaves the contact with the adsorbed one. If no overlap is detected with a second disk, it will be irreversibly adsorbed on the line at a distance $1+\sigma$ from particle 1, as shown in Fig.2.5a. If overlap occurs with a second adsorbed disk at the right of particle 1, then one should look again if $\Gamma'$ is at the right or left hand side of the line $\Gamma$ corresponding to the second particle.

The lines $\Gamma$ will be also referred to as *separation lines* since they will determine towards which side of the overlapping adsorbed disk the incoming particle will roll. Note that in standard BM half of the incoming particles which overlap with an adsorbed disk will try to reach the substrate at its right hand side and half at its left hand side. Now, due to the fact that the separation line is inclined, a fraction $1/(2+\sigma)$ of the incoming particles that overlap a preadsorbed disk will roll to its left hand side, while a fraction $(1+\sigma)/(2+\sigma)$ will do it to its right. As we will see, this asymmetry in the deposition around a preadsorbed particle will influence both the coverage and the structure of the adsorbed layer.

Now, we will consider that the adsorbing disk arrives at the line in the presence of two adsorbed disks , separated by a gap of length $l$. As we will see, depending on their distribution, the incoming disk can roll towards the right hand side of both adsorbed particles, which constitutes a new adsorption mechanism appearnot present in BM.

We will concentrate on the situation of interest, in which the incoming disk rolls to the right of disk 1. If the gap $l$ is larger than $1+\sigma$, then the incoming disk will arrive at a distance $1+\sigma$ at the right of disk 1 without touching disk 2. If the gap is smaller, the incoming particle will overlap disk 2 before reaching the line. However, as shown in figs.2.5b and 2.5c it can either leave disk 1 before touching disk 2, or can overlap disk 2 before arriving at the line $\Gamma'$. When the incoming disk leaves its contact with particle 1, the distance between their centers is 1, and its direction is normal to the direction of $\Gamma'$ at which the incoming disk will move thereon. The most unfavorable situation is when the incoming disk also touches particle 2, so that the distance between their centers is also 1. This implies that the incoming disk will overlap disk 2 after leaving its contact with disk1 for gaps of length $\min(0, \frac{1-\sigma}{1+\sigma}) < l < 1+\sigma$, and that it will

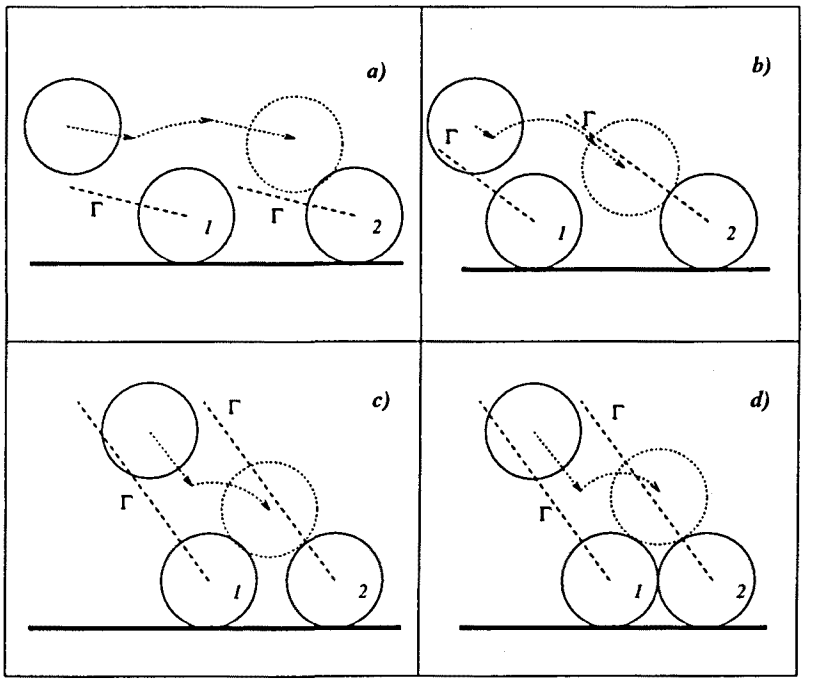


Figure 2.6: a) and b) Disk rolling to the left and to the right of the second disk, respectively, after having left the contact with disk 1. c) and d) Disk rolling to the left and to the right of the second disk, respectively, when it overlaps at the same time with both adsorbed disks.

touch both disks for gaps smaller than $\min(0, \frac{1-\sigma}{1+\sigma})$. This means, that the screening of disk 1 over disk 2 increases with $\sigma$, and that, in particular, for incident angles greater than 60° ($\sigma > 1$) an incoming particle cannot overlap two adsorbed disks at the same time.

If the incoming particle leaves disk 1 before touching disk 2, then it would arrive at the line at a distance $1 + \sigma$ from disk 1, after moving along a straight line. Since this trajectory is by construction parallel to the line $\Gamma$ of disk 2, the incoming disk will roll to the left of particle 2. Then, this will happen when $l > \sigma$. Otherwise, it will roll to the right of disk 2. However, it is important to note that we also have

the restriction that $l < (1-\sigma)/(1+\sigma)$, which implies that rolling to the right is only allowed for $\sigma > 1$ (or $\alpha > 45°$). Figures2.6a) and 2.6b) show both situations.

On the other hand, if the incoming disk overlap both disks at the same time, then its motion depends on the relative location of the center of the incoming disk with respect to the separation line $\Gamma$ of particle 2 (see figs.2.6c and 2.6d). One way to know how it will roll is to assume that the incoming disk reaches the wall following a straight line from the point in which it touches both disks. If the final point is at the right of the center of disk 2, then it rolls to the righ; otherwise, it rolls to the left. In terms of the gap length, one obtains that the incoming disk rolls to the right of particle 2 whenever $l < -1 + \frac{2}{1+\sigma}\sqrt{\sigma^2+2\sigma}$. Again, there exists the restriction that this kind of situation may appear as long as $l < \frac{1-\sigma}{1+\sigma}$, which implies that for $\sigma > -1+\sqrt{2}$ (or $\alpha > 45°$) all particles touching two adsorbed disk at the same time will roll necessarily to the right hand side of disk 2. In this case, we should also take into account that $l > 0$, which implies that for $\sigma < -1 + 2/\sqrt{3}$ (or $\alpha < 30°$) all particles in this situation will try to reach the line to the left of particle 2. Since they will not be able to reach it, will be rejected.

We have shown that for arrival angles $\alpha > 30°$, depending on the relative distribution of the adsorbed particles, the incoming disk may roll to the right of two consecutive disks. This mechanism is not present in BM and implies that the adsorption of a particle may depend on the distribution of three particles (or two gaps). Depending on the distance between the second and the third adsorbed disk, the incoming particle may also roll to the right of this third particle. This means that incoming disks may roll over a number of adsorbed particles before reaching the substrate, or being rejected. Then, for $\alpha > 30°$ the adsorption kinetics becomes non-local in the sense that the final position of a particle on the line is not restricted to the initial gap tried. In fig.2.7 we show a summary of the different rolling mechanisms for an incoming disk after having rolled at the right of a preadsorbed particle, when a second one is at the right on tha line at a distance $l+1$ from the first adsorbed particle. One can see that, when $\alpha < \pi/6$, all particles will roll to the left of disk 2. For larger angles, depending on $l$ particles will be allowed to roll either to the left or to the right of disk 2. On the other hand, if $\sigma > 1$, ( $\alpha > \pi/3$) the center of all particles rolling to the right of disk 1 will reach $\Gamma'$ before touching disk 2.

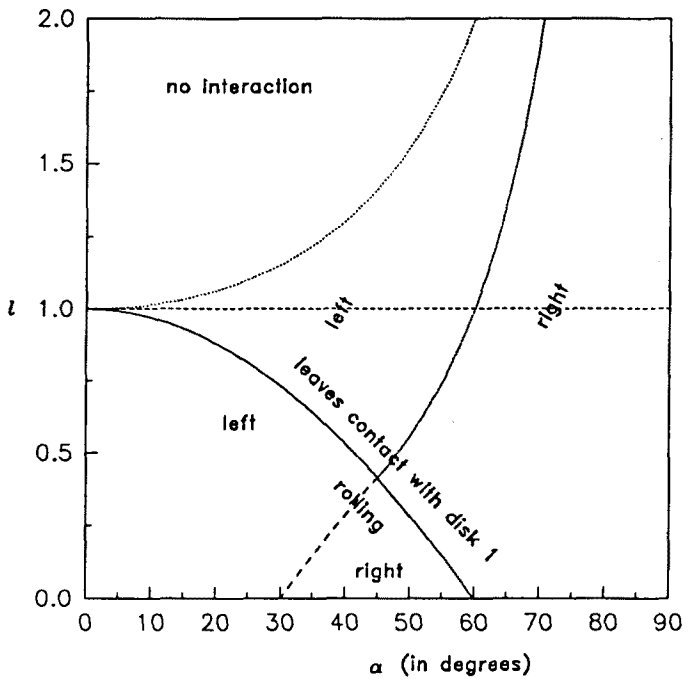


Figure 2.7: Different rolling mechanisms for a particle arriving along a direction forming an angle $\alpha$ with the normal, overlapping disk 2 at the right of disk 1 with which has interacted before. Disks 1 and 2 are separated a distance $1 + l$. In the figure, right and left means particle trying to reach the line at the right or left hand side of disk 2, respectively, and *rolling* means that it overlaps disks 1 and 2 at the same time, while *leaves contact with disk 1* means that at the right of that limiting curve, it rolls sequentially over both. If $l < 1$ the incoming particle is rejected if it rolls to the left (see text).

It is important to realize that due to this new non-local mechanism , when $\sigma \geq 1$ ($\alpha > 60^o$), all incoming particles will be able to reach the line (see fig.2.7). This implies that there will be no rejected particles, and that the coverage will increase linearly until jamming. Then, in this case, the function $\phi$, interpreted as the available line fraction is simply $\phi(\theta, \sigma) = H(\theta^{\infty}(\sigma) - \theta)$, with $H(x)$ being the Heaviside step function.

So far, we have not specified what happens to those particles which arrive along the separating line $\Gamma$ of disk 1. In standard BM this is neither specified, because it is irrelevant since only a fraction of zero measure of the incoming disks will follow this trajectory. In our models, the situation is more involved because a finite fraction of the particles overlapping a sphere will roll to its right trying to reach the line $\Gamma'$. If there is a second disk at a distance $l = \sigma$, then the line $\Gamma'$ of the preadsorbed particle at the left will coincide with the line $\Gamma$ of disk 2, which means that a finite fraction of overlapping particles will arrive along that separating line. Therefore, we have to decide whether those particles will turn to the right or to the left of disk 2. Since there will always exist an attractive interaction between the disks and the substrate, which makes it possible that the particles are irreversibly adsorbed at the positions at which they arrive, we have taken the convention that such particles arriving along the separating line will roll to the left of the second disk.

### 2.3.1 Analytic Solution

As in the inclined RSA, it is possible to find an analytic expression for certain physical quantities in this one-dimensional version of the model. The same tools used in standard BM[7] by introducing the distribution function of gaps can be applied now. However, these techniques make use of the shielding property of the kinetic 1-d models. The non-local adsorption mechanism introduced in the previous paragraph breaks down the shielding property, and, therefore, it is not possible to find an exact analytic expression for $\alpha > 30°$. We will restrict our analytical study to the inclined BM neglecting the non-local adsorption mechanisms, and we will compare these exact results with computer simulations to have an idea of the effect of these mechanisms in the overall behavior of the system. In order to account for the non-local kinetic mechanisms, new theoretical techniques should be introduced, and, in principle, only

approximated solutions can be expected.

Let us introduce the one-gap distribution function $G(l,t)$, expressed in the appropriate dimensionless variables introduced in chapter 1. In that chapter we have shown that there exists a singular contribution to $G(l,t)$ due to the rolling mechanism. Therefore, we expect that here the same contribution will exist. Instead of deriving equations for the global one-gap distribution function, we will write separately the evolution equation for the regular and the singular gaps. To this end, we decompose $G(l,t)$ as[12]

$$G(l,t) = g(l,t) + g_0(t)\delta(l) + g_1(t)\delta(l-\sigma) + g_2(t)\delta(l-\sigma+1)\theta(\sigma-1) \quad (2.3.26)$$

where $g(l,t)$ refers to the regular contribution to the gap distribution function, and $g_0(t)$ and $g_1(t)$ to the fraction of gaps of lengths 0 and $\sigma$, respectively. Note that the singular contributions are related to the minimum gap lengths, and that in our model, besides the fact that disks cannot overlap, we should take into account that an incoming particle cannot be closer than $1+\sigma$ at the left of a preadsorbed disk. Finally, $g_2(t)$ will only appear when $\sigma \geq 1$. This term takes into account that there exists a finite fraction of disks which will roll to the left of an adsorbed disk which has previously rolled to the right of an older adsorbed particle. This is due to our last assumption of the last paragraph referring to the particles which arrive along a separation line. It only appears for $\alpha > 60^\circ$ because for smaller angles there is no room for them at the left of the disk.

We will follow the same scheme followed to solved the generalized RSA model. Then, in order to derive the evolution equation for the one-gap distribution functions, we have to identify the different ways in which gaps of length $l$ are created and destroyed, according to the mechanisms introduced before.

Gaps of length smaller than $\max(1,\sigma)$ can only be created, as in the previous model. For the particular case $l=\sigma$ and $\sigma > 1$ they can be destroyed by particles rolling to the right of a second disk at a distance $1+\sigma$ from another disk. In this case, a gap of length 0 at the right of the adsorbing particle and another of length $\sigma-1$ at the left are created at a rate proportional to $1+\sigma$.

Gaps of length $\max(1,\sigma) < l < \sigma+1$, can be destroyed by rolling of incoming

particles over adsorbed disks at rate proportional to $1+l$. Two new gaps are created as a result,one of length 0 at the right of the adsorbing disk, and the other of lengt $l-1$ at the left.

Finally, gaps of length $l > 1+\sigma$ can be destroyed either by rolling or by direct adsorption. An incoming disk can roll over the disk which delimits the gap at its left. Then, at rate proportional to $1+\sigma$, two new gaps appear, one of length $\sigma$ at its left, and a second of length $l-1-\sigma$ at its right. An incoming particle may also roll to the left of the disk which delimits the gap at its right. Then, at a rate proportional to 1, two new gaps appear, one of length 0 at its right, and a second of length $l-1$ at its left. Direct destruction of the gap will happen at a rate proportional to $l-1-\sigma$, produncing a gap of length $l' \epsilon [0, l-\sigma-1]$ at its rigth, and a second of length $l-l'-1$ at its left. All these processes give a total rate of destruction $l-1$ for a gap of length $l$.

Note that in this model an incoming particle will touch 0, 1 or 2 disks before adsorbing. Then, we can also consider that the analytic model we present is an approximation to the real kinetics in which interactions with more than two disks are neglected. Then, this approximation is exact for $\alpha < 30^o$, where interactions with more than two particles are forbidden.

We can now proceed to find the evolution equation for the one-gap distribution functions. The dynamics will depend on whether $\sigma$ is greater or smaller than one. We have seen that in the first case a new singular adsorption mechanism appears.

Let us first consider the adsorption kinetics when $\sigma < 1$. In this case we will obtain an exact expression for small values of $\sigma$. We can write the evolution equations looking how a gap of length $l$ is destroyed and created from larger gaps. Each term accounts for one of these mechanisms, and is multiplied by the corresponding relative rate. We arrive at the set of equations

$$\begin{aligned} \frac{\partial g_I(l,t)}{\partial t} &= -(l+1)g_I(l,t) + (1+\sigma)g_I(l+1+\sigma,t) + g_I(l+1,t) + \\ &\int_{l+1}^{\infty} dl' g_I(l',t) + \int_{l+1+\sigma}^{\infty} dh' g_I(l',t) \qquad l \geq 1 \end{aligned} \tag{2.3.27}$$

$$\frac{\partial G_2(l,t)}{\partial t} = (1+\sigma)g_I(l+1+\sigma,t) + g_I(l+1,t) + \int_{l+1}^{\infty} dl' g_I(l',t) + \int_{l+1+\sigma}^{\infty} dl' g_I(l',t) \qquad \sigma < l < 1 \qquad (2.3.28)$$

$$\frac{\partial g_{III}(l,t)}{\partial t} = (1+\sigma)g_I(l+1+\sigma,t) + (l+2)g_I(l+1,t) + \int_{l+1+\sigma}^{\infty} dl' g_I(l',t) \qquad l < \sigma \qquad (2.3.29)$$

$$\frac{dg_0(t)}{dt} = \int_{1+\sigma}^{\infty} g_I(l',t)dl' + \int_{1}^{1+\sigma} (l'+1)g_I(l',t)dl' \qquad (2.3.30)$$

$$\frac{dg_1(t)}{dt} = (1+\sigma)\int_{1+\sigma}^{\infty} g_I(l',t)dl' \qquad (2.3.31)$$

where the first three equations define the regular contribution to the gap distribution function, according to the separation introduced in eq.(2.3.26), and the last two the singular component. Note that in this case $g_2(t)$ does not exist. As in the previous model, we have introduced the subscripts $I, II$ and $III$ to distinguish the regular contribution in the three domains in which the kinetic mechanisms are different. Eq.(2.3.27) takes into account that such gaps may be destroyed either by rolling over any of the limiting disks or directly, and that they can be created from larger ones either at the left or right of the incoming disk. Eq.(2.3.29) considers that gaps smaller than 1 and larger than $\sigma$ cannot be destroyed, but are created through the same mechanisms as the larger gaps. Finally, eq.(2.3.30) indicates that these gaps cannot be destroyed, and cannot created at the left of an incoming disk which adsorbs directly. It also considers that they can be created by rolling over the two disks which delimit the gap. The equations for the singular contributions take into account that gaps of length $1+\sigma$ can only be created by rolling at the right of a disk.

Eqs.(2.3.27)-(2.3.31) can be solved following the procedure we have introduced to solve the previous models. We should solve first the integro-differential equation for $G_1(l,t)$, and from it the rest of the equations become differential equations which can be solved. We always start from an empty line, and then the same initial condition for the one-gap distribution function applies here as well. To solve eq.(2.3.27) we introduce the "ansatz"

$$g_I(l,t) = t^2\alpha(t)F(t)e^{-(l+1)t} \qquad (2.3.32)$$

where $F(t)$ is the function obtained in the RSA model, eq.(2.2.7), and the dependence in $\sigma$ is implicit in both $F(t)$ and $\alpha(t)$. Introducing this expression for $g_I(l,t)$ in eq.(2.3.27), we derive an ordinary differential equation for $\alpha$, which has as solution

$$\alpha(t,\sigma) = \exp\left(2 - 2t - e^{-t} - e^{(1+\sigma)t}\right) \tag{2.3.33}$$

satisfying the initial condition that the line is empty. We can now also determine $G_2(l,t)$ and $g_{III}(l,t)$, as well as the singular contributions, as quadratures, by substituting eq.(2.3.32) in eqs.(2.3.28)-(2.3.31). One obtains

$$g_{II}(l,t) = \int_0^t \alpha(\tau)F(\tau)e^{-l\tau}\left[\tau^2 + \tau + (\tau^2(1+\sigma)+\tau)e^{-\sigma\tau}\right]\, d\tau \tag{2.3.34}$$

$$g_{III}(l,t) = \int_0^t \alpha(\tau)F(\tau)e^{-l\tau}\left[(l+2)\tau^2 + e^{-\sigma\tau}(\tau + (1+\sigma)t^2)\right]\, d\tau \tag{2.3.35}$$

$$g_0(t) = \int_0^t d\tau\alpha(\tau)F(\tau)\left[1 + 2\tau - e^{-\sigma\tau}(1 + (1+\sigma)\tau)\right] \tag{2.3.36}$$

$$g_1(t) = \int_0^t d\tau(1+\sigma)\tau\alpha(\tau)F(\tau)e^{-\sigma\tau} \tag{2.3.37}$$

Note that in the limit $\sigma \to 0$, the singular contributions $g_0$ and $g_1$ will coincide. The sum of both will then give the delta function characteristic of BM. On the other hand, the function $g_{III}$ dissapears when performing this limit. Therefore, the behavior for $l \to 0$ will differ depending on whether $\sigma$ vanishes or not. By letting the time go to infinity, one can see that in the jamming there are no gaps larger than 1.

We can now derive an expression for the time evolution of the coverage $\theta$. In chapter 1 we have pointed out that, due to the singular contributions to the one-gap distribution function of BM, the coverage cannot be calculated using the same method employed to obtain the coverage in RSA[7]. However, if the whole $G(l,t)$, including its singular points, is considered, then one gap corresponds to one particle[12]; therefore, using the first equality of eq.(1.1.10), and eq.(2.3.26) for the gap distribution function, we arrive at

$$\theta(t) = \int_0^t (1+2\tau)\alpha(\tau)F(\tau)\quad d\tau \tag{2.3.38}$$

which has the same form as the one obtained in standard BM, eq.(1.2.19), the dependence on $\sigma$ being now introduced through the definitions of $\alpha(t)$ and $F(t)$. Again, one can study the at short and long time behavior, giving

$$\theta(t) \sim t + \left(4 + 2\sigma + \sigma^2\right) \frac{t^3}{4} + \mathcal{O}(t^4) \tag{2.3.39}$$

Note that the effects of the inclination appear in the third power, since three particles are needed to make clear the rolling mechanisms. Note that the second power is missing because if only one particle is adsorbed on the substrate, all particles can reach the line. The asymptotic approach to the jamming is exponential, as in standard BM, its amplitude depending on the incident angle,

$$\theta^{\infty} - \theta(t) \sim \frac{e^{2-2\gamma}}{1+\sigma} \frac{e^{-2t}}{t} + \mathcal{O}\left(e^{-3t}\right) \tag{2.3.40}$$

The maximum fraction of the line covered with particles can be expressed as a quadrature,

$$\theta^{\infty}(\sigma) = \int_0^{\infty} (1+2t)\alpha(t)F(t)e^{-2t}\, dt \tag{2.3.41}$$

which can be calculated perturbatively as a power series of $\sigma$. To first order one obtains

$$\theta^{\infty} = \theta_{bm}^{\infty} - \left[\theta_{bm}^{\infty} + e^{2-2\gamma} \int_0^{\infty} \frac{1+3t+t^2}{t^2} e^{-3t-3e^{-t}-2E_1(t)}\, dt\right] \sigma + \mathcal{O}l(\sigma^2) \tag{2.3.42}$$

We will now study analytically the same model in which non-local effects have been neglected for arrival trajectories such that $\sigma > 1$. The results we will obtain will not describe all the processes that can take. We will concentrate in the jamming coverage in order to compare the result of this approximation with the results we have obtained from computer simulations.

We will follow the same analysis we have done for $\sigma < 1$. The only new thing we have to take into account is that there appear new adsorption mechanisms, as

explained at the beginning of this section. The decomposition (2.3.26) still holds, with a new singular contribution with respect to the previous region. One can derive again the evolution equations,

$$\frac{\partial g_I(l,t)}{\partial} = -(l+1)g_I(l,t) + (1+\sigma)g_I(l+1+\sigma,t) + g_I(l+1,t) + \int_{l+1}^{\infty} dl' g_I(l',t) + \int_{l+1+\sigma}^{\infty} dl' g_I(l',t) \quad l \geq \sigma \tag{2.3.43}$$

$$\frac{\partial g_{II}(l,t)}{\partial t} = (1+\sigma)g_I(l+1+\sigma,t) + (l+2)g_I(l+1,t) + \int_{l+1+\sigma}^{\infty} dl' g_I(l',t) \quad \sigma - 1 < l < \sigma \tag{2.3.44}$$

$$\frac{\partial g_{III}(l,t)}{\partial t} = \int_{l+1+\sigma}^{\infty} dl' g_I(l',t) \quad (1+\sigma)g_I(l+1+\sigma,t) \quad l < \sigma - 1 \tag{2.3.45}$$

$$\frac{dg_0(t)}{dt} = \int_{1+\sigma}^{\infty} g_I(l',t)dl' + \int_1^{1+\sigma} (l'+1)g_I(l',t)dl' + (1+\sigma)g_1(t) \tag{2.3.46}$$

$$\frac{dg_1(t)}{dt} = (1+\sigma)\int_{1+\sigma}^{\infty} g_I(l',t)dl' - (1+\sigma)g_1(t) \tag{2.3.47}$$

$$\frac{dg_2(t)}{dt} = (1+\sigma)g_1(t) \tag{2.3.48}$$

which, as before, have been constructed by looking which processes contribute to create and destroy gaps in the different intervals. Note that eq.(2.3.43) is equal to eq.(2.3.27), which means that the form of $G_1(l,t)$ is the same for all the values of $\sigma$, varying only its domain of validity. Then, we can substitute eq.(2.3.32) in eqs.(2.3.44)-(2.3.48), and by solving the differential equations, we can obtain the whole one-gap distribution function. As before, integrating $G(l,t)$ in $l$, we can know the evolution of the fraction of the line covered by particles,

$$\theta(t) = \int_0^t e^{-(1+\sigma)t}[\alpha(\tau)F(\tau)(1+(1+\sigma)\tau)+$$

$$(1+\sigma)^2 \int_0^\tau \tau' \alpha(\tau') F(\tau') e^{-\tau'} d\tau' \Big] d\tau \qquad (2.3.49)$$

It is worth pointing out that in this region, the kinetics predicted by this solvable model is not consistent. As we have mentioned at the beginning all incoming disks will be able to roll over all the disks it needs until it finds room on the line. In these kinetics models the scale of time is the arrival of particles to the substrate, and it is fixed. Therefore, the coverage will increase linearly in time until jamming. The jamming coverage in this model is obtained as a quadrature from eq.(2.3.49) by letting the lime go to infinity. Then, this limit, together with eq.(2.3.41), gives the jamming coverage as a function of the incident angle $\alpha$, for the solvable model.

We have performed numerical simulations of the adsorption of disks of diameter one on a line of length 1000, using the rules of the inclined BM introduced in this section, in which incoming disks may roll over as many disks as they are allowed before either reaching the substarte or being rejected. We start with an empty line, which is sequentially filled until jamming is achieved. In fig.2.8 we show the jamming coverage as a function of the angle of arrival of disks, and we compare with the analytic expressions, eqs.(2.3.41) and the limit of eq.(2.3.49).

As a major feature, one can see that despite the approximate character of the analytic solution for $\sigma > \pi/6$, it reproduces quite well the jamming coverage, except in the neighborhood of $\sigma = 1$. When increasing the incident angle $\alpha$ from 0, initially one observes a decrease of the jamming, indicating that a finite fraction of particles roll at the right of preadsorbed spheres, creating gaps of length $\sigma$ which cannot be covered by further particles. For angles greater than $\pi/6$, particles can roll over preadsorbed spheres. This mechanism increases the probability that a gap of length $\sigma$ is produced, and this fact explains that the jamming coverage obtained from the simulations are systematically smaller than the ones obtained from the approximate analytic expression. Close to $\sigma = 1_-$, the jamming has decreased a 20% with respect to standard BM. At $\sigma = 1_+$, a jump in the jamming is observed. The jump in the coverage is reproduced properly by the analytic model, which means that the increase is basically due to the possibility of the incoming particles to adsorb at a distance $\sigma$ at the right of a disk, given that a doublet of particles preadsorbed at a distance $1+\sigma$ exists. Therefore, the magnitude of the jump equals the fraction of particles which have reached the line according to this mechanism.It is $(1/2)\int_0^\infty u\alpha(u)F(u)e^{-3u}du$

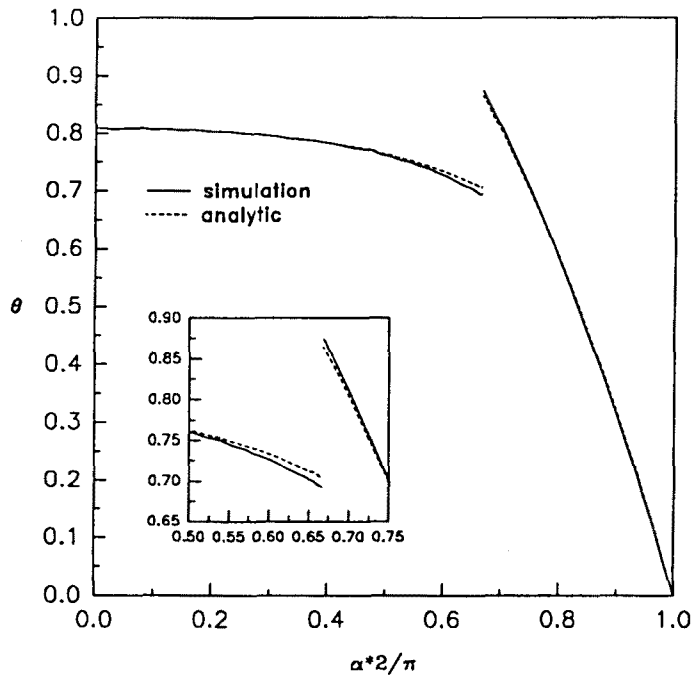


Figure 2.8: Jamming limit of the inclined BM. The line corresponds to the analytic solution, which is approximate for $\alpha > \pi/6$, and the dotted line to the simulation results, in which all possible processes affecting the arrival of spheres at the substrate have been taken into account. In the inset, an enlargment of the region where the discontinuity takes place.

for the analytic model, and the difference in the magnitude of the jump between the simulations and the analytic model is equal to the fraction of particles which have rolled over more than one preadsorbed sphere before reaching the line. For angles larger than $60^o$ a fast decrease of the coverage is observed. In this region all incoming particles reach the line, and moreover, rolling at the right of an adsorbed disk is the most favourable event, which tends to create larger gaps.

We have also observed in the simulations which has been the average last movement of the incoming disks. In fig.2.9 we show the fraction of particles which arrive at the line directly, after having rolled the last time to the right, and those which have done it to the left of a preadsorbed particle. For $\alpha < 30^o$, the variations are simply due to the fact that rolling to the right is a factor $1/\cos\alpha$ most probable than doing it to the right. At $\alpha = 30^o$, the non-local mechanism starts to appear, favouring rollings to the right, and both mechanisms are equivalent. Since more particles arrive at the line rolling, the fraction which do it through direct adsorption decreases. At $\alpha = 60^o$, particles rolling at the left on a pair are now accepted. This produces a large increase in the fraction of particles which arrive rolling to theleft, which is directly related to the fraction of pairs present on the substrate. The change in the structure also favors that particles arrive rolling to the right.

### 2.3.2 Structure of the Adsorbed Layer

The numerial simulations we have performed to study the kinetic process until jamming enable us to study also the pair distribution function of disks on the substrate. As in BM, now the pair distribution function consists of a regular part and a series of delta functions. In BM, these delta functions appear at distances multiple of the diameter, indicating the formation of clusters. In fig.2.10a, we have depicted the function at jamming for two values of $\sigma = 0.165, 1.015$, which correspond approximately to inclination angles of $\alpha = 30^o$ and $\alpha = 60^o$, respectively. It can be seen that, besides the peaks at multiples of the diameter, a number of new peaks appear. The peaks observed correspond again to clusters of particles, which originate from the rolling mechanisms. The separation between disks in a given cluster is 1 or $1+\sigma$. Therefore, the number of peaks increases at distances in multiples of the diameter, since particles can be distributed in two different sets of lengths which are incommen-

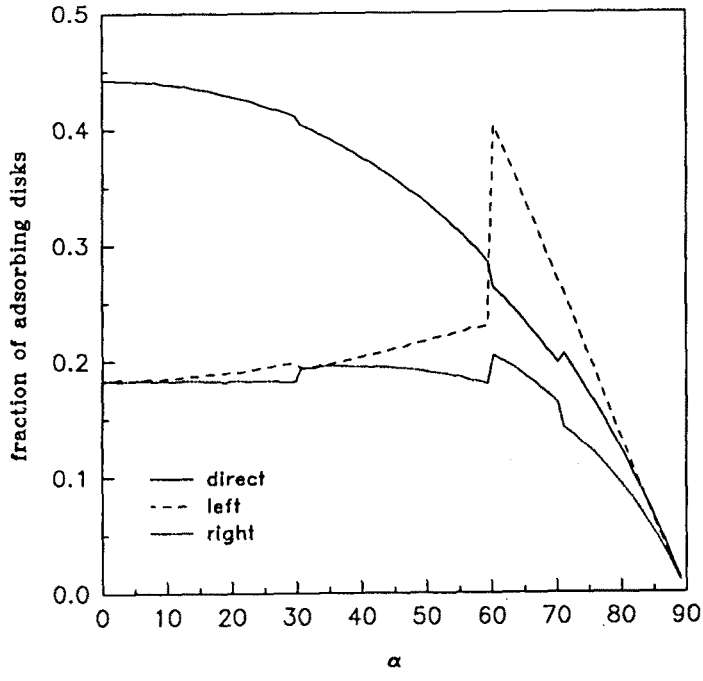


Figure 2.9: Fraction of particles which have arrived at the line: (- - -) rolling to the left, (—) rolling to the right.

surable when $\sigma$ is irrational. For example, for $\sigma = .165$, we observe two peaks near $r = 1$, corresponding to separations $r = 1$ and $r = 1 + \sigma$, three peaks near $r = 2$, corresponding to distances $r = 2$, $r = 2 + \sigma$ and $r = 2(1 + \sigma)$, and so on. The relative areas under the peaks are equal to the relative probability for each configuration of disks. A qualitative different structure is observed when $\sigma = 1$. In this case, both kinds of distances are commensurable, so when two particles are separated by $1 + \sigma$, there is exactly enough room for another particle. Then, an ordered sequence of peaks is obtained, showing a much more locally ordered substrate. Note that due to the instrinsically stochastic nature of the process, the height of the peaks decay with the distance. One expects to have locally higly ordered structures separated by some sort of domain walls.

In fig.2.10b) we have shown the pair distribution function for $\sigma > 1$. In this case the number of peaks increases also due to the new singular contribution, which introduces a new singular length, $\sigma$, for particles which roll in a doublet. It should be noted that the larger the value of $\sigma$, the more ordered the structure of the adsorbed layer, the reason being that when increasing $\sigma$, the probability of being at a distance $1 + \sigma$ increases relative to that at a distance 1 from a preadsorbed disk.

# Appendices

## 2.A Generalized RSA inclined model

An obvious way to generalize the inclined RSA model developed in this chapter is to introduce a new exclusion length $\sigma'$. Then, an incoming disk of diameter one overlaps with an adsorbed disk if the distance between their centers is smaller than $1 + \sigma$ if the incoming disk is at the right hand side of the adsorbed particle, and if it smaller than $1 + \sigma'$ otherwise. To be specific, we will assume $\sigma > \sigma'$.

We can deduce the evolution equations for the one-gap distribution functions in a way analogous to the RSA model solved in the main text. We have to take into account that now gaps smaller than $1+\sigma+\sigma'$ cannot be destroyed because an incoming disk whose center lies in such a gap is bound to overlap with one of the disk which

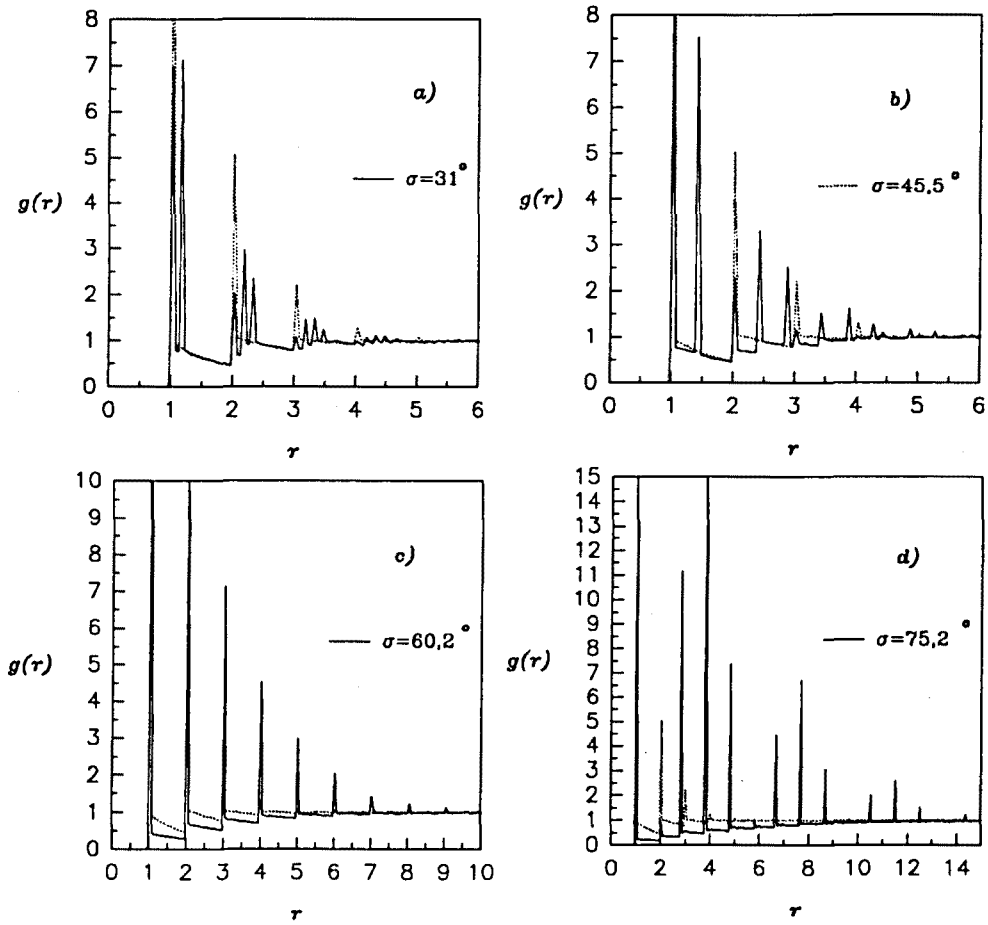


Figure 2.10: Pair distribution function at jamming for the inclined BM for different values of the arrival angle. a) (—) $\alpha = 30°$, (- - -) $\alpha = 60°$. b) (—) $\alpha =$ .

delimit the gap. Moreover, there are no gaps smaller than $\sigma'$ because $1+\sigma'$ is the closest distance at which two disks are allowed to approach. Finally, gaps of length $l$ larger than $1+\sigma+\sigma'$ are destroyed at a rate proportional to $l-1-\sigma-\sigma'$ and two new gaps are created in such a process, one of length $l'\epsilon[\sigma', l-1-\sigma]$ at the right, and another of length $l-l'-1$. According to these mechanisms, the evolution equations for the one-gap distribution function are

$$\frac{\partial G_1(l,t)}{\partial t} = -(l-1-\sigma-\sigma')G_1(l,t) + \int_{l+1+\sigma}^{\infty} G_1(l',t)\,dl' + \int_{l+1+\sigma'}^{\infty} G_1(l',t)\,dl' \quad l > 1+\sigma+\sigma' \tag{2.A.50}$$

$$\frac{\partial G_2(l,t)}{\partial t} = \int_{l+1+\sigma}^{\infty} G(l',t)\,dl' + \int_{l+1+\sigma'}^{\infty} G(l',t)\,dl' \quad \sigma < l < 1+\sigma+\sigma' \tag{2.A.51}$$

$$\frac{\partial G_3(l,t)}{\partial t} = \int_{l+1+\sigma}^{\infty} G(l',t)\,dl' \quad \sigma' < l < \sigma \tag{2.A.52}$$

where the notation $I, II, II$ has the same meaning as in the previous sections. We will be interested in the kinetics of this system when initially the line is empty. Then, we can solve the integro-differential equation (2.A.50 ) making the "ansatz"

$$G_1(l,t) = e^{-(l-1-\sigma-\sigma')t}\tilde{F}(t) \tag{2.A.53}$$

Substituting this expression in eq.(2.A.50 ), and solving the ordinary differential equation for $\tilde{F}(t)$ gives

$$\tilde{F}(t) = \frac{e^{-2\gamma}}{(1+\sigma)(1+\sigma')} e^{-E_1((1+\sigma)t)-E_1((1+\sigma')t)} \tag{2.A.54}$$

Once $G_1(l,t)$ is knwon, it can be used to determine the gap distribution function of the smaller gaps. In this case we get

$$G_2(l,t) = \int_0^t \frac{\tilde{F}(\tau)}{\tau}\left[e^{-(l-\sigma')\tau} + e^{-(l-\sigma)\tau}\right] d\tau \tag{2.A.55}$$

$$G_3(l,t) = \int_0^t \frac{\tilde{F}(\tau)}{\tau} e^{-(l-\sigma')\tau}\, d\tau \qquad (2.A.56)$$

$$(2.A.57)$$

As expected, $G_2(l,t)$ can be expressed in function of $G_3(l,t)$, similarly to the additivity property eq.(2.2.10). In this case

$$G_2(l,t) = G_3(l,t) + G_3(l-\sigma+\sigma',t) \qquad (2.A.58)$$

This means that, again, at jamming both $G_{iii}(l,t)$ and $G_2(l,t)$ will exhibit the same logarithmic divergence at $l=\sigma$ and $l=\sigma'$.

The coverage as a function of time can be obtained by using the fact that one gap corresponds to one particle. One arrives at

$$\theta(t) = \int_0^t \tilde{F}(\tau)\, d\tau \qquad (2.A.59)$$

which is formally equivalent to eq.(2.2.19), and expresses the fact that in this model $\tilde{F}(t)$ is the available line fraction.

# References


[1] J. J. Ramsden, Phys. Rev. Lett. **71**, 295 (*1993*); J. Stat. Phys. **73** 853 (*1993*).

[2] J. Sjollema and H.J. Busscher, Colloids Surfaces **47**, 337 (*1990*).

[3] T. Dabros and T.G.M. Van de Ven, Int. J. Multiphase Flow **18**, 751 (*1992*).

[4] B. Widom, J. Chem. Phys. **44**, 3888 (*1966*)

[5] P. Schaaf and J. Talbot, Phys. Rev. Lett. **62**, 175 (*1989*).

[6] G. Tarjus, P. Schaaf and J. Talbot, J. Stat. Phys. **63**, 167 (*1991*).

[7] J. Talbot and S. Ricci, Phys. Rev. Lett. **68** 958 (*1992*).

[8] D. Boyer, J. Talbot, G. Tarjus, P.R. Van Tassel and P. Viot, Phys. Rev. E **49** 5525 (*1994*).

[9] B. Bonnier, D. Boyer and P. Viot, J. Phys. A **27**, 3671 (*1994*).

[10] Y. Pomeau, J. Phys. A **13**, L193 (*1980*).

[11] E.L. Hinrichsen, J. Feder and T. Jossang, J. Stat. Phys. **44**, 793 (*1986*).

[12] P. Viot, G. Tarjus and J. Talbot, Phys. Rev. E, **48** 480 (*1994*).

[13] A. Rényi, Publ. Math. Inst. Hung. Acad. Sci., **3**, 109 (*1958*) (translated in Selected Transl. Math. Stat. Prob. **4**, 203 (*1963*)).

# Chapter 3

# Hydrodynamic Interactions and the Adsorption Process

The models presented in the previous chapters allows one to obtain precise results on the behavior of the model, with a thorough understanding of the essentials controlling the different aspects of the adsorption process. However, we have shown in the previous chapter that there exists a close connection between the adsoprtion mechanisms and the imposed conditions on the bulk transport. These effects, however, have to be introduced in a simplified way in these models and therefore, it is not clear a priori that some of the features which are not considered may have a significant influence in the adsorption. Only through a detailed study of the transport mechanisms, incorporating appropriately the behavior of the particles at the solid surface, it is possible to elucidate which are the different aspects which will be important.

In this chapter we will analyze in detail the influence of the bulk transport to the surface, taking into account the effects of hydrodynamic interactions on the adsorption colloidal particles when diffusion is negligible, considering both the rate of arrival of particles to the surface, and the local structure of the adsorbed layer which is formed as a result of this process. We will show how these interactions affect the transport of suspended objects when they come close to the surface or other particles, and will

compare the results with the predictions of the kinetic model BM, which only takes into account the geometric aspects of the adsorption process.

## 3.1 Nature of hydrodynamic interactions

The motion of small particles suspended in a viscous incompressible fluid depends on the viscous transport of the host fluid. Moreover, due to the viscosity, the fluid exerts a friction force on the suspended particle so that a moving particle attains almost instantaneously a terminal velocity. This resistive force is linear with respect to the instantaneous particle velocity if the Reynolds number characterizing fluid motion is vanishingly small[1]. This kind of fluid typically describes the motion of particles of sizes not larger than a few microns in common solvents[1]. In this situation, the fluid velocity field obeys the linearized Navier-Stokes equation, a linear diffusion-like differential equation. This linearity ensures that the velocity of the moving particles will be proportional to the force exerted on it.

Then, in general, the frictional force that the fluid exerts on a particle which moves at velocity $\vec{u}$ is written as $\vec{\vec{\xi}} \cdot \vec{u}$. The proportionality constant is called the *friction* coefficient, $\vec{\vec{\xi}}$, and it depends not only on the mass of the particle, but on its particular geometry. For a sphere of radius $a$ in a fluid of viscosity $\eta$, one has the well-known Stokes law, $\vec{\vec{\xi}} = 6\pi\eta a \vec{\vec{1}}$, but there exists no exact expression for the friction coefficient of an object of a general shape. As a consequence of this friction force, if we want that a particle moves in a fluid at constant velocity, we have to exert an force in the direction of the motion of the particle, which, due to the absence of inertial effects, is equal in magnitude and opposite in sign to the frictional force. The external force is necessary in order to maintain the transport of momentum towards the fluid induced by the motion of the particle. For an incompressible fluid, a force acting on a point induces a velocity field which decays slowly, as a power law with the distance from the point where the force is applied. This slow decay is due to the fact that velocity perturbations have no particular lengthscale when the Reynolds number is zero.

[1]Non zero Reynolds numbers appear when inertial motion in the host fluid is not negligible in front of the viscous relaxation of the perturbations caused by the presence of the particles

If a second particle is suspended in the fluid, its motion will be influenced by the perturbations in the velocity field induced by the motion of the first particle. This means that even in the absence of any other interaction forces, both particles interact through the host fluid. This interaction mediated by the solvent and due to the motion of the particles is called *hydrodynamic interaction.* The friction force is again in this case proportional to their velocity, but now the friction becomes a tensor which depends both on the geometry of both particles and on their relative position in space[2]. Moreover, new crossed friction tensors appear because the force on particle 1 will not only depend on its velocity, but also on the velocity of particle 2. According to these ideas, if we consider two equal spheres, in order that they move with center of mass velocities $U_1$ and $U_2$, and rotating with angular velocities $\omega_1$ and $\omega_2$, respectively, forces $\vec{F}_1$ and $\vec{F}_2$ and torques $\vec{T}_1$ and $\vec{T}_2$ should be applied such that

$$\begin{pmatrix} \vec{F}_1 \\ \vec{F}_2 \\ \vec{F}_3 \\ \vec{F}_4 \end{pmatrix} = - \begin{pmatrix} \vec{\vec{A}}_{11} & \vec{\vec{A}}_{12} & \vec{\vec{B}}_{11} & \vec{\vec{B}}_{12} \\ \vec{\vec{A}}_{11} & \vec{\vec{A}}_{12} & \vec{\vec{B}}_{11} & \vec{\vec{B}}_{12} \\ \vec{\vec{B}}_{11} & \vec{\vec{B}}_{12} & \vec{\vec{C}}_{11} & \vec{\vec{C}}_{12} \\ \vec{\vec{B}}_{12} & \vec{\vec{B}}_{22} & \vec{\vec{C}}_{12} & \vec{\vec{C}}_{22} \end{pmatrix} \cdot \begin{pmatrix} \vec{U}_1 \\ \vec{U}_2 \\ \vec{\omega}_1 \\ \vec{\omega}_2 \end{pmatrix} \tag{3.1.1}$$

where the matrix is called the *generalized resistance matrix*, whose wlwments are the matrices, $\vec{\vec{A}}_{ij}, \vec{\vec{B}}_{ij}, and \vec{\vec{C}}_{ij}$, which depend on the relative distance between the two spheres. These equations are valid only for a quiescent fluid. If there exists an external homogeneous flow, however, replacing in the last equation the velocities of the particle by its relative velocity respect the unperturbed ones, then it is still valid. We have also used the symmetry properties between. The different elements of the friction tensors satisfy symmetry properties derived from Onsager's relations, which permit to relate the crossed terms[1]. For general geometries of the objects, analytic expressions for the friction tensors are not known. In fact, the determination of these coefficients requires in principle the solution of the flow field equation with the appropriate boundary conditions on the surface of the objects. For the special case of two spheres, Jeffrey and Onishi[3] have given analytic expressions for the different friction tensors for any separations between the spheres, but for many spheres, the corresponding expressions are only known in series form. For example, in the specific case of interest in this chapter in which sphere 2 is kept at rest by applying forces

and torques, and on particle 1 no external torques are exerted, its motion is governed by the equation

$$-\vec{F}_1 = \left(\vec{\vec{A}}_{11} - \vec{\vec{B}}_{11} \cdot \vec{\vec{C}}_{11}^{-1} \cdot \vec{\vec{B}}_{11}\right) \cdot \vec{U}_1 \equiv \vec{\vec{\xi}}_{eff} \cdot \vec{U}_1 \tag{3.1.2}$$

which has been obtained by combinig the appropriate equations of (3.1.1). $\vec{\vec{C}}^{-1}$ means that the inverse of the matrix is considered. The whole combination of tensors can be interpreted as if sphere 1 was alone, but moving with an effective friction tensor, $\vec{\vec{\xi}}_{eff}$. Note that due to linearity, translational motion is decoupled from rotational , which in this case simply reads

$$\vec{\omega}_1 = -\vec{\vec{C}}_{11}^{-1} \cdot \vec{\vec{B}}_{11} \cdot \vec{U}_1 \tag{3.1.3}$$

The explicit expressions for the friction tensors are given explicitly in appendix 3.A, after Jeffrey and Onishi[3]. The inverse of the friction tensor, called the mobility tensor, $\vec{\vec{\mu}}$, satisfies $\vec{\vec{\mu}} \cdot \vec{\vec{\xi}} = \vec{\vec{\xi}} \cdot \vec{\vec{\mu}} = \vec{\vec{1}}$, and is the proportionality factor relating the velocity of the particle to the external force imposed.

Hydrodynamic interactions are not additive as a consequence of the slow decay of perturbations of the velocity field. Then, if a third particle is suspended in the fluid, the expressions obtained for the friction tensors in the two-particle case cannot be used to construct the new friction tensors. Rather, the global problem including the three particles should be solved at once. Due to the complexity that this treatment requires, there exists no analytic expression for the friction tensors for more than two spheres. Basically all the analytic results up to date consist of perturbative calculations for far apart spheres. Expressions for the friction tensors, or their inverse mobility tensors, have been obtained either using the method of reflections[2], which require the knowledge of the velocity field everywhere, or using the so-called induced force method[4], where an appropriate inclusion of the boundary conditions can avoid the calculation of the fluid velocity field everywhere in space. This method has been applied frutifully to determine the friction coefficients of cylinders[5] and of general axisymmetric objects[6], and has been used to describe the motion of drops in the

presence of external gradients, when the fields at the surface of the drop are coupled through general linear laws[7], although always in the low density regime.

These expressions for the frictions obtained for distant particles, however, cannot be applied when two spheres come close, and therefore, they are then of restricted use when applied to the study of the dynamics of suspensions. When two spheres are close together, their relative motion is controlled by the fluid flow in the gap between them giving rise to strong lubrication forces, because they cannot overlap. This is basically a two-body problem, even in the presence of more suspended spheres, and it is described by lubrication theory[8]. There exist, however, no perturbative analytic expressions for the whole range of separations for more than two spheres, which are the kind of expressions of interest in the study of the dynamics of non-dilute suspensions.

We will be interested in the motion of spheres close to a wall. From the point of view of hydrodynamic interactions, a wall plays an analogous role as a second spherem, in the sense that it will modify the friction tensors of the moving sphere. However, due to the different geometry, also different techniques have been developed to find explicit expressions for the corresponding friction tensors. In principle, a set of equations equivalent to (3.1.1) can be written, where now the subindex 2 will refer to the wall. However, since it will not move, it is usually directly rewritten in terms only of the forces and velocities acting on the sphere, by defining effective friction tensors. In the absence of external torques one simply has

$$-\vec{F}_1 = \vec{\vec{\xi}}^{w}_{eff} \cdot \vec{U}_1 \tag{3.1.4}$$

where the superscript $w$ in the effective friction tensor is introduced to avoid confusion with the tensor introduced in eq.(3.1.2). In appendix 3.A we give the analytic expressions of the different functions entering $\vec{\vec{\xi}}^{w}_{eff}$ which will be used later on. There exists no exact solution for the effective friction tensor at any separation except for the perpendicular motion of a sphere relative to a plane wall[9]. For the parallel motion, there are perturbative solutions very close[10] and far away from the wall[2]. More recently, Perkins and Jones[11] have obtained expressions for the mobility tensor perturbatively for a sphere away from the wall. However, they have calculated enough terms in the series so that their expressions are valid up to almost touching.

Beenakker and Mazur[12], using the induced force method, have also obtained perturbative expressions for the mobility of N spheres in the presence of a wall. Their approach, however, is only valid if all the spheres are far away from it, and then these results are more useful in the study of sedimentation than to consider the dynamics close to a surface. Vasseur and Cox[13] have also analyzed the sedimentation of two spheres parallel to a wall. We are interested, however, in the motion of a sphere close to a substrate when a second one is already fixed at the surface. Up to now, there exists no analytic expression for the friction tensors of this three body problem. Only numerical studies based on the boundary element method have been performed to study the trajectories of an incoming sphere close to an adsorbed one[14].

We have started to implement the induced force method to obtain expresions for the friction coefficients of spheres in the presence of a wall. If the sphere is far from the wall, we have recovered the results by Brenner[9]. We have incorporated the velocity field propagator which incorporates the boundary condition of stick at the wall. In this way, the problem reduces to the study of a single sphere, instead of being a two body problem, involving both the sphere and the wall. In order to obtain the corresponding expression for the friction coefficient when the sphere is close to the wall, we have to take into account that the force which the fluid exerts on the particle is not homogheneous, and has a singularity in the region closest to the wall. An accurate description of the force distribution in this region, which can be obtained from lubrication theory, is crucial to obtain consistent expressions for the friction coefficients[15]. The advantage of this method is that, once developed, would allowed to deal also with the problem of two spheres close to the wall, where there is a lack of analytic results.

Besides the numerical methods used to evaluate friction coefficients of different kind of objects[16], in the last decade a number of simulation techniques have been developed to study the dynamics of suspended particles incorporating hydrodynamic interactions in a more or less exact fashion. Bossis and Brady[17] introduced a method analogous to molecular dynamics to simulate the trajectories of colloidal particles, in which the global friction tensors are constructed assuming pairwise additivity of hydrodynamic interactions. Later, they coined the term Stokesian dynamics to denote a generalized simulation technique in which the non-additive character of hydrodynamic interactions was introduced to some extent as well as diffusion[18], and have

applied it to study the rehology of suspensions[19]. The dynamics of colloids when Brownian motion is relevant has also been considered within the framework of Brownian Dynamics[20], although hydrodynamic interactions here are introduced in a more simplified way, without considering lubrication effects. More recently, Lattice Gas Cellular Automata and Lattice Boltzmann techniques, which are more powerful computationally, have been combined with the method introduced by Brady and Bossis to study the sedimentation of interacting spheres[21]. Hybrid methods in which the singular part of the friction tensor associated to the lubrication forces is included analytically, have been developed to simulate highly concentrated suspensions[22][23]. Bafaluy *et al.* have studied the effect of hydrodynamic interactions on the adsorption of Brownian particles at low coverages, using a refined version of Brownain dynamics [24]. Then, the effect of hydrodynamic interactions in the diffusion coefficient should be considered.

Due to the absence of exact analytic expressions for the friction tensors when a number of particles are close to the wall, we will make use of numerical simulations in order to study the effects of hydrodynamic interactions on the adsorption of colloidal particles, by implementing them in an appropriate approximate way.

## 3.2 Hydrodynamic Effects in the Adsorption of Large Colloidal Particles

We will center our attention in the case of large or heavy hard spheres, whose motion is characterized by a large Péclet number, $Pe$, comparing gravitational and thermal energies, $Pe = 4\pi\Delta\rho a^4 g/(3k_BT)$, where $\Delta\rho$ is the difference between the density of the object and that of the host fluid, $a$ the typical size of the particle, and $g$ the gravity acceleration. This study is interesting because it allows to study the effect of transport in an adsorption situation in the opposite case of that considered up to know[24]. Moreover, in the limit of heavy particle adsorption, BM has been introduced as an adequate model to describe these adsorption processes[25], and there exist recent experimental result on the adsorption of melamine particles which have shown discrepancies with BM results[26]. Finally, we will consider hard spheres to avoid

other interactions which could mask the role played by hydrodynamic interactions on adsorption kinetics.

We are interested in the process in which initially the wall is empty. Particles come to the wall due to the action of an external force which acts perpendicular to the substrate, to which we will refer to as the gravity force, and when they touch the line are irreversibly adsorbed at that position, without allowing any further movement. This adsorbed particle will influence the motion of the spheres which arrive later at the substrate, and in this way the exclusion volume effects at the interface will interfere with the transport mechanism of the spheres to the substrate.

We will first study the adsorption on a line. Although this corresponds to an unrealistic experimental situation, this idealized model will be useful to introduce in a simpler way the techniques we have used, and will serve to show the characteristic features introduced by hydrodynamic interactions, and compare in detail with the kinetic model. Afterwards, we will on its two dimensional version, and will compare with experimental results.

### 3.2.1 One-dimensional Model

In this model, the substrate is one-dimensional, and a dilute quiescent suspension is in contact with it. The particles suspended in the fluid will move through it due to the presence of an external field perpendicular to the line and, if during their motion they touch the surface, they will irreversibly adsorb at that position as a result of strongly attractive short-range substrate-particle interactions. We will restrict ourselves to the case of high Péclet number particle motion for the reasons explained at the beginning of the section, which implies that the Brownian motion of the particles in the fluid can be neglected with respect to the effect of the external field. However, due to the fact that the typical particle size is of a few tens of microns, the Reynolds number associated to their motion is negligible. Although the bulk solution is considered dilute, and therefore the motion of suspended particles will not depend on their relative distribution, the interactions with the adsorbed particles are relevant when the suspended colloids move close to the wall. Moreover, high concentrations are achieved in the substrate.

In order to describe the adsorption of particles which move in the bulk according to the mechanisms explained in the previous paragraph, we have to solve the evolution equation for the different particles subject to the boundary condition that the motion ceases when the particle touches the substrate. For all purposes, it is enough to consider the motion of a single sphere, due to the low concentration of the suspension in the bulk. In the absence of Browninan motion, the dynamics of a suspended sphere at position $\vec{r}$ in the bulk is governed by the equation

$$\frac{d\vec{r}}{dt} = \vec{\vec{\mu}}_{eff}(\{\vec{r}_i\}) \cdot \vec{F}_{ext} \tag{3.2.5}$$

where $\{\vec{r}_i\}$ refers to all the vectors pointing from all the preadsorbed spheres to the incoming one, as well as the vector position of the suspended particle, and $\vec{\vec{\mu}}_{eff}$ is the inverse of the effective friction tensor defined in eq.(3.1.2). In this case, $\vec{F}_{ext} = -m_{app} g \hat{z}$ with $m_{app}$ the apparent mass of the suspended sphere. We have assumed that the line is perpendicular to the $\hat{z}$ direction, and that the fluid in which the colloidal particles are suspended is above the line, geometry which will be assumed hereafter.

We have to implement an appropriate expression either for the friction or mobility tensor if we want to look at the particle trajectories in the presence of the line, and its effect on adsorption kinetics. As we have shown in the previous section, however, there exist no general analytic expression for the friction of a number of suspended spheres in the presence of a wall. We need expressions for the friction in the whole range of separations, because the adsorption will be composed of regions where the incoming sphere is far both from the adsorbed particle and from the wall, regions where it will be close either to the wall or to the adsorbed particle, and intermediate regions where the distance between the incoming particle and the interfacial objects is of the order of the diameter of the spheres. Then, neither the exact expressions for two spheres in an unbounded fluid[3] and one sphere in the presence of a wall[9][11], nor the expansions in powers of the inverse of the distance for a number of spheres in the presence of a wall[12] are completely satisfactory to describe the effect of hydrodynamic interactions in this process.

As a result, some approximation has to be introduced in order to obtain an homogeneous analytic expression for the friction tensor. Due to the high dilution of the

suspension, the fact that the gravity force drives the particles towards the substrate because diffusion can be neglected, and also that the incoming sphere interacts with immobile particles[27], the non-additivity effects of hydrodynamic interactions are not expected to play a major role in the dynamics of the incoming particles. On the other hand, lubrication effects, which essentially constitute two-body interactions, will play a dominant role when the adsorbing sphere comes close either to the wall or to a preadsorbed sphere. In accordance with these ideas, we have assumed that the total friction tensor can be constructed as the sum of the friction tensors of the different pair of objects as if they were isolated in the host fluid from the rest of particles. The global friction tensor for a situation in which a particle adsorbs on a substrate in the presence of $m$ preadsorbed particles is expressed as

$$\vec{\vec{\xi}}_{eff}(\{\vec{r}_i\}) = \vec{\vec{\xi}}_{sp}(\vec{r}) + \sum_{j=1}^{m} \left( \vec{\vec{\xi}}_{ss}(\vec{r}_{i1}) - \vec{\vec{\xi}}_0 \right) \tag{3.2.6}$$

where $\vec{\vec{\xi}}_{sp}(\vec{r})$ refers to the friction tensor for a configuration made up of a sphere and a plane, with $\vec{r}$ being the position vector of the particle, because we have taken the origin of coordinates on the line. $\vec{\vec{\xi}}_{ss}(\vec{r}_{i1})$ is the friction tensor for two spheres suspended in an unbounded fluid. Here, $\vec{r}_{i1}$ refers to the position vector of the suspended particle relative to the $i$-th adsorbed sphere. Finally, $\vec{\vec{\xi}}_0 = 6\pi\eta a\vec{\vec{1}}$ is the Stokes friction tensor, with $\eta$ being the viscosity of the solvent, $a$ the radius of the particle, and $\vec{\vec{1}}$ the identity matrix. One should subtract the Stokes' friction to ensure that the overall friction tensor reduces to the usual Stokes law when the colloidal sphere is far from any other object. Expressions for both $\vec{\vec{\xi}}_{sp}$ and $\vec{\vec{\xi}}_{ss}$ are known exactly, and are given in appendix 3.A. This additivity assumption was introduced by Bossis and Brady[17]. They showed that it is equivalent to assume that the forces acting on the incoming particle are additive. They showed that with this approximation lubrication forces are properly incorporated. Moreover, they constructed the global mobility matrix directly from the mobilities of two isolated spheres and a sphere and a plane. This second approximation is equivalent to assume additivity of velocities, and the lubrication forces are not properly incorporated. They observed that overlapping between particles was not prevented within this second approximation scheme.

Within our approximation scheme, the effective mobility matrix is determined in-

verting the effective friction tensor obtained using the force additivity approximation, eq.(3.2.6). Note that the fact that the order in which the inverse of the friction tensor is performed leads to different mobility matrices indicates that, to some extent, the non-additivity of hydrodynamic interactions is taken into account when inverting the effective friction tensor.

Finally, note that the expressions of the friction tensors that we are using correspond to three dimensional hydrodynamics, although adsorption takes place on a line. We will consider three dimensional spheres, and from the point of view of hydrodynamic interactions the line will be considered as a plane. In the absence of diffusion, one can see this restriction as if one had some symmetry in the solution which limited the motion of the suspended particles to a line.

The non-linear dependence of the friction tensors as a function of the distance between the particles, together with the fact that the friction tensors associated with the sphere-sphere configuration have a spherical symmetry different from the cylindrical one of the sphere-plane friction tensors, make it impossible to find an analytic solution for eq.(3.2.6) even in the simplest case in which a single sphere is adsorbed on the line. In the general problem of adsorption kinetics one has to take into account that besides this problem, the number of particles on the line increases with time. Therefore, a numerical simulation study has to be performed.

We have integrated numerically the trajectories of the incoming particles, described by eq.(3.2.5) and the expression for the friction tensor eq.(3.2.6), with the appropriate functions given in appendix 3.A, implementing a 4th order Runge-Kutta algorithm [28] with variable time step. In the numerical integration is important to take into account that the behavior of the friction changes qualitatively along the trajectory of the particle. When the sphere is far from any other object, the mobility is of order unity, and changes slowly. However, when it comes close to an adsorbed sphere, the mobility becomes anisotropic. Then, while the component associated to the displacement along their lines of centers vanishes linearly with the clearance between the spheres (see eq.(3.A.21 ), the component related to the displacement at constant separation goes to zero as the inverse of the logarithm of the clearance (see eqs.(3.A.22 )-(3.A.24 )). In this region, the mobility changes rapidly, and in a different fashion depending on the direction. In fact, the displacements in this region will

consist basically on angular displacements at practically constant distance between the spheres. The variable time step is chosen to ensure that the displacement is never larger than a tenth of the clearance. Moreover, to take the anisotropic behavior of the mobility properly into account, eq.(3.2.5) is solved in spherical coordinates centered in the closest adsorbed sphere to the incoming one.

The fact that the mobility goes to zero when the spheres come into contact, due to the stick boundary condition, introduces an additional computational difficulty, because the velocity in that region can become so small that the computer time needed to describe the trajectory becomes exceedingly large. We have decided to stop a trajectory when the distance between the incoming and an adsorbed sphere becomes smaller than $10^{-4}$ times the diameter of the particles, and place the particle in contact with the adsorbed sphere along the steepest descent path. This motion seems reasonable because at that point, the trajectory is basically controlled by the geometrical constraints, and the external force drives the particle to the line. In the next section, however, we will comment on the limitations introduced by this loose of precision in the analysis of the relative distribution of spheres on the line.

When the sphere comes close to the line, again the mobility becomes anisotropic and exhibits the same behavior explained in the previous paragraphs (see eqs.(3.A.28 ) and (3.A.29 )). Again, the time step allows displacements up to a tenth of the clearance, and since the mobility goes to zero, if the simulation is not stopped, the particle would need an infinite amount of time to actually touch the line. We have considered that when the gap between the sphere and the plane is smaller than $10^{-2}$ diameters, the particle is placed at that position. Due to the driving force, this approximation is reasonable. The situation would be completely different in case the diffusion was present. In that case, the sphere would have a large tendency to diffuse parallel to the line, leading to deslocalization in the final adsorption position[24].This truncation procedure can be seen as an effective way to account for the attractive short-range particle-surface potential, which binds the sphere to the substrate. In all the simulations the diameter of the spheres is taken as the unit length, and $6\pi\eta/(2mg)$ is the unit of time.

We will start by considering the distribution of incoming spheres around a single adsorbed sphere. This simpler situation will help to understand the basic effects of

hydrodynamic interactions in the adsorption, which will be necessary to understand afterwards the results obtained from the simulation of the whole kinetic process.

### Relative Distribution Around a Preadsorbed Particle

We consider the specific geometry in which one sphere has been adsorbed on the line, whose center is taken as the coordinates origin. We will first analyze at which position on the line an incoming particle which is initially at a certain distance from the fixed sphere will be adsorbed. To this end, initial positions are chosen at a height 50, where the influence of hydrodynamic interactions are negligible, and the eq.(3.2.5) is solved numerically until the particle reaches the line. As shown in fig. 3.1, initial positions of the incoming spheres are characterized by the distance off-centers $x_i$.

In fig.3.2 we show the final position from the fixed sphere, $x_f$, as a function of the initial displacement $x_i$. It can be seen that for initial separations larger than 0.3 diameters, the incoming sphere is not in contact with the preadsorbed particle. According to BM, the particle has to roll and end on the line in contact with the adsorbed sphere while the initial displacement is smaller than one diameter, and the final and initial positions coincide for larger separations. Therefore, hydrodynamic interactions introduce an effective repulsion between the incoming and the adsorbed particles. This effective repulsion, which introduces significant deviations with respect to BM, depends on the initial displacement. In the inset of fig. 3.2, the difference in the final positions when hydrodynamic interactions are considered (HI) and when the motion is ballistic, relative to the ballistic prediction are depicted. One can see that the difference in the final position is up to an 18% when the initial separation is of one diameter. When the initial displacement grows, the final position obtained in HI tends to the value of BM. However, from fig. 3.2 one can see that differences are still observed for initial separations for $x_i \sim 5$, which is a feature of the long-range character of hydrodynamic interactions.

One can extend the previous analysis to the case where there are two preadsorbed particles on the line at a given distance $l$. In fig. 3.3 we show the behavior for $l = 5$ and $l = 10$. One can see that when a second sphere is present on the line, the differences with respect to BM in the nearby of the adsorbed particles is not

3.1

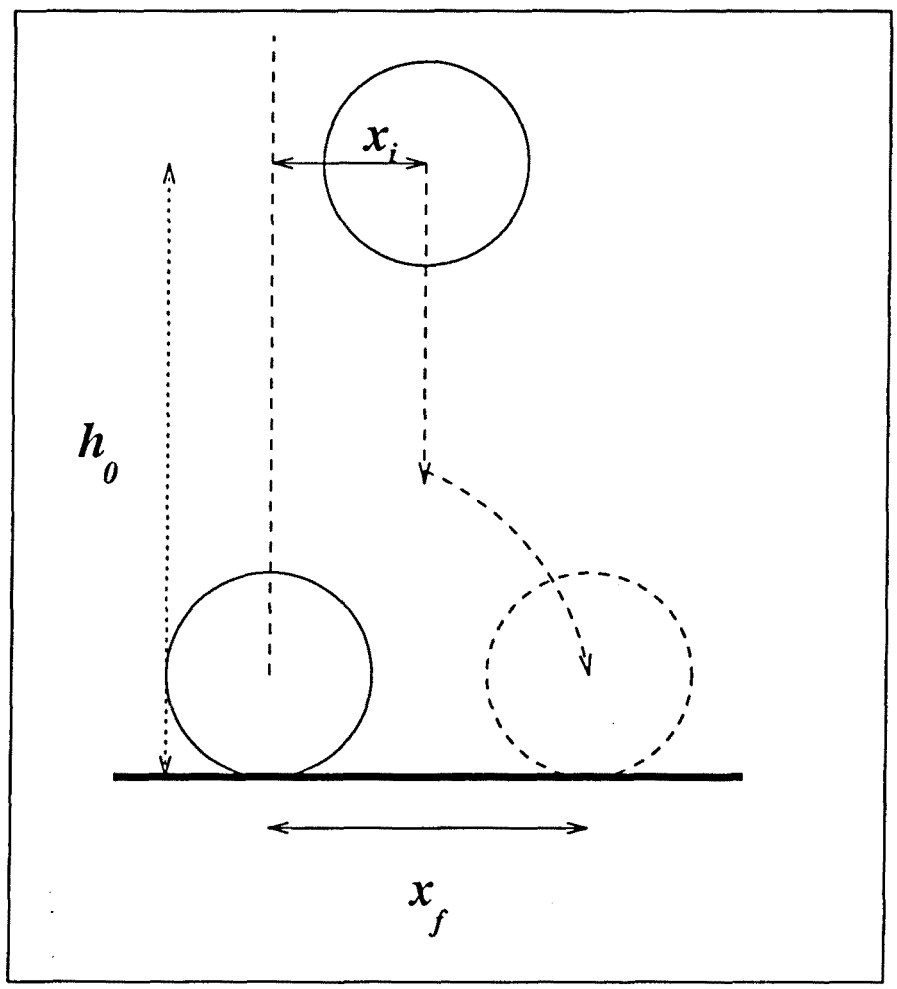


Figure 3.1: The incident sphere is located at a separation $x_i$ from the preadsorbed one (at the origin), at a height $h_0 = 50$; $x_f$ the final adsorbed position on the line.

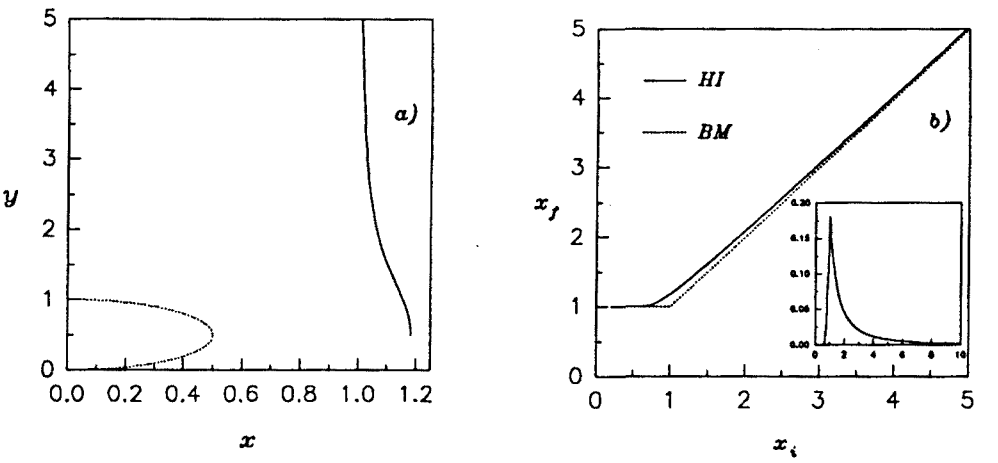


Figure 3.2: a) Example of the trajectory for an incoming particle initially separated one diameter. b)Final distance to the fixed sphere, $x_f$, as a function of the initial displacement, $x_i$. (—) with hydrodynamic interactions (HI), (- - -) BM prediction. Inset, the relative difference between BM and HI.

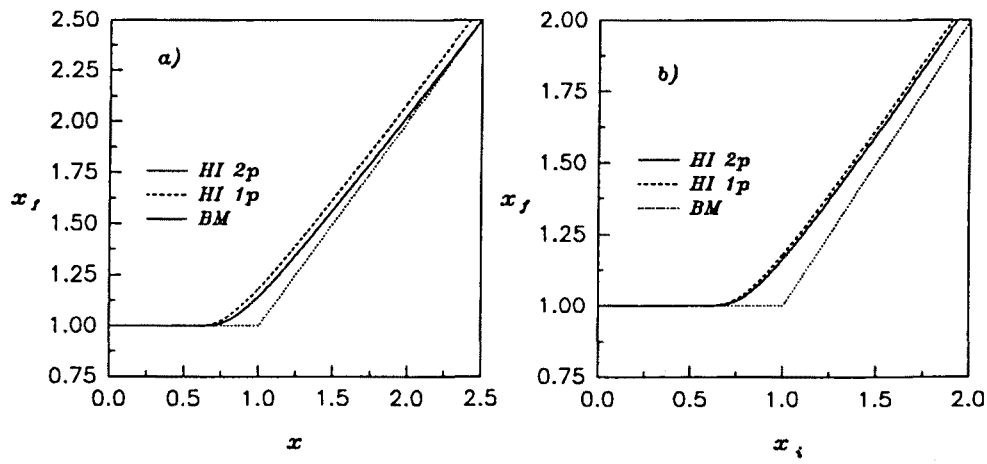


Figure 3.3: Final distance , $x_f$, as a function of the initial displacement, $x_i$. Comparison of BM model with Hi when one particle is in the substrate (HI1p), and when two adsorbed particles are on the substrate (HI2p) when the gap between them has a length: a) 5 diameters, b) 10 diameters.

substantially modified. In fact, the final position is a little bit closer to the adsorbed sphere, but the differences with BM remain of the order of 15%. This deviation is due to the repulsion produced by the distant sphere, and diminishes for larger gaps. On the other hand, the convergence of HI to BM is faster now, than in the one-particle geometry, screening the long-range effects of hydrodynamic interactions. For gaps larger than 10, the overall curve can be constructed from an appropriate superposition of curves of the kind shown in fig. 3.2.

We have also checked the effect of the wall in the final positions of the particle. To this end, we have considered the geometry of fig. 3.1 in which there is one particle, and we have compared the predictions both when the wall is present and absent. In this last case, the expression for the friction coefficient is not given by eq.(3.2.6). Rather, the exact result of Jeffrey and Onishi[3] can be used. In fig. 3.4a) we compare the final positions obtained when the wall is present and absent. One can see that the differences are small, which shows that the wall introduces small perturbations in the motion of the spheres, due to the driving introduced by the external field.

This last result indicates that we can study some of the properties of HI disregarding the wall. In this case, the adsorption reduces to the settling of a sphere in the presence of a fixed one. The mobility matrix in this case has spherical symmetry, and is given by the inverse of eq.(3.A.25 ). Then, if we take polar coordinates centered in the fixed sphere, and the origin of angles coincides with the vertical direction, eq.(3.2.5) reduces to

$$\frac{\xi_r}{r\xi_t}\frac{dr}{d\theta} = -\frac{\cos\theta}{\sin\theta} \tag{3.2.7}$$

where $\xi_r = X^A_{11}$, and $\xi_t = Y^A_{11} - (Y^B_{11})^2/(3Y^C_{11})$ (see appendix 3.A). If the trajectory of the incoming spheres starts at an infinite distance but at finite displacement $x_0$, the final position at the height of the fixed particle is obtained from the previous equation,

$$x_0 = x_f \exp\left\{-\int_{x_f}^{\infty}\frac{dr}{r}\left(\frac{\xi_r}{\xi_t}-1\right)\right\} \tag{3.2.8}$$

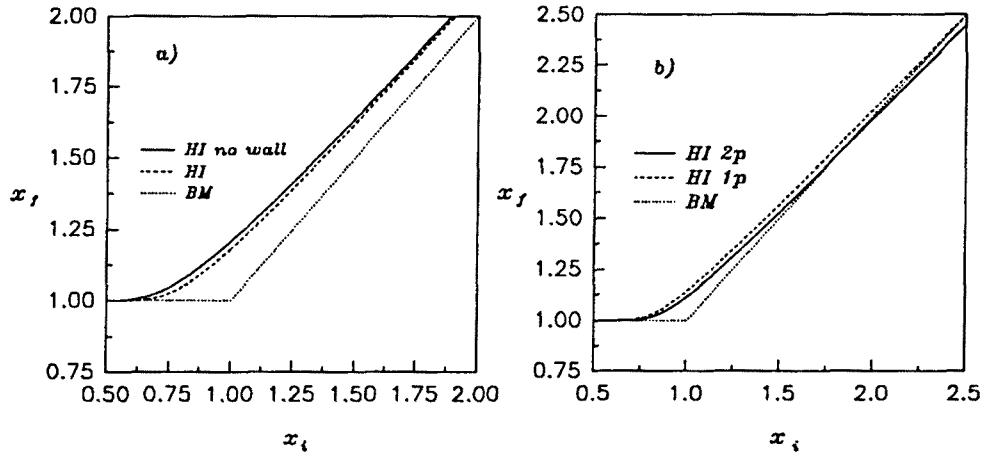


Figure 3.4: a) Final position as a function of the initial displacement of a single adsorbed sphere with hydrodynamic interactions and (—) a wall, (- - -) no wall. b) Final position as a function of initial displacement from the sphere at the origin when there is a second at a distance 5 (- - -) and when there is a second at a distance 5 and a third sphere in contact with the second (—).

We can now use the expressions for the friction coefficients near contact to obtain the behavior of the final position near contact. From eqs.(3.A.21 )-(3.A.25 ) one gets

$$\xi_r \sim -\frac{1}{4(r-1)} \quad , \quad \xi_t \sim -\frac{1}{6}\log\left(\frac{1}{r-1}\right) \tag{3.2.9}$$

which, upon substitution in eq.(3.2.8), gives

$$x_f \sim 1 + e^{-\left(\frac{K}{\epsilon_t}\right)} \tag{3.2.10}$$

with $K$ an integral of the quotient of frictions. This equation indicates that the incoming particles will never touch a preadsorbed one. This is in contrast with the numerical result shown in fig. 3.1, where the incoming particle touches the adsorbed one until the initial displacement becomes of order $10^{-1}$. This spurious consequence of numerical limitations, however, introduces small changes in the distribution, because the function obtained in eq.(3.2.10) shows that the departure from touching is very smooth.

We have also addressed the effect of a third adsorbed sphere on the line by considering the situation in which one sphere is taken as the origin of coordinates, a second one is placed at a distance $l$, and a third is located in contact with this second one. In Fig 3.4b), we show the differences with respect to the results obtained in fig. 3.3a) when only two spheres are present on the line. The relative differences observed in the final position are always smaller than 1%. This means that in the one dimensional model, the geometrical restrictions tend to cancel the effects of many particles, and that the interaction is properly taken into account considering the interaction with a limited number of particles. Moroever, we expect that the geometrical distribution discussed above will keep the largest deviations with respect to the results obtained for two adsorbed spheres. When more particles are adsorbed, they will tend to cancel each other's effects.

Finally, we have also checked the effect of the interactions with the wall on the final location of the incoming sphere. There will exist an attractive interaction between the adsorbing spheres and the wall, which keep the particles fixed to the substrate. Although the interactions at the surface can be of different kinds, we have considered

that it is of van der Waals type. For the case of an isolated sphere in the presence of a plane, it is characterized by an energy $U_{vdw}$[29]

$$U_{vdw} = -\frac{A_h}{6}\left(\frac{a}{z-a} + \frac{a^2}{(z+a)^2} + \log\left(\frac{z+a}{z-a}\right)\right) \tag{3.2.11}$$

with $A_h$ being the Hamaker constant, with a typical value of $A_h = 10^{-20}J$[30], $z$ the minimum distance between the sphere and the surface. Van der Waals forces play a significant role in the adsorption of Brownian particles when hydrodynamic interactions are considered[24]. Then, one may think that also if gravity is present, this attractive interaction may have some importance. We have included this new force in eq.(3.2.5) besides gravitational force, and we have studied the final position on the line around a preadsorbed one as a function of the initial displacement. The differences observed in the final positions are practically equivalent to the ones obtained for a hard wall. Despite the power-law decay of van der Waals potential, the force is significant only at distances of the order of a fraction of the radius of the particle, when the adsorbing sphere is already very close to the substrate. The opposite case in which there exists an attractive potential between the adsorbing spheres has been considered in ref.[31]. In that case, larger deviations with respect to the hard sphere situation are found, and the particles tend to end closer.

If we choose the initial displacements $x_i$ with a certain probability distribution $P(x_i)$ along the line at a height $h_0$, and we consider that there is a single adsorbed sphere on the substrate, then we can use the previous study on the trajectories of incoming particles to obtain the relative distribution of particles around a fixed adsorbed sphere, that is, the probability of having a second one at a distance $x_f$, $P(x_f)$. It satisfies the equation

$$P(x_i)dx_i = P(x_f)dx_f \tag{3.2.12}$$

with $P(x_i)dx_i$ being the probability of having initially a particle between $x_i$ and $x_i + dx_i$, and, accordingly, $P(x_f)dx_f$ is the probability of having a sphere on the line between $x_f$ and $x_f + dx_f$. An interesting feature of the probability $P_f$ is that it is equivalent to the pair distribution function at low coverages. We will consider

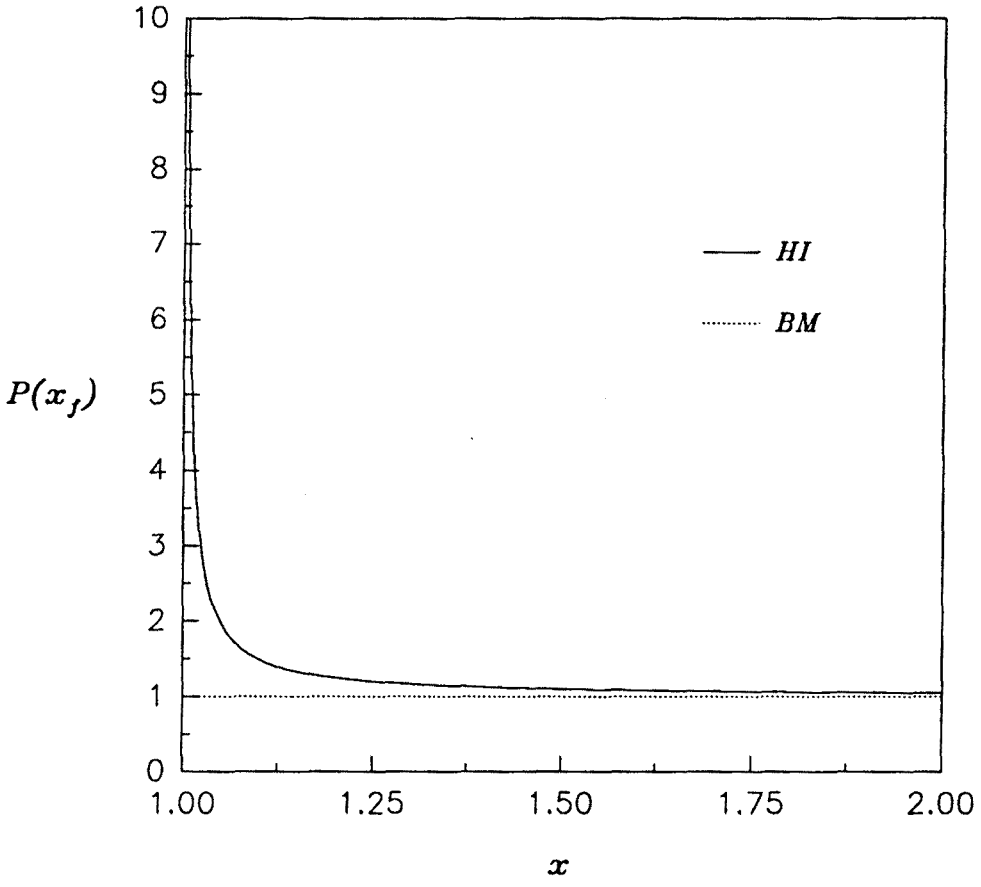


Figure 3.5: Relative distribution of particles around a fixed adsorbed sphere: (—) HI, (•) BM. It coincides with the pair distribution function at low coverages, once normalized.

that the probability distribution of initial positions is uniform, which constitutes the standard assumption in the kinetics sequential adsorption models. In this case, the probability distribution for the final positions can be written as

$$P(x_f) \propto \frac{dx_i}{dx_f} \tag{3.2.13}$$

which can be obtained by numerically differentiating fig. 3.2, and its result is shown in fig.3.5b), without being normalized. We also compare with the predictions of BM. In that case, the initial position coincides with the location on the substrate for $r > 1$, and therefore the relative distribution is homogeneous. One only has to take into account that a delta function appears at $r = 1$ because all trajectories which start at $|x_0| < 1$ end at contact with the sphere on the line.

An estimate of the behaviour of $P_f$ near contact can be carried out by using the fact that the substrate produces small changes in the location on the line. If we consider that the incoming sphere moves in the presence of a single fixed sphere, we have calculated the distance when both are at the same height, eq.(3.2.8). If we differentiate it, we will obtain a function proportional to the probability distribution function, $P_f$,

$$P(x_f) \propto \frac{\xi_r}{\xi_t} \exp\left\{ -\int_{x_f}^{\infty} \frac{dr}{r} \left( \frac{\xi_r}{\xi_t} - 1 \right) \right\} \tag{3.2.14}$$

and, although a general expression cannot be obtained, using the expressions of the friction coefficients close to contact, eq.(3.2.9), we can estimate the asymptotic behavior. Performing the integrals, and disregarding various normalization factors, one obtains

$$P(x_f) \sim \frac{1}{(x_f - 1)|\log(x_f - 1)|^5} \tag{3.2.15}$$

which clearly shows that the effective repulsive interaction induced by hydrodynamic interactions prevent particles from touching, and therefore, destroy the delta function

characteristic of BM. On the other hand, the fast decay obtained in eq.(3.2.15), indicates that a large fraction of the particles will be extremely close to the adsorbed particle. As we will see in the next section, the intrinsic limitations of numerical simulations will induce delta functions in the pair distribution functions. These can be thought as averages of the actual logarithmic decay in a small gap close to the adsorbed particle.

Introducing in eq.(3.2.14) the expression for the friction coefficients when incoming particle is far from the fixed one,

$$\xi_r \sim 1 + \frac{9}{4}\frac{1}{r^2} \quad , \quad \xi_t \sim 1 + \frac{9}{16}\frac{1}{r^2} \tag{3.2.16}$$

gives the asymptotic behavior

$$P(x_f) \sim 1 + \frac{27}{16 x_f^2} \tag{3.2.17}$$

which shows the slow decay associated to the slow decay of hydrodynamic interactions. Although qualitatively interesting, this slow decay will not be of great interest from the point of view of adsorption kinetics.

### The Adsorption Process: Kinetics and Structure

The previous section has served us to understand the new features that the incorporation of hydrodynamic interactions, when the detailed transport of particles from the bulk to the substrate is considered, introduce in the distribution of adsorbed particles. We will now study the adsorption process, taking hydrodynamic interactions into account, and following the basic ideas of the adsorption kinetics models introduced in chapter 3. The line is initially empty. Adsorbing spheres are chosen sequentially, in such a way that there is only one sphere adsorbing at a time. Initial positions for the incoming spheres are chosen uniformly random at a height 50, to be sure that initially hydrodynamic interactions can be disregarded. The particle evolves according to eq.(3.2.5), and the appropriate boundary conditions are implemented: If the particle touches the wall, then it is irreversibly adsorbed at that position, with no

further motion; if it is trapped on the top of two adsorbed particles, and is unable to reach the line, it is rejected. This last boundary condition ensures that only one layer of adsorbed particles is formed. Then, the kinetic process will reach a jamming limit, when no more particles can be added to the line.

The study of this kinetic process has to be performed with the aid of computer simulations. We have considered a line of length 800. Initial positions are chosen using a standard uniform random generator. Then for each trial particle, eq.(3.2.5) has to be integrated numerically. In view of the results of the previous section, and also in order to save computer time, the incoming sphere is assumed to interact only with its nearest neighbors. As we have seen, in the most unfavorable case, differences of 1% are expected. Then, the expression for the friction tensor, eq.(3.2.6) simplifies considerably, and has a constant structure along the simulation. Note, however, that the neighbors may change along the trajectory of the incoming sphere. Periodic boundary conditions have been considered to diminish finite size effects, and a number of configurations of the order of 1000 have been simulated in each situation to have a reasonable statistics.

In order to be able to compare our results with BM predictions, simulation of BM of the same system explained in the previous paragraph have also been carried out, following [25]. Positions are chosen uniformly random on the line. If no overlap occurs with a preadsorbed particle, the incoming sphere is irreversibly located at that position. Otherwise, its position is shifted one diameter to the right or the left of the corresponding preadsorbed particle, depending on whether the incoming sphere is at its right or left hand side, respectively. If at the new position there is an overlap with another preadsorbed particle, the incoming one is rejected and a new position is chosen randomly.

In fig. 3.6 we show the fraction of covered line as a function of time, and compare with BM results. The unit time in both cases is the number of particles which have tried to reach the wall. In this sense, we follow the kinetic models, which do not have a characteristic time scale, instead of counting the time from the differential equation. In the absence of Brownian motion, however, both time scales will be practically equivalent, except perhaps near the jamming. The differences observed in the figure are small, and relative differences do not exceed 1% along the whole

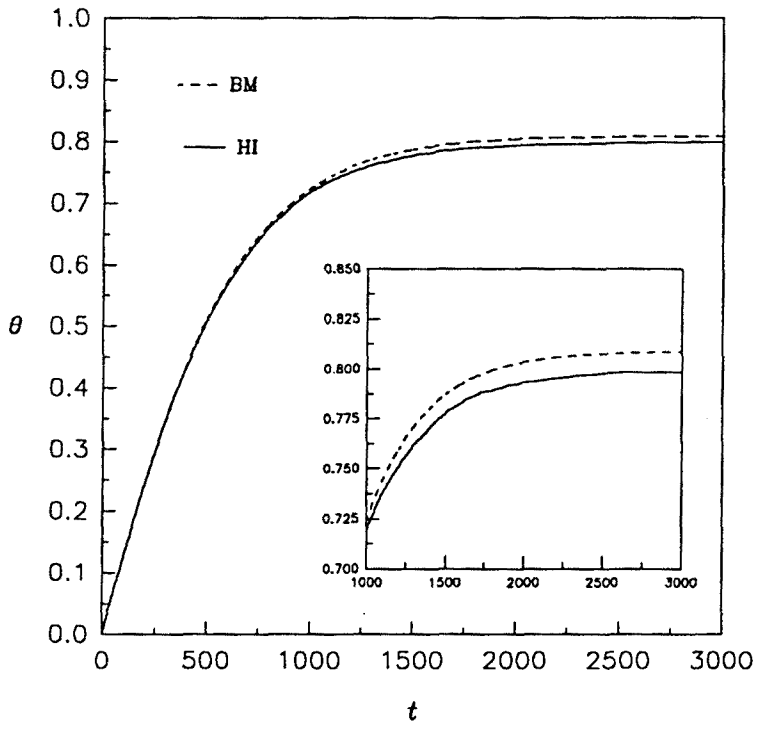


Figure 3.6: Coverage as a function of time. (—-) with hydrodynamic interactions, (- - -) ballistic model. Inset, differences in the asymptotic regime.

process, leading to a difference in the jamming limit of a 1.3%. The jamming limit we have obtained is $\theta_\infty^{HI} = 0.797 \pm .001$, while BM predicts $\theta_\infty^{BM} = 0.808 \pm .001$, therefore the differences are small, and almost impossible to be detected from an experimental point of view. Nonetheless, they are larger than the ones observed in the jamming limit when comparing RSA and DRSA[32].

In the inset of fig. 3.6, the asymptotic kinetics for both HI and BM is shown. It is the same, due to the fact that the asymptotic regime is controlled by the available area of isolated targets, and in both models these areas do not go to zero since incoming

particle can roll on preadsorbed ones. This means that the asymptotic kinetics is not sensitive to the actual transport process from the suspension to the line. We have computed the number of trials needed to succeed in adding a sphere to the line, as a function of coverage. The mean value of its inverse gives us the available fraction of the line as a function of the coverage, which we have plotted in fig. 3.7. Again, the differences between HI and BM are at most of 1%. These results show that in these systems, global quantities are not very sensitive to hydrodynamic interactions, although small deviations are observed, which suggests that other physical properties may be more sensitive to the transport mechanisms.

We will next focus our interest on the local structure of the adsorbed layer, that is, on the relative distributions of the particles on the line. Most of the structure information is contained in the pair distribution function, $g(r)$. In appendix 3.B we introduce it and explain how it can be numerically computed.

We have studied the pair distribution function of both HI and BM as a function of the coverage, using the method described at the end of appendix 3.B. To determine this quantity, it is necessary to introduce a spatial resolution $\delta r$, and take the average number of particles in boxes of such a width. On the other hand, the numerical method used to simulate the adsorption process produces a finite fraction of adsorbed spheres at contact, and a large fraction of pairs of particles separated at a distance close to contact. Then, the specific form of the curve in the vicinity of distances a multiple of the diameter, will depend strongly on the value of $\delta r$ considered. In principle, the smaller the value of $\delta r$, the more accurate the description of the curve, which consists on a delta function, which appears as a pronounced peak, and a smooth curve. On the other hand, the smaller its value, the least smooth the curve. A compromise has been reached by taking $\delta r = 0.05$. By varying $\delta r$ around this value, we have verified that the form of the curve is stable, and only the precise value of the height of the peak changes.

In fig. 3.8 we show $g(r)$ at low, $\theta = 0.25$, intermediate, $\theta = 0.5$, and close to jamming, $\theta = 0.79$, coverages. Peaks are obtained at distances multiple of the diameter, which are followed by a slow decay. The peak is due both to the existence of particles at contact, and the existence of a singular contribution due to the fact that the repulsion induced by hydrodynamic interactions favors the appearance of

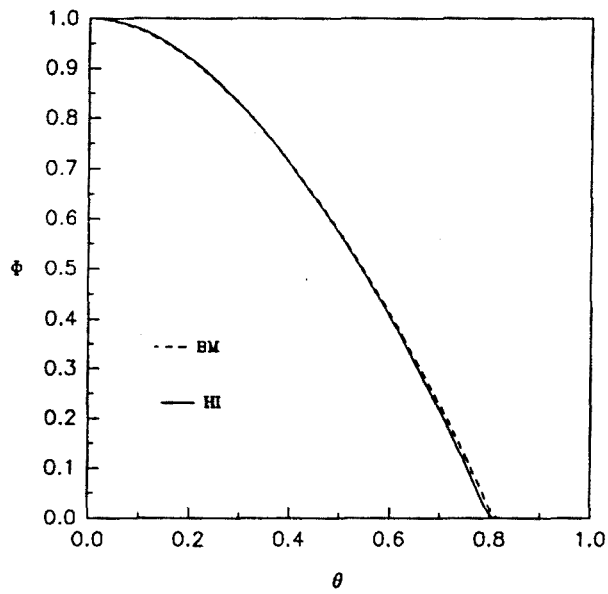


Figure 3.7: Available line fraction as a function of coverage. (—-) with hydrodynamic interactions, (- - -) ballistic model.

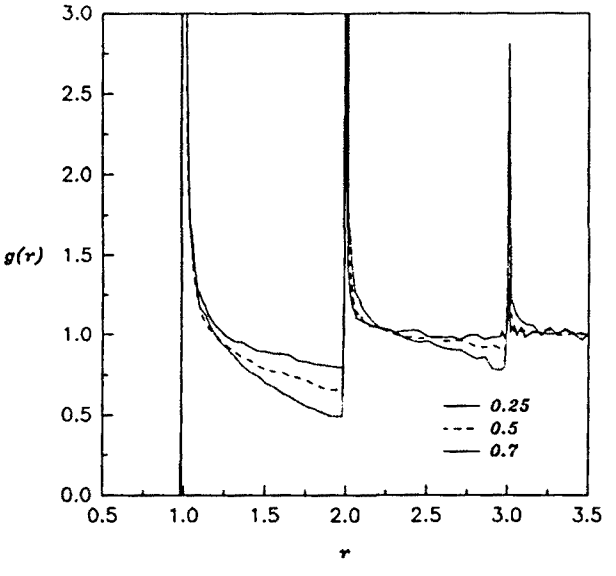


Figure 3.8: Pair distribution function for HI at coverages $\theta = 0.25(---), 0.5(---)$, and close to jamming (- -).

small gaps between spheres. In fact, from the results of previous section, we know that the pair distribution function in the absence of substrate has to decay after the peak at contact as the product of the clearance times a power of its logarithm (see eq.(3.2.15)). The decay of $g(r)$ is not sensitive to coverage, because it is basically a two-body effect. As the coverage increases, the relative distances tend to be smaller, as expected, concentrating in values around the multiples of contact. The height of the peaks, which are not shown in the figures except for the third, also increase with coverage, indicating that the fraction of particles forming clusters increase, as well as the fraction of particles at distances close to multiples of diameters, forming dense structures, although without touching. Due to finite size effects, no peaks at distances larger than 6 have been obtained, even close to jamming.

We have also compared the pair distribution functions obtained in HI with those of BM, as shown in fig. 3.9. The peaks obtained in BM are always higher than the

corresponding ones for HI. This can be expected, since from fig.3.2, one can predict that the fraction of particles at contact in HI will be a around a third of the fraction obtained in BM. The decay of the curves after the peak is faster in BM, because in this case the interaction is only by contact. After the first peak, differences for the values of $g(r)$ up to a 40% are observed. At higher coverages, the differences in the height of the peaks remains, but the convergence of HI to BM curve is faster, indicating that the possible positions on the line become progressively dominated by the geometrical restrictions, and that the relative distances decrease in average. Note that the $g(r)$ obtained in HI is always larger than the one obtained with BM, except at the peaks. This can be seen as another feature of hydrodynamic interactions, which prefer to move the incoming spheres away from the adsorbed ones.

From this one-dimensional analysis one can see that, while the averaged global quantities, are not sensitive to the precise transport process, the structural local properties are more sensitive to the specific transport mechanism of the particles towards the line, and its interaction with surface exclusion effects. The results we have obtained from the $g(r)$ agree qualitatively with the ones observed experimentally on the adsorption of melamine spheres on a glass surface[26]. However, in order to be able to perform precise comparisons, one should consider the adsorption on a real two-dimensional substrate, which constitutes the topic of the next section.

### 3.2.2 Two-dimensional Model

In this section we will proceed to analyze a more realistic situation in which particles adsorb on a planar bidimensional surface. As happened in the one-dimensional case, the study of the adsorption will have to be carried out numerically. Again, particles will be launched at a certain height over the plane, and its trajectory, eq.(3.2.5) will be numerically integrated until they reach the surface. The expression for the effective friction tensor, eq.(3.2.6) using the force additivity approximation, is still valid. The same expressions for the friction coefficients, given in Appendix 3.A, can still be used, because three-dimensional spheres have considered in the previous model. The Runge-Kutta algorithm is analogous to the one used in the previous section, and a variable time step has also to be introduced to take properly into account the trajectory in the regions where the mobility components go to zero. Finally, the trajectories that

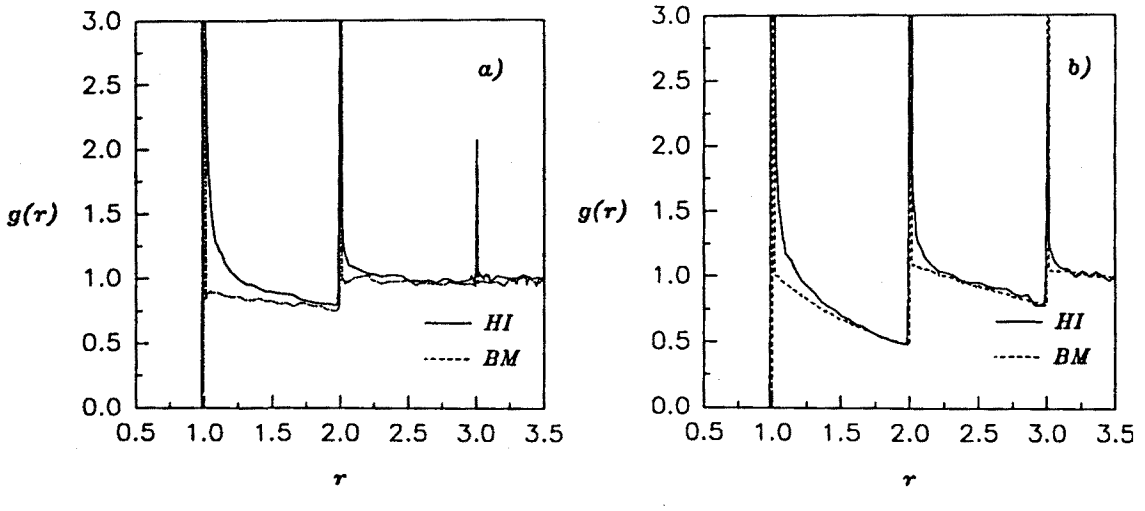


Figure 3.9: Pair distribution function for HI (—), and BM (- - -). a) At $\theta = 0.25$; b) at $\theta = 0.79$.

go too close to a preadsorbed sphere need such an amount of time to be performed, because the velocity goes to zero in those regions, that the program has to be stopped, and the particles then try to reach the wall rolling over the preadsorbed sphere, as in BM.

### Relative distribution

However, before studying the global kinetic process, we will concentrate on the basic features introduced by hydrodynamic interactions, which are better understood by considering the simplified situation in which a sphere arrives at the plane in the presence of one or two spheres.

Let us consider first an adsorbing sphere in the presence of a single adsorbed particle. In this case, and due to the symmetry, we reproduce the behavior discussed in the previous section.

However, new phenomena appear when adsorption takes place in the presence of two adsorbed particles. In fact, we will study the adsorption in the presence of a doublet of adsorbed particles. One is at the center of coordinates, and the other one in contact with it, as shown in fig. 3.10. Initial positions for the incoming sphere, $r_i$, are chosen as shown in fig. 3.10, for values which correspond to contact with particle 1 if sphere 2 would not be present. In fig. 3.11a) we present the final angle on the plane for initial displacements from sphere 1, for different initial orientations. As a general feature, the incoming sphere has a tendency to move apart from sphere 2 due to the effective repulsions induced by hydrodynamic interactions, ending at angles smaller than the initial one. This effect is specially pronounced when the initial separation from sphere 1 is smaller, and for smaller values of the initial angle. Note that BM predicts no change in the orientation, because if the incoming sphere touches sphere 1, it will reach the surface through the steepest descent path. This deviation shows a tendency to form aligned triplets on the surface, where BM would predict the appearance of isotropic clusters. From the point of view of the deposition process, this tendency to align would affect only a small part of the incoming spheres, because they should arrive close to one of the particles forming a doublet. In fact, the study of the structure of the clusters remains as an open subject also experimentally.

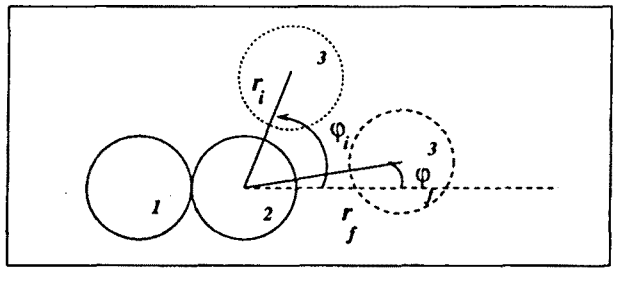


Figure 3.10: Top view of the geometry considered. Sphere 1 and 2 are adsorbed, and sphere 3 (continuous line) is at a height 50, while the discontinuous sphere corresponds to its final position on the surface.

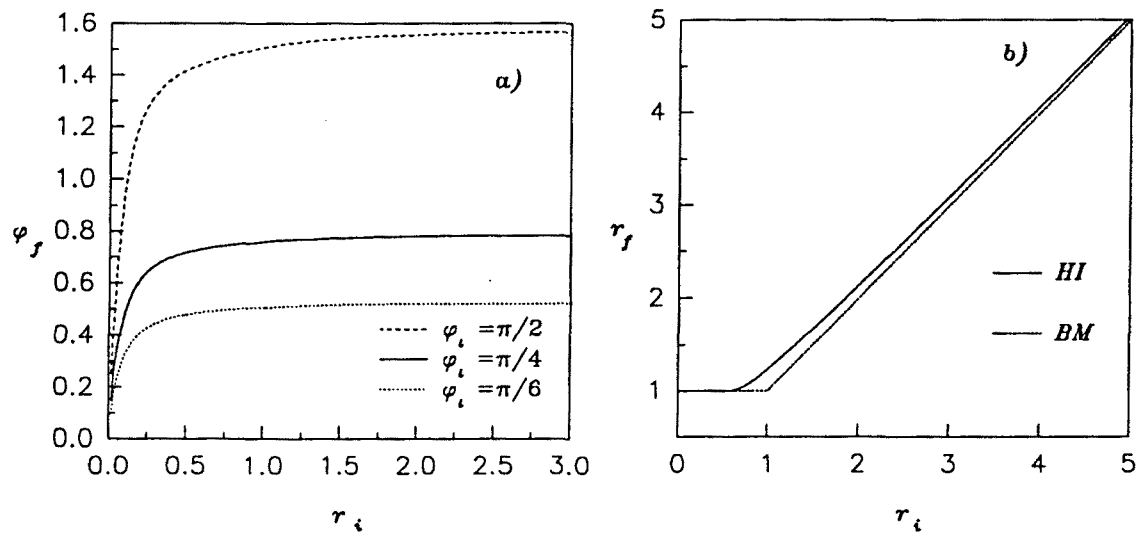


Figure 3.11: a) Final angle as a function of the distance for initial angles $\varphi_i$ = $30°(---), 45°(---)$, and $90°(--)$; dotted lines correspond to BM predictions. b) Final distance for $\varphi_i = 0$). (See previous figure for notation).

For $\varphi_i > 90^o$, the incoming sphere will move to the intermediate region between the adsorbed spheres. In this case, due to the symmetry, the particle will end in contact with both spheres, in agreement with BM. However, as shown in fig. 3.11b), if the initial positions are chosen $\varphi_0 = 0^o$, the mutual repulsion and its long range produce important differences in the final position, with respect to BM.

In the adsorption on a line, because of the geometrical restrictions, the effect of a second sphere is a shadowing of the effective repulsion produced by the nearest preadsorbed sphere. Now, due to the angular degree of freedom, the combined repulsion effects of the two adsorbed spheres can also change the direction of movement of the incident sphere, leading to more complex interaction of the transport process with the surface exclusion effects.

### The radial distribution function

We will generalize the basic principles introduced in the previous one-dimensional model, to this system. We will consider again that spheres approach the planar surface one at a time in a sequential way, which corresponds to the situation when the bulk concentration is small. Again, the boundary conditions are introduced considering that as soon as a sphere touches the surface, it is irreversibly located at that position, and that if it touches a preadsorbed particle, it will try to reach the surface following the steepest descent path[2]. If during this motion, it is trapped on the top of some adsorbed particles, then it is rejected. Now, there exist more trapping possibilities than in 1-D. In order to know when a particle is unable to reach the surface, the 2-D BM algorithm[33] has been implemented. In app. 3.C, we show the different rolling mechanisms, and which ones leads to trapping.

In the 1-D model, we have further argued that, because of the geometric restrictions, the effective friction tensor could be constructed by considering only the nearest neighbours of the adsorbing particle. We have seen now that the angular dependence becomes very important. Then, a particle which is not nearest neighbor, but which is in a direction different from the nearest neighbours may cause significant changes

[2]Remember that in the simulations, if the distance between the particles is smaller than $10^{-4}$, the incoming spheres starts to move according to BM

in the direction of the incoming trajectory. Therefore, a more general scheme for the interactions has to be introduced. Although in principle, we would have to consider the interaction of the adsorbing sphere with all the adsorbed particles, the computer time increases rapidly with the number of interacting particles. As a compromise, we will consider that the adsorbing sphere, as it approaches the surface, is located in the center of an imaginary cylinder of a certain radius $R$. The particle will then interact with all preadsorbed spheres located in the interior of such cylinder, which will be referred to as *interaction cylinder*. On the other hand, we have seen that if a single sphere is adsorbed, the incoming one ends practically at the same initial position for initial displacements larger than 10. This fact suggests that $R$=10 is a reasonable choice for the radius of the interaction cylinder. If there are no adsorbed particles in the cylinder, the particle adsorbs at the initial position.

However, even with this restriction, the time that a particle needs to reach the surface is too large. In order to speed up the simulation, we have considered that, as the particle approaches the surface, the radius of the interaction cylinder initially decreases linearly with the height. In fact, if one observes the trajectory of one particle in the presence of a preadsorbed one, as the one shown in fig. 3.2a), one can see that initially the trajectory is controlled by gravity, and the displacement parallel to the surface is a small correction of its initial value. The major part of the parallel displacement takes place when the distance to the adsorbed particle is of the order of 2 or 3. Though these trajectories are obtained with a small number of particles on the surface, it seems reasonable that this behavior holds in more complex situations. Therefore, in this region the trajectory of the particle will not be especially sensitive to the local enviroment. When the sphere approaches the surface, then the previous assumption is no longer valid. For this reason, when the height is smaller than 5, we then take the radius of the interaction cylinder constant and equal to 5. The introduction of this radius-varying interaction cylinder, saves an order 10 the computer time needed to perform the simulation.

We have checked the errors induced by the use of such a varying cylinder by covering a surface both using a constant-radius and a varying-radius interaction cylinder, as shown in fig. 3.12. At an intermediate coverage, as shown in fig.3.12a)[3], all the

[3]the jamming value of BM in 2-D is 0.6105 [34]

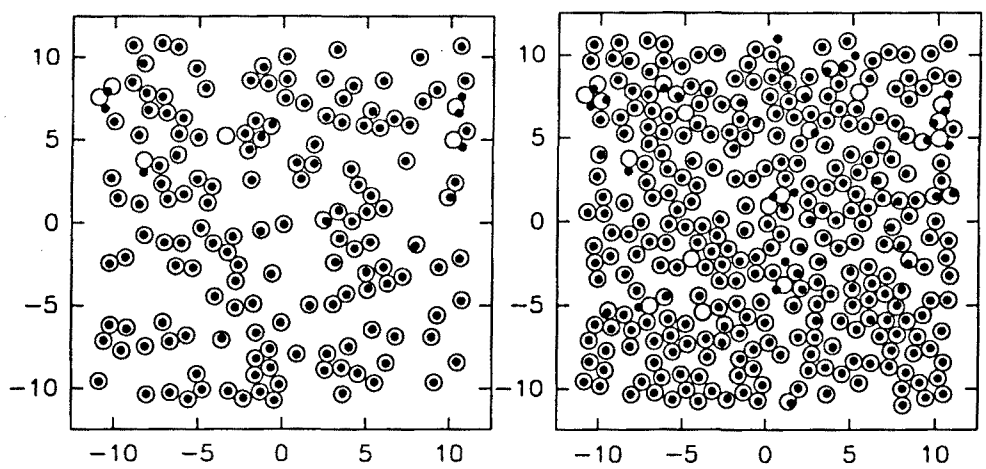


Figure 3.12: Surface covered with a varying-radius , and a constant-radius interaction cylinder, at a) $\theta = 0.25$, and b) $\theta = 0.5$.

particles end at the same positions on the plane using both methods, although at higher coverages a small fraction of the particles are placed at different positions, as seen in fig. 3.12b). This is due to the fact that if an incoming sphere arrives close to an aggregate, a small initial deviation may lead to a completely different final position. Then, due to the infinite memory of the adsorption process, all the particles arriving afterwards will be sensitive to this difference. leading to a completely different configuration. From the point of view of average quantities, it is doubtful that this change may lead to a significantly different results.

Finally, the initial height at which particles are left has also been changed with respect to the 1-D model. We have checked that if it is taken 10 diameters using the same argument exposed to choose the interaction radius 10, then the changes in the configurations on the surface relative to the ones obtained upon choosing it for example 12 diameters, are smaller than the ones produced by taking a constant or varying cylinder. Now, the possibility of taking 10 as the initial height is important, since it is related to the initial value of $R$ and therefore to the minimum value of the sides of the studied surface, because, obviously, the diameter of the interaction cylinder cannot be larger than the system size.

We have performed numerical simulations of the adsorption process on a rectangular surface, of sides 23.5 and 24.7, up to a coverage of $\theta = 0.5$. The size of the system has been chosen for convenience in order to compare with experimental results[26]. We have focused on the study of the radial distribution function, since we expect, from the results obtained in the 1-D model, that both the jamming and the kinetics will be similar to those of 2-D BM. Note, in particular, that this means that in our simulations we will arrive at a 18% away from jamming. At this concentration, we can already obtain an idea of the behavior of the system near jamming. From the computer time point of view, it is difficult to reach higher coverages.

We have covered 200 surfaces, and from them, we have constructed the radial distribution function, according to the procedure explained in app. 3.A. We do not need as many surfaces as lines in 1-D to obtain reasonably smooth $g(r)$, due to the additional angular average which is performed in a 2-D model. As in the previous model, simulations of the deposition of BM have also been carried out, under the same conditions exposed in the previous paragraph, in order to compare both models. The

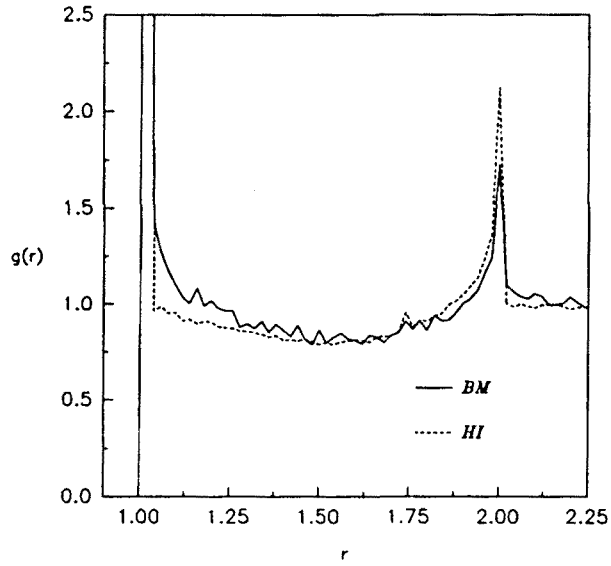


Figure 3.13: Radial distribution functions in 2-D at $\theta = 0.5$. (—) HI, (- - -) BM.

algorithm simulated follows the one in Ref.[33], and which is outlined in app. 3.C.

In fig. 3.13 we compare with the results obtained from BM. Again, we will focus our attention on the curves after the first peak. One can see that the effective repulsion introduced by hydrodynamic interactions produces a curve which decay slower than the one of BM due to the fact that a portion of the particles that according to BM should be in contact, now will be at slightly larger distances. Now, at a separation around one and a half diameter, both curves cross, while in the 1-D model the probability was always higher for HI. As expected, the second peak is higher for BM, and again, the decay after the second one is slower for HI. This peak appears due the rolling on an aligned trimer, but it is not a delta peak as the ones produced by rolling over connected clusters. It is due to the behavior of the angular probability distribution, which exhibits a maximum when the three particles are aligned. At high coverages a third peak at a distance $\sqrt{3}$ can be observed. Such a peak appears due to the rolling on a connected trimer. The strength of the divergence in $g(r)$ at r=2 will

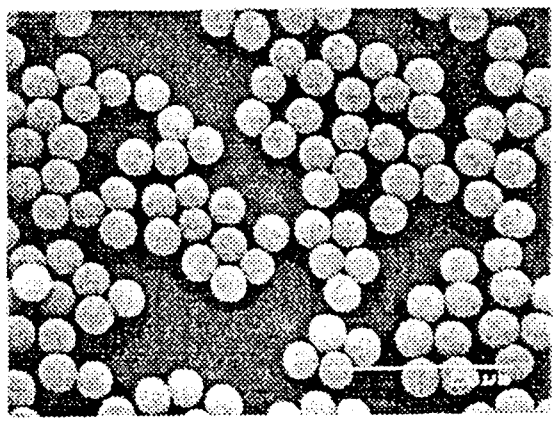

Figure 3.14: Photograph of the adsorbed layer of melamine latex spheres.

be sensitive to the fact that there is a tendency to form aligned clusters because of hydrodynamic interactions. Looking at the figures, however, one can see that there is a lack of resolution to distinguish to what extent the difference is due to this alignment or it is due to the effective repulsion which decreases the number of particles at contact. As in the 1-D model, the behavior right after the peaks is quite unsensitive to the coverage, but at higher coverages, a faster convergence between both models is observed after the peak regions, where differences are always observed.

We have also compared our results with recent experimental results by Wojtaszczyk *et al.* on the deposition of melamine particles on a silicon surface [26]. These authors used an optic microscope which allowed them to actually see the melamine spheres on the surface. In fig. 3.14 a photograph of a surface of glass covered with melamine spheres of diameter 4.2$\mu$m is shown. In order to see them they should focus appropriately, having to determine which particles are actually adsorbed on the surface. In order to compute the $g(r)$, it is necessary to digitalize the images, which

introduces a certain rounding error in the evaluation of the function, which has a significant influence in the specific form of the peaks of $g(r)$. As mentioned for the 1-D model, the form of the curve in the region around the peaks is very sensitive to the specific way in which $g(r)$ is constructed, which means that if we want to compare our results to theirs, we should proceed exactly in the same way in his way to determine $g(r)$. To this end, our simulation data have been digitalized exactly in the same way in which the data files for the positions of the particles are obtained from the experimental photographs. In this way, we can compare the results, although both are not reliable in the peak region. In fig. 3.15 we show a comparison of the experimental and computer results for two different coverages[35]. One can see that the agreement behind the first peak is quite good, and in general, one obtain a better agreement than comparing the experiments to BM. From the experimental point of view, the suspension of melamine particles is not completely monodisperse, and then it was thought that the discrepancies observed between the experimental $g(r)$ and the BM one could be due to this fact. Simulations of BM introducing the same degree of polydispersity as in experiments have also been performed[36], and the comparison of the pair distribution function still showed basically the same discrepancies, as the ones shown in fig.3.15.

## 3.3 Discussion

In this chapter we have studied the effects of hydrodynamic interactions in the adsorption of colloidal particles at high Péclet numbers, and compared with BM, which has been used up to now to compare with experimental results. This model disregards the transport process of the colloids to the surface, and, as described in app. 3.C, the arrival at the surface only depends on the local geometry of the previously adsorbed particles.

We have developed numerical studies for both 1-D and 2-D models including hydrodynamic interactions. From the study of the first model, which is simpler to implement, we have shown that hydrodynamic interactions introduce an effective repulsion between the incoming and the preadsorbed colloids, which is long ranged and starts to produce a distortion of the trajectory of the incoming sphere for distances

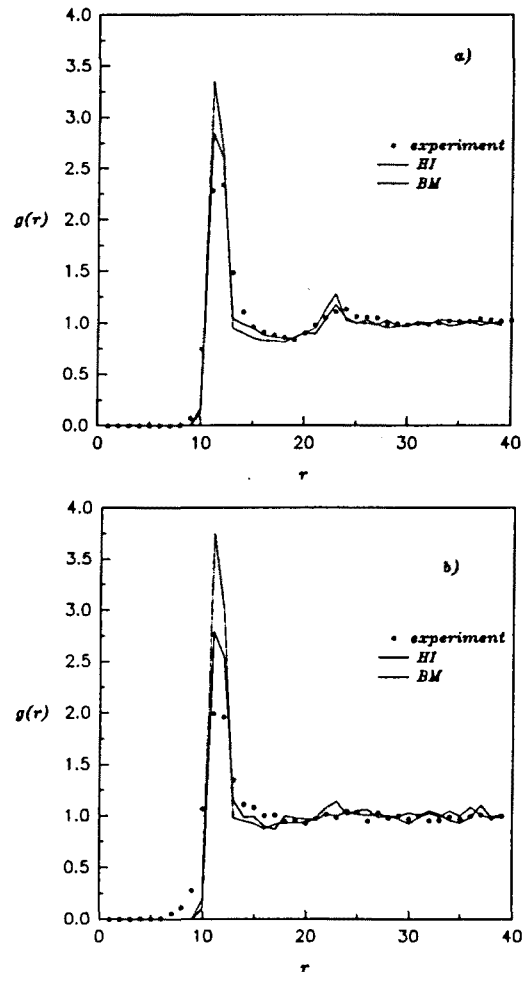


Figure 3.15: Radial distribution functions at coverages for HI(—), BM(- - -), and experimental results (*). a)30%, b) 17%

between particles of the order of a few diameters, which means that the interactions are not short ranged. This result shows that a detailed knowledge of the transport mechanism is necessary because it changes the structure of the adsorption layer.

In our analysis we have first considered the effect on the relative distribution of adsorbing particles around a single particle, as well as around two preadsorbed spheres. The first study has shown the effective repulsion introduced by hydrodynamic interactions. When two spheres are considered, while in 1-D a screening effect is shown, which limits the long range effect of HI on the final positions on the line, a new effect appear associated to the angular variation of the incoming particle in 2-D, leading to a tendency to form aligned clusters, a qualitative difference with respect to BM. We have then studied both the kinetics and the structure of the kinetic process. On one hand, the effect of hydrodynamic interactions on the kinetics is small, producing corrections which are never larger than 1%. On the other hand, when considering the pair distribution function, larger effects are observed. As a consequence of the effective repulsion, after the first peak which corresponds to the existence of a finite fraction of dimers, differences in the probability of adsorption up to a 40 % are observed both in 1-D and 2-D. The results obtained from both models show the same qualitative differences with respect to $g(r)$ predicted by BM that the ones observed when comparing the experimental results on the adsorption of melamine particles with BM[26]. Moreover, quantitative comparisons have been carried out of our 2-D results with their experimental data, obtaining a quite good agreement for the whole function, specially after the first peak.

In the literature, BM had been introduced as the limiting case when the deposition is controlled by gravity instead of diffusion[25]. However, from the above analysis one can conclude that in the regime when gravitational effects become important, HI introduces significant effects with respect to the kinetic model. BM will represent a good model of the deposition process only when inertial effects become dominant, since in this regime the friction term in the dynamics of the particle is negligible. Note that if damping dominates the inertial terms, the results presented in this chapter are the same for any value of the density in this regime, due to the structure of eq.(3.2.5), in which we have been able to find an dimensionless time scale incorporating the details of the system. Therefore, by appropriately rescaling the time we will always obtain the same results. The inertial contribution to the motion of the colloidal

particles will dominate when the deposition of one sphere takes place during a time interval not larger than the inertial decaying time $\tau \equiv m/\xi = 2a^2\Delta\rho/(9\nu\rho_f)$. In usual experimental situations, as the one reported in ref.[26] for melamine particles, $\tau \sim 10^{-6}s$, while the experimental time scale is of the order of minutes. Consequently, in this situation inertial effects are negligible, which explains the disagreement between the radial distribution function obtained experimentally and the one calculated from BM, and justifies the validity of eq.(3.2.5). Therefore, the applicability of BM is severely restricted in experimental situations.

Finally, it is also interesting to note that the fact that HI affect the local distribution of adsorbed particles implies that these interactions will be relevant when studying other physical properties of adsorbed layers which depend on the local structure of the deposits, as for example the dielectric susceptibility of adsorbed particles [37].

# Appendices

## 3.A Expressions for the friction tensors

For the two-sphere problem, Jeffrey and Onishi[3] computed the corresponding friction tensors. We will follow the notation of eq.(3.1.2), and we concentrate on the tensor components of interest. The two spheres have a radius $a$ and are separated a distance $r$. We will call $\hat{e}$ the unit vector of the center-to-center direction. Then, due to the symmetry, the matrices appearing in eq.(3.1.2) can be expressed as

$$(A_{11})_{ij} = X^A_{11} e_i e_j + Y^A_{11}(\delta_{ij} - e_i e_j) \qquad (3.A.18)$$

$$(B_{11})_{ij} = Y^B_{11} \epsilon_{ijk} e_k \qquad (3.A.19)$$

$$(C_{11})_{ij} = X^C_{11} e_i e_j + Y^C_{11}(\delta_{ij} - e_i e_j) \qquad (3.A.20)$$

with the different functions being given by

$$X_{11}^A = \frac{1}{4}\frac{1}{1-4r^{-2}} - \frac{9}{40}\ln\left(1-\frac{4}{r^2}\right) - \frac{3}{112}\left(1-\frac{4}{r^2}\right)\ln\left(1-\frac{4}{r^2}\right)$$
$$+ \frac{3}{4} + \frac{17}{70}\frac{1}{r^2} + \frac{127}{560}\frac{1}{r^4} - \frac{4057}{2240}\frac{1}{r^6} + \ldots \quad (3.A.21)$$

$$Y_{11}^A = -\frac{1}{6}\ln\left(1-\frac{4}{r^2}\right) + 1 - \frac{5}{48}\frac{1}{r^2} + \frac{371}{768}\frac{1}{r^4} + \frac{1633}{36864}\frac{1}{r^6} + \ldots \quad (3.A.22)$$

$$Y_{11}^B = -\frac{1}{4}\left[1+\frac{1}{2}\left(1-\frac{4}{r^2}\right)\right]\ln\left(\frac{r+2}{r-2}\right) + \frac{3}{2r} - \frac{9}{8r^3} + \frac{125}{24r^5} + \ldots \quad (3.A.23)$$

$$Y_{11}^C = -\frac{1}{5}\left[1+\frac{47}{50}\left(1-\frac{4}{r^2}\right)\right]\ln\left(1-\frac{4}{r^2}\right) + 1 - \frac{194}{125}\frac{1}{r^2}$$
$$+ \frac{327}{500}\frac{1}{r^4} - \frac{14801}{800}\frac{1}{r^6} + \ldots \quad (3.A.24)$$

In these expressions the radius has been taken as the unit length, and the friction unit is $6\pi\eta a$, with $\eta$ being the viscosity of the solvent. The effective friction tensor given in eq.(3.1.2) can be expressed in terms of these functions, giving

$$\vec{\vec{\xi}}_{eff} = X_{11}^A \hat{e}\hat{e} + \left[Y_{11}^A - \frac{(Y_{11}^B)^2}{3Y_{11}^C}\right] \quad (3.A.25)$$

For the situation of a single sphere in the presence of a plane wall, due to the cylindrical symmetry, the effective friction tensor given in eq.(3.1.4) can be decomposed as

$$\vec{\vec{\xi}}^{w}_{eff} = \xi_\perp \hat{z}\hat{z} + \xi_{||}(\vec{\vec{I}} - \hat{z}\hat{z}) \quad (3.A.26)$$

where $\hat{z}$ is a unit vector perpendicular to the wall. The function $\xi_\perp$ is related to the motion of the sphere perpendicular to the plane, its exact expression found by Brenner[9], is

$$\xi_\perp = \frac{4}{3}\sinh\alpha \sum_{n=1}^{\infty} \frac{n(n+1)}{(2n-1)(2n+3)} \left(\frac{2\sinh((2n+1)\alpha) + (2n+1)\sinh(2\alpha)}{4\sinh^2((n+1/2)\alpha) - (2n+1)^2\sinh^2\alpha} - 1\right) \quad (3.A.27)$$

where $\alpha = \text{arc}\cosh(z)$, with $z$ the distance from the center of the sphere to the wall measured in units of te radius of the sphere. Although this function is expressed as an infinite series, in the simulations it was never necessary to compute more than 20 terms of the series to get a good estimate of its value. Close to the wall, the dominant contribution diverges as the inverse of the distance of the bottom of the sphere to the surface,

$$\xi_{\perp} \sim \frac{1}{z-1} \quad , \qquad z \to 1 \tag{3.A.28}$$

The function $\xi_{||}$ is not known exactly. There exist expressions of the function for small and large distances. We have used those given in ref.[10],

$$\xi_{||} = \frac{1}{1 - \frac{9}{16z} + \frac{1}{8z^3} - \frac{45}{256z^4} - \frac{1}{16z^5} + ..} \tag{3.A.29}$$

for $z > 1.1$, and

$$\xi_{||} = -\frac{8}{5}\ln(z-1) + 0.9588 + ... \tag{3.A.30}$$

when $z < 1.1$.

## 3.B The pair distribution function

Let us consider a system composed by $N$ particles. One can define the $n-$particle density function, $\rho^{(n)}(\vec{r}_1, ...\vec{r}_n)$, such that $\rho^{(n)}(\vec{r}_1, ...\vec{r}_n)d\vec{r}_1...d\vec{r}_n$ gives the probability to have the center of a first particle in the volume element $d\vec{r}_1$ centered at $\vec{r}_1$, the center of a second particle in the volume element $d\vec{r}_2$ centered at $\vec{r}_2$,... and the center of an $n-$th particle in the volume element $d\vec{r}_n$ centered at $\vec{r}_n$, irrespective of the positions of the remaining $N-n$ particles. The simplest function of this family is $\rho^{(1)}(\vec{r})$, which represents the probability density of having the center of one particle of the system in the volume element $d\vec{r}$ centered at $\vec{r}$, and is related to the local density of the system.

If there exist no correlations between the different particles of the system, then the probability to find the center of one particle in the volume element centered in $\vec{r}_2$ will be independent of that of finding another particle in the volume element centered at $\vec{r}_1$. Then,

$$\rho^{(n)}(\vec{r}_1,...,\vec{r}_n)d\vec{r}_1 \ ... \ d\vec{r}_n = \rho^{(1)}(\vec{r}_1)d\vec{r}_1 \ ... \ \rho^{(n)}(\vec{r}_n)d\vec{r}_n \qquad (3.B.31\ )$$

In general, the probabilities will not be independent, since correlations between the particles will usually exist, the most obvious one due to the excluded volume associated to the finite size of the particles. Then, one way to account for such correlations is to introduce an $n$-particle distribution function, $g^{(n)}(\vec{r}_1,...,\vec{r}_n)$ such that

$$\rho^{(n)}(\vec{r}_1,...\vec{r}_n) = \rho^{(1)}(\vec{r}_1)...\rho^{(1)}(\vec{r}_n)g^{(n)}(\vec{r}_1,...,\vec{r}_n) \qquad (3.B.32\ )$$

Then, the deviations of $g^(n)$ from unity will account for the existence of correlations in the system, indicating to what extent the structure of the fluid deviates from completely randomness. For homogeneous systems, eq.(3.B.32 ) simplifies to

$$\rho^{(n)}(\vec{r}_1,...\vec{r}_n) = \rho^n g^{(n)}(\vec{r}_1,...,\vec{r}_n) \qquad (3.B.33\ )$$

with $\rho$ being the average density of the system. From the above definition, it is clear that, in the absence of long-range order, all the functions $g^{(n)} \rightarrow 1$ when the mutual separations become large in the thermodynamic limit. Of particular physical relevance is the pair distribution function $g^{(2)}(\vec{r}_1,\vec{r}_2)$. For isotropic systems, it will only depend on the relative distance $r_{12} = |\vec{r}_1 - \vec{r}_2|$. Then, it is more useful to consider the radial distribution function $g(r_{12})$. In equilibrium, the thermodynamics of the system can be deduced from it in the case that the interactions between the particles be pairwise additive. Anyway, this is not our case because we are dealing with nonequilibrium systems.

Nevertheless, the probabilistic interpretation of $g(r)$ relates it with the fluctuations in the number of particles of the system, irrespectively of the fact that the system is

in equilibrium or out of it. Specifically, one has,

$$1 + \rho \int [g(\vec{r}) - 1]\, d\vec{r} = \frac{< N^2 > - < N >^2}{< N >} \qquad (3.B.34)$$

where at the r.h.s.one can recognize $\sigma$, which in equilibrium is related to the isothermal compressibility [38].

Despite the formal definition given above, the pair distribution function can be easily thought of as giving us the number of particles at a distance $r$ from a given one, relative to the number of particles at the same distance in an ideal gas at the same density. This point of view is closer to the way in which $g(r)$ is calculated from a computer simulation[39], and which we have used in the present chapter to calculate $g(r)$.

Once $N$ surfaces (lines) are covered by $N_p$ spheres (disks), and their center positions have been recorded, the minimum separations of all the pairs of particles are calculated in turn up to a maximum distance for each surface (line), which we take as half the size of the system. Then, we introduce a step $\delta r$ which allows us to group these minimum separations into an array. Therefore, we can compute an histogram, $n^{his}(i)$, $i = 1, 2, ...$, which is related to the distance $r$ by $i = \text{int}(r/\delta r)$, int(x) referring to the integer part of x. Once we have constructed the histogram, the average number of particles at a distance $b$ from a given one can be known, since it is given by $n(b) = n^{his}(b)/(N * A)$, where $A$ is the size of the system. The average number of particles in the same volume in an ideal gas at the same density $\rho = N_p/A$ is $n^{id}(b) = \pi\rho((r + \delta r)^2 - r^2)$ for a surface, and $n^{id}(b) = 2\rho\delta r$ for a line. Finally, the radial distribution function is obtained as the quotient of these two quantities, that is, $g(r + \frac{1}{2}\delta r) = n(b)/n^{id}(b)$, and it is evaluated at half the space interval to avoid fluctuations[39].

## 3.C The 2-D Ballistic Model

We will describe in this appendix the two dimensional version of BM[33], since it is used in the III algorithm when the incoming particle is almost touching a preadsorbed

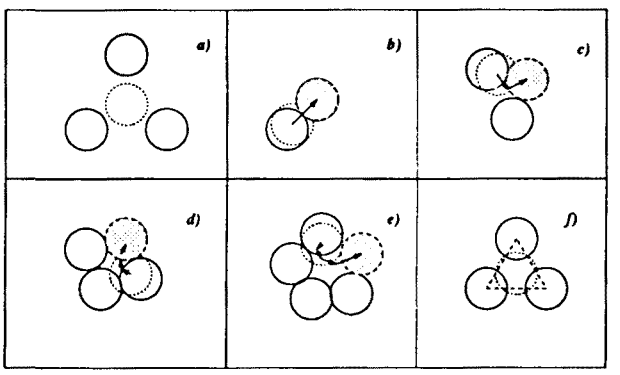


Figure 3.16: Different rolling mechanisms in 2-D BM. The dashed circle is the initial trial position, and the arrows the consecutive movements trying to reach the substrate. Only the last process leads to rejection.

one. It is also employed to simulate BM in order to compare the results with III. An initial position, $\vec{r}_0$, for the center of an incoming sphere is chosen randomly over the area of the adsorbing surface. A greater variety of configurations appear when compared to 1-D BM. The particle may roll over up to five preadsorbed spheres before reaching the surface, existing also the possibility that it gets trapped before arriving at the wall, as shown in fig. 3.16.

If no overlap with a preadsorbed sphere is detected, the incoming particle is irreversibly located at the same position, $\vec{r}_0$ (process a). If an overlap occurs, then it will roll over the adsorbed one following the path of steepest descent, that is, moving radially apart from the adsorbed particle, until being at a distance of one diameter. This results in a new position $\vec{r}_1$. If no overlap occurs, it adsorbs at this new position (process b). If overlap occurs with a second preadsorbed sphere, a new position on the

surface, $\vec{r}_2$ is chosen as the nearer of the two possible points which are one diameter away from the center of the two preadsorbed particles (process c). If overlap occurs at $\vec{r}_2$ with a third preadsorbed particle, and the triangle formed by the three preadsorbed spheres is acute, then the particle is trapped, and it has failed to reach the surface, being rejected (process f). If the triangle is obtuse, a new position $\vec{r}_3$ is tried as the point outside the triangle that is one diameter from the pair of preadsorbed particles which determine the longest side of the triangle (process d). If again, overlap occurs with a fourth particle, if the triangle formed by the center of this fourth one and the two previous ones which determined the longest side of the previous triangle is acute, the particle has been trapped before reaching the wall and is therefore rejected (process f). If the triangle is obtuse, again the new position, $\vec{r}_4$ is chosen as the point outside the triangle that is one diameter from the particles which lie on the extremes of the longest side (process e). If at this new position overlap occurs with a fifth sphere, the particle has got trapped and is rejected (process f).

This constitutes the basis for the computer algorithm of the filling of the surface according to BM rules, which then circumvents the need to explicitly follow the particle trajectory by making small steps along the path of steepest descent, and it is able to locate the incoming particle by looking at its environment.

# References


[1] S. Kim and S.J. Karrila, *Microhydrodynamics: Principles and Selected Applications*, Butterworth-Heinemann, Boston *1991.*

[2] J. Happel and H. Brenner, *Low Reynolds Number Hydrodynamics*, Kluwer Academic Publishers, Dordrecht, *1991.*

[3] D.J Jeffrey and Y. Onishi, J. Fluid Mech **139**, 261 (*1984*).

[4] P. Mazur and W. van Saarloos, Physica A **115**, 21 (*1982*).

[5] J. Bonet-Avalos, J.M. Rubí and D. Bedeaux Macromolecules **26**, 2550 (*1993*).

[6] J. Bonet-Avalos, J.M. Rubí, D. Bedeaux and G.Z. van der Zwan, Physica **A211**, 193(*1994*).

[7] J. Bafaluy, I. Pagonabrraga, J.M. Rubí and D. Bedeaux, Physica **A213**, 277 (*1995*).

[8] G.K. Batchelor *Fluid Mechanics*, Oxford University Press, Oxford *1972.*

[9] H. Brenner, Chem. Eng. Sci. **16**, 242 (*1961*).

[10] A.J. Goldmann, R.G. Cox and H. Brenner, Chem. Eng. Sci. **16**, 637 (*1967*).

[11] G.S. Perkins and R.B. Jones, Physica A **189**, 447 (*1992*).

[12] C.W.J. Beenakker and P. Mazur, Physica A **120**, 398 (*1983*).

[13] P. Vasseur and R.G. Cox, J. Fluid Mech. **80**, 561 (*1977*).

[14] T. Dabros and T.G.M. Van de Ven, Int. J. Multiphase Flow **18**, 751 (*1992*).

[15] I. Pagonabarraga and J.M. Rubí, in preparation.

[16] S. Weinbaum, P. Ganatos and Z.Y. Yan, Annu. Rev. Fluid Mech. **22**, 275 (*1990*).

[17] G. Bossis and J.F. Brady, J. Chem. Phys. **80**, 5141 (*1984*).

[18] J.F. Brady and G. Bossis, Ann. Rev. Fluid Mech. **20**, 111 (*1988*).

[19] G. Bossis and J.F. Brady, p.119 in *Hydrodynamics of Dispersed Media*, eds. J.P. Hulin, A.M. Cazabat, E. Guyon, F. Carmona, Elsevier Sci. Publs., North Holland, *1990*.

[20] D.L. Ermak and J.A. McCammon, J. Chem. Phys. **69**, 1352 (*1978*).

[21] A.J.C. Ladd, J. Chem. Phys. **95**, 3484 (*1990*); A.J.C. Ladd and D. Frenkel, Phys. Fluids, **2**, 1921 (*1990*)

[22] A.S. Sangani and G. Mo, Phys. Fluids **6**, 1653 (*1994*).

[23] X.F. Yuan and R.C. Ball, J. Chem. Phys. **101**, 9016 (*1994*).

[24] F.J. Bafaluy, B. Senger, J.C. Voegel and P. Schaaf, Phys. Rev. Lett. **70**, 623 (*1993*).

[25] J. Talbot and S. Ricci, Phys. Rev. Lett. **68** 958 (*1992*).

[26] P. Wojtaszczyk, P.Schaaf,B. Senger, M. Zembala and J.-C. Voegel, J. Chem. Phys. **99**, 7198 (*1993*).

[27] C.W.J. Beenakker, J. Chem. Phys. **85**, 1581 (*1986*) (see ref. 6).

[28] M. Abramowitz and I.A. Stegun, *Handbook of Mathematical Functions*, Dover Publishers, New York *1972*.

[29] Hamaker, Physica (*1940*)

[30] J. Israelachvilii, *Forces*, Academic Press, London *1992*

[31] Joosten, J. Chem. Phys. , (*1992*).

[32] B. Senger, P. Schaaf, Europh. Lett. , (*1992*).

[33] A.P. Thompson and E.D. Glandt, Phys. Rev. A **46**, 4639 (*1992*); H.S. Choi, J. Talbot, G. Tarjus and P. Viot, J. Chem. Phys. **99**, 9296 (*1993*).

[34] R. Jullien and P. Meakin, J. Phys. A **25**, L189 (*1992*).

[35] I. Pagonabarraga, P. Wojtaszczyk, M. Rubí, B. Senger, P. Schaaf and J.-C. Voegel, (in preparation).

[36] P. Wojtaszczyk, PhD dissertation CNRS Strasbourg (*1995*).

[37] M.T. Haarmans and D. Bedeaux, Thin Solid Films **224**, 117 (*1993*).

[38] J.-P. Hansen and I.R. McDonald, *Theory of Simple Liquids*, Academic Press, London *1991*; T.L Hill, *Statistical Mechanics Principles and Selected Applications*, Dover ().

[39] M.P. Allen and D.J. Tildesley, *Computer Simulations of Liquids*, Clarendon Press, Oxford (*1987*).

# Chapter 4

# Continuum Description of the Adsorption Process

In the previous chapters we have studied the adsorption of colloids from a *microscopic* scale, so that we were able to follow the movement of the colloidal particles themselves. We employ the word *microscopic* to emphasize that in adsorption there are basically two length scales of interest: on the one hand, the characteristic length of the interaction potential between the wall and the particles (which is also of the order of the size of the colloids), $l$,and on the other hand the macroscopic length scale $L$, at which bulk gradients change.

When describing the transport and configurational processes associated with a liquid-solid interface at this *microscopic* scale, it is not necessary to introduce any specific property associated to the interface. Apart from introducing an attractive potential close to the wall, one can use the same concepts as for unbounded fluids. For example, if diffusion is considered, the dynamics can be expressed in terms of the appropriate Smoluchowski equation, and the behavior close to the interface is enough to characterize the properties of the system near the interface.

On the contrary, in a thermodynamic theory, one is interested in describing the

system at the macroscopic scale $L$. In this case, one is forced to treat the interface as a new phase. Then, one has to introduce new physical quantities, such as adsorption or surface diffusion, which are specifically associated with the interface, as distinct from the bulk phase[1].

Consider, as a simple example, a suspension of Brownian spheres of radius $a$ in the presence of a wall, neglecting excluded-volume effects for the moment. From a *microscopic* point of view, it is clear that the attractive surface force will produce a non-homogeneous distribution of particles as we move perpendicular to the interface. Let us focus in more detail on the variation of the local number density of particle centers, which we will call $c$, as a function of the distance to the interface, $y$. For $y < a$, obviously $c = 0$, and far from the wall the bulk concentration $c_\infty$ should be reached. In fact, since the interaction potential is of order $l$, deviations from $c_\infty$ will be observed for $y \sim \mathcal{O}(l)$. Note, however, that in the absence of Brownian motion, eventually all the particles will finish their motion at the minimum of the attractive wall potential, $y_m$, yielding a concentration profile,

$$c \sim \delta(y - y_m) \tag{4.0.1}$$

Brownian motion will smooth out this sharp profile, producing a Boltzmann-like distribution with a large peak at $y = y_m$, which relaxes to its bulk value at distances large compared to the attractive potential decay length. Then, from this *microscopic* point of view, there is no new phenomenon which can be identified with adsorption. At this level of description, there is a continuous variation in the solute number density $c(y)$ with distance, although with a large maximum at $y_m$. Therefore, this implies that adsorption, as a new physical phenomenon, can only have a meaning when the system is viewed at a *macroscopic* or continuum length scale $L$.

At such *macroscopic* level of description, the bulk concentration at a point in the bulk is measured experimentally averaging a probe of a length $h$, small compared to $L$, but large enough to retain statistically a large number of particles in the probe. It is clear that such a probe will not resolve the very local concentration variations near the wall. Only the bulk value $c_\infty$ will be obtained for any $y$. Then, it is only through the discrepancy between the actual number of solute particles initially put in the system, and the number obtained taking $c = c_\infty$ for all $y$, which is called the

excess density, that information on the adsorption can be obtained. Therefore, this "excess" quantity is introduced merely in order to account for the total solute number of particles solely in terms of the point concentration values which are relevant at the macroscale. Finally, the inability to distinguish between the wall and the region of extent $\mathcal{O}(l)$ close to it, when the whole system is viewed with resolution $\mathcal{O}(L)$, leads to adscribe the "excess" of solute to the bounding surface.

Alternatively, one can consider the surface effect as accounting for discrepancies that would otherwise be observed between experiments on real bounded systems, which, at the thermodynamical level of description, would give a value of the density $d(\vec{r},t)$, and the predicted outcome of such experiments based upon the assumption of physicochemically inert boundary, giving $d^+(\vec{r},t)$. The "excess" density can be then expressed as the difference of both quantities, $d_{ex}(\vec{r},t) = d(\vec{r},t) - d^+(\vec{r},t)\Theta(\vec{r},t)$, where $d^+(\vec{r},t)$ accounts for the "bulk" density for an inactive interface, and $\Theta(\vec{r},t)$ is the characteristic function of the bulk phase, which is 1 in the bulk fluid, and 0 otherwise. Bedeaux *et al.* [2] showed that an alternative description of the interfacial phenomena at the thermodynamical level, would be to consider the interface as a surface of discontinuity (in our case the wall) in equilibrium with the bulk phase. Then, $d(\vec{r},t)$ at any point of the space can be written as $d(\vec{r},t) = d^+(\vec{r},t)\Theta(\vec{r},t) + d^s(\vec{r},t)\delta^s(\vec{r},t)$, where $d^s(\vec{r},t)$ the value of the density at the new phase, and $\delta^s(\vec{r},t)$ the characteristic function for the surface of discontinuity. Albano *et al.* [3] later showed that the formulation in terms of excess quantities was equivalent to the latter one, where the contributions appearing in the surface of discontinuity can be expressed as integrals of the excess ones.

Our purpose in this chapter is to address the adsorption phenomena at the continuum level. Instead of particles, we will talk now of concentration profiles, where the relevant transport process are diffusion in the bulk and in the surface. Moreover, due to the existence of attractive forces between the wall and the suspended particles, we should take into account that diffusion takes place in the presence of a potential field close to the interface. Different qualitative situations will be found depending on the nature of this attractive potential. In the case of suspensions, London-van der Waals forces give rise to an attractive potential, but there also exists a repulsive contribution at very short distances due to Born forces, whereas at larger distances double layer forces must be considered. If the first two contributions dominate, then the potential

can be regarded as purely attractive, as shown in fig. 4.1a), and it is usually the case for aerosols[8]. In this situation, adsorption from the bulk is controlled by usual diffusion[4][5]. On the contrary, if double layer forces are present, there will be a maximum in the energy potential, as usually found in hydrosols[8]. Therefore, the diffusing particles will have to overcome a potential barrier before being adsorbed at the wall[4][6][7], see fig.4.1b). In this last case, depending on the balance between the repulsive and attractive forces, there may appear a secondary minimum near the wall before overcoming the energy barrier, and two adsorbed states will coexist in the interface.

We will use non-equilibrium thermodynamics formalism to deduce the mass balance equations for the adsorbed phase, as well as its coupling to the bulk phase, in the case in which the transport to the interface is controlled by the attractive energy potential, which exhibits a maximum. We will generalize the standard formalism to take into account non-linear relations between the thermodynamic flux and force. We will then take advantage of the thermodynamic formalism to derive the appropriate fluctuation-dissipation theorem, and we will see which applications can have in the study of steady adsorbed states.

## 4.1 Adsorption as an Activated Process

Non-equilibrium thermodynamics provides a general framework which allows to identify the relevant thermodynamic fluxes and forces, once the appropriate expression for the local entropy production is formulated, and then obtain general linear relations between them. Such relations are appropriate to describe transport processes, such as diffusion. However, in relaxation processes, non-linear relations between fluxes and forces are known to hold, as for example the law of mass action in chemical reactions. Prigogine and Mazur[10][12] devised a general method to obtain non-linear relations between fluxes and forces within non-equilibrium thermodynamics by introducing an additional degree of freedom to the system.

Let us consider the particualr case of the unimolecular chemical reaction $A \rightleftharpoons B$. They considered that the chemical reaction should be regarded as a series of coupled

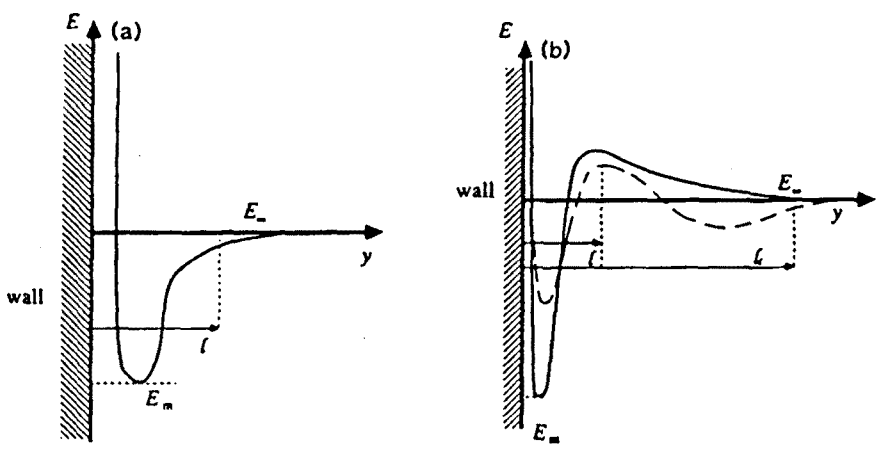


Figure 4.1: Examples of interfacial potentials. a) Purely attractive potential b) Appearence of a potential barrier due to the competition between attractive and repulsive forces (—) a single interfacial minimum exists, and (- - -) appearence of a secondary minimum in the interfacial region.

intermediate reactions $A_1 \rightarrow A_2 \rightarrow ... \rightarrow A_n$, where $A_i$ describe intermediate products $i$, and where $A_1$ corresponds to the actual reactant $A$, and $A_n$ to the actual product $B$. In the image of the activated complex theories of chemical reactions[15] the intermediate reactions can be thougth of as different internal configurations of the activated comples. If we denote $c_i$ the mass fraction of the component $A_i$, its corresponding mass balance equation, as deduced from non-equilibrium thermodynamics gives

$$\rho_t \frac{dc_i}{dt} = -\nabla \cdot \vec{J}_i + J_{i-1} - J_i \tag{4.1.2}$$

with $\vec{J}_i$ being the mass diffusion flux, and $J_i$ refers to the reaction rate associated to reaction $i$. If one lets now the index $i$ vary continuously[1], indicating that there exists an infinite series of intermediate reactions between $A$ and $B$, the balance eq.(4.1.2) becomes

$$\rho_t \frac{dc(\gamma)}{dt} = -\nabla \cdot \vec{J}(\gamma) - \frac{\partial J(\gamma)}{\partial \gamma} \tag{4.1.3}$$

A new variable $\gamma$ is introduced, referred to as an *internal variable*, and the flux along this new variable can be interpreted as a diffusion flux for going from $A$ to $B$. In appendix4.A, we describe the formulation of non-equilibrium thermodynamics in the presence of an internal variable, and show how in general, non-linear relations between fluxes and forces are obtained, and in the particular case of a chemical reaction, it leads naturally to the law of mass action.

Note that, according to our previous interpretation in which the different "chemical" constituents of the coupled chemical reactions correspond to the different states of the activated complex when going from the reactant to the product state, passing through an intermediate state with a maximum energy, which corresponds to the "activated state", this limit of taking an infinite number of intermediate chemical species can be thought as if the chemical reaction is characterized by very smooth activated complex configurational changes.

[1] This technique has also been applied to describe the kinetics of the liquid→vapor phase transition in its relation to nucleation theory[11]

Kramers[9] showed that a chemical reaction could be treated as the thermally activated passage of an energy barrier. We are interested in describing the diffusion across an energy barrier, of the type shown in fig.4.1b). As we have seen in the previous chapters, we expect to obtain non-linear relations between the flux of particles across the energy barrier and the concentration of adsorbed particles. Therefore, we will use Kramers' analogy in the opposite sense, and we will consider the diffusion in the presence of an energy barrier as a chemical reaction. This will allow us to use a thermodynamic formalism in which general non-linear relations between fluxes and forces can be obtained.

The basic difference we will found in the adsorption with respect to what has been explained for chemical reactions is that now the activated process is localized at the interface. As explained in the introduction, at the thermodynamic level, the interfacial phenomena should be introduced carefully. We will follow the formalism developed by Bedeaux *et al.*[2], hereafter referred to as BAM, in which the interface is located at the surface of separation between the two bulk phases, and in appendix4.B we summarize the basic assumptions of BAM.

### 4.1.1 Thermodynamic description of the system

We will consider a bulk phase in contact with a wall. The suspension of colloidal particles is described as a binary mixture, which is characterized by the local concentration of particles, $\rho(\vec{r})$, or its mass fraction $c(\vec{r}$. According to BAM's formalism, these quantities have a buk and a surface component, accounting for the existence of a wall in contact with the bulk.

We have shown in the previous section that an internal variable has to be introduced to describe properly the chemical reaction which takes place at the interface,as a model of the diffusion across an energy barrier. However, we will derive explicitely the internal variable again, because now new couplings between the bulk and the interface will appear. Then, in order to deal with the chemical reaction at the interface we will follow the method described in the previous section, in which an mixture constitued by $n$ species is considered, characterized by the mass fractions $c_i$, $i = 1, ..., n$, and where only $c_1$ and $c_n$ correspond to actual mass fractions of suspended and ad-

sorbed particles. We will now decompose all the physical quantities in their bulk and surface component. For example, the mass fractions will be expressed as[2]

$$c_i(\vec{r},t) = c_i^+(\vec{r},t)\Theta^+(\vec{r},t) + c_i^s(\vec{r},t)\delta^s(\vec{r},t) \tag{4.1.4}$$

For simplicity's sake, the wall will be assumed to be flat, and its position will coincide with the origin of heights, $z = 0$. Additionally, it will be assumed at rest. In this conditions, $\Theta^+(\vec{r},t) = \theta(z)$, and $\delta^s(\vec{r},t) = \delta(z)$, $\theta(\vec{r})$, and $\delta(\vec{r})$ being the Heaviside and the delta functions, respectively. Moreover, $c_i^+$ refers to the mass fraction of component $i$ in the bulk phase, while $c_i^s$ gives the mass fraction of the same component on the interface.

As we have already explained, the chemical reaction is localized in the interface. According to this idea, we will take $c_i^+(\vec{r},t) = 0$ for $i > 1$, but $c_1^s$ is in principle different from zero. Regarding the dynamics at the surface, according to the previous picture, a chain reaction $c_1^s \rightarrow c_2^s \rightarrow ... \rightarrow c_n^s$ will exist.

We can now derive the corresponding mass balance equation for this system. According tp BAM's formalism the global balance equations have the same form that the ones for unbounded systems. In particular, the mass balance equation for a mixture of $n$ components, where $n-1$ reactions take place is of the form

$$\frac{\partial \rho_k}{\partial t} + \nabla \cdot (\rho_k \vec{v}_k) = \sum_{j=1}^{n-1} \nu_{kj} J_j \qquad , k = 1, ..., n \tag{4.1.5}$$

where $\rho_k$ stands for the density of the $k$-th component, $\vec{v}_k$ its velocity, $\nu_{kj}J_j$ refers to the rate of production of component $k$ in reaction $j$, $\nu_{jk}$ divided by the molecular mass of component $k$ being proportional to the corresponding stoichiometric coefficient with which $k$ appears in reaction $j$. From the global balance equation one can derive the balance equations for the bulk and the interface, if the different physical quantities are decomposed in thei bulk and interface contributions, as in eq.(4.1.4. Both[13] and [14] derived such balance equations for the case in which chemical reactions are present in the bulk and the interface. In our case, one arrives at

$$\frac{\partial \rho_i^+(\vec{r},t)}{\partial t} = -\nabla \cdot (\rho_i^+ \vec{v}_i^+(\vec{r},t)) \tag{4.1.6}$$

$$\frac{\partial \rho_i^s(\vec{r},t)}{\partial t} = -\nabla \cdot (\rho_i^s \vec{v}_i^s(\vec{r},t)) - [\rho_i(v_{i,n} - v_n^s]_- + \sum_{j=1}^{n-1} \nu_{ji} J_i^s \tag{4.1.7}$$

The first equation is the usual balance equation valid in the bulk[12], while the interfacial balance equation contains an additional term accounting for the flux of mass arriving from the bulk to the surface. The subscript $-$ indicates that one should evaluate the quantity in brackets at both sides of the interface at contact with it, and substract them. In this case, since one of the bulk phases is the solid, where the relevant thermodynamic fields are assumed constant, this term reduces to the value of the magnitude in brackets in the fluid phase, evaluated at the interface. Moreover, in our case the interface does not move, and then, according to eq.(4.B.123 ), $v_n^s = 0$. In this case, the term in brackets gives directly the component of the bulk mass flux perpendicular to the interface, evaluated at contact with it, accounting for the mass interchange between the bulk and the wall.

After summing over all $i$, eqs.(4.1.6)-(4.1.7) give the balance equation for the total volume and surface densities, $\rho^+$ and $\rho^s$,

$$\frac{\partial}{\partial t}\rho^+ + \nabla \cdot (\rho^+ \vec{v}) = 0 \tag{4.1.8}$$

$$\frac{\partial}{\partial t}\rho^s + \nabla \cdot (\rho^s \vec{v}) + \rho^+(v_n^+ - v_n^s) = 0 \tag{4.1.9}$$

where $\vec{v}^+$ and $\vec{v}^s$ are the surface and fluid baricentric velocities, respectively, which in our case are zero, since we are assuming for simplicity that the both bulk and interfacial fluid are at rest.

It is more useful to write the mass balance equations (4.1.6)-(4.1.7) in terms of the mass fractions $c_k$, introduced above, and which are defined as

$$c_k^+ = \frac{\rho_k^+}{\rho^+} \qquad , c_k^s = \frac{\rho_k^s}{\rho^s} \tag{4.1.10}$$

If we introduce the bulk and interfacial diffusion fluxes

$$\vec{J}_k^+ \equiv \rho_k^+(\vec{v}_k^+ - \vec{v}^+) \qquad , \vec{J}_k^s \equiv \rho_k^s(\vec{v}_k^s - \vec{v}^s) \tag{4.1.11}$$

then, after using eqs.(4.1.8)-(4.1.11) and the above definitions in eqs.(4.1.6)-(4.1.7) one arrives at

$$\rho^+ \frac{d^+}{dt} c_1^+ + \nabla \cdot \vec{J}_1^+ = 0 \tag{4.1.12}$$

$$\rho^s \frac{d^s}{dt} c_k^s + \nabla \cdot \vec{J}_k^s + \vec{n} \cdot \vec{J}_k^+ = \sum_{j=1}^{n-1} \nu_{kj} J_j^s \tag{4.1.13}$$

where $\frac{d^{+,s}}{dt}$ is the baricentric time derivative in the corresponding phase, the superscript indicating which baricentric velocity should be considered. For fluids at rest, this derivative coincides with the partial time derivative. In eq.(4.1.12) we have explicitely expressed the fact that in the bulk there is a single diffusing species, while in the surface there is an ensemble of species, which will be related later on with the interfacial coupled chemical reactions. Note that due to the definition of the diffusion fluxes and that of baricentric velocity, $\sum_{k=1}^{2} \vec{J}_k^+ = \sum_{k=1}^{n} \vec{J}_k^s = 0$, which implies that in the bulk and interfacial phases there are only 1 and $n-1$ independent diffusion fluxes, respectively.

Non-equilibrium thermodynamics lies on the basis that out of equilibrium, locally equilibrium is fullfilled, and that therefore, a Gibbs relation can be locally formulated. BAM's formulation also relies on the fact that out of equilibrium, a Gibbs relation is satisfied locally both in the bulk and in the interface, as shown in appendix 4.B, eqs.(4.B.129 )-(4.B.130 )). If both thermal and viscous effects can be neglected and the surface density is assumed constant, the Gibbs relations read

$$T \frac{d^+ s^+}{dt} = -\mu_1^+ \frac{d^+ c_1^+}{dt} \tag{4.1.14}$$

$$T \frac{d^s s^s}{dt} = -\sum_{k=1}^{n-1} \mu_k^s \frac{d^s c_k^s}{dt} \tag{4.1.15}$$

where $s^+$ is the entropy per unit mass in the fluid, and $s^s$ the entropy per unit mass in the surface. The entropy per unit mass at the bulk and at the interface will satisfy balance equations of the same kind that eqs.(4.B.121 ) and (4.B.122 ). Therefore,

$$\rho^+ \frac{d^+ s^+}{dt} = -\nabla \cdot \vec{J}_s^+ + \sigma^+ \tag{4.1.16}$$

$$\rho^s \frac{d^s s^s}{dt} = -\nabla \cdot \vec{J}_s^s - J_{sn}^+ + \sigma^s \tag{4.1.17}$$

with $\vec{J}_s$ and $\sigma$ being the entropy flux and entropy production, respectively.

Substituting eqs.(4.1.12) and (4.1.13) in eqs.(4.1.14) and (4.1.15), and comparing their form with the one predicted by the balance equations (4.1.16) and (4.1.17), one can identify the entropy fluxes,

$$\vec{J}_s^+ = -\frac{1}{T}\mu_1^+ \vec{J}_1^+ \tag{4.1.18}$$

$$\vec{J}_s^s = -\frac{1}{T}\sum_{k=1}^{n-1} \mu_k^s \vec{J}_k^s \tag{4.1.19}$$

as well as the terms of entropy productions

$$\sigma^+ = -\frac{1}{T}\vec{J}_1^+ \cdot \nabla \mu_1^+ \tag{4.1.20}$$

$$\sigma^s = -\frac{1}{T}\sum_{k=1}^{n-1} \vec{J}_k^s \cdot \nabla \mu_k^s - \frac{1}{T}\sum_{r=1}^{n-1} J_r^s A_r^s - \frac{1}{T}\sum_{k=1}^{n-1} J_{kn}^+ (\mu_k^+ - \mu_k^s)\delta_{k,1} \tag{4.1.21}$$

where $A_r^s = \sum_{j=1}^{n-1} \mu_j^s \nu_{jr}$ is the affinity of reaction $r$, and $\delta_{a,b}$ is the Kronecker delta function. The entropy production accounts for all the irreversible processes taking place in the system, namely, diffusion, surface diffusion, surface chemical reactions, and diffusion from the bulk to the interface. The entropy production and Curie's

symmetry principle, according to which only those quantities having the same tensorial character can be coupled, applied both at the bulk and interface, allows to derive the phenomenological equations, relating linearly the fluxes and forces,

$$\vec{J}_1^+ = -\vec{\vec{L}}^+ \cdot \nabla \mu_1^+ \tag{4.1.22}$$

$$\vec{J}_k^s = -\sum_{i=1}^{n-1} L_{ki}^s \nabla \mu_i^s \tag{4.1.23}$$

$$J_r^s = -\sum_{i=1}^{n-2} L_{ri}^{(1)} A_i^s - \sum_{i=1}^{n-1} L_{ri}^{(2)} (\mu_i^+ - \mu_i^s)\delta_{i,1} \tag{4.1.24}$$

$$J_{1n}^+ = -\sum_{i=1}^{n-2} L_{1i}^{(3)} A_i^s - L_{11}^{(4)} (\mu_1^+ - \mu_1^s) \tag{4.1.25}$$

where $L_{ki}^+$, $L_{ki}^s$, and $L_{ij}^{(p)}, p = 1, ..., 4$ are phenomenological coefficients which, due to Onsager's symmetry principle, satisfy the relations $L_{ij}^+ = L_{ji}^+$, $L_{ij}^s = L_{ji}^s$, $L_{ij}^{(1)} = L_{ji}^{(1)}$, $L_{ij}^{(2)} = L_{ji}^{(3)}$, and $L_{ij}^{(4)} = L_{ji}^{(4)}$, although only a fraction of them appear in the previous equations because different number of species are present in the bulk and the interface. While eqs.(4.1.22) and (4.1.23) correspond to Fick's law in the solution and at the surface, respectively, eq.(4.1.24) relates the reaction rate both to the corresponding affinities and to the mass flux from the bulk at the interface. Note that such a coupling can only appear at the interface, because in the bulk the mass flux and the reaction rate have different tensorial character. Finally, eq.(4.1.25) can be interpreted as the boundary condition for the perpendicular component of the mass flux of the fluid at the interface.

### 4.1.2 Non-equilibrium thermodynamics of the adsorbing surface

In order to describe the diffusion across the surface energy barrier we have to let the number of intermediate interfacial chemical species go to infinity. As explained at the beginig of the chapter, then the chemical reaction is equivalent to the diffusion across

an energy barrier. Note that the formalism we are formulating does not depend too much on the specific form of the potential. The only requirement is that it has an barrier large compared with $k_BT$, to ensure that it controls the diffusion towards the adsorbed state. Note that since the interfacial potential is characterized by a maximum, the density will be concentrated at the minima, which constitute the significant thermodynamic states[12]. If there is only one relative minimum, then there will be only one thermodynamic phase. If it has a secondary relative minimum before crossing the barrier, then two thermodynamic adsorbed states will exist. Obviously, the state appearing due to the secondary minimum will lead to a more mobile adsorbed phase.

In this continuum limit, the label identifying the chemical species, $k$, becomes the internal degree of freedom, $\gamma$, which is a continumm variable. This internal variable will be defined in a finite interval. However, due to the form of the potential, we know that the thermodynamic properties will be controlled by the values of the magnitudes around the energy minima. Therefore, we may restrict the values of $\gamma$ to a segment in which its initial value, which we will call $\gamma_i$, corresponds either to the secondary minimum, or to a certain initial configuration, and its final value, $\gamma_f$, will be taken equal to the value corresponding to the minimum close to the surface.

We should reformulate then the results of the previous section in this continuum limit. Both the balance equations for the density and the entropy in the bulk phase are not affected by this modification. The balance equation for the surface concentration eq.(4.1.13) will now read

$$\rho^s \frac{d^s c^s(\gamma)}{dt} = -\nabla \cdot \vec{J}^s(\gamma) - J_n^+ \delta(\gamma - \gamma_i) - \frac{\partial}{\partial \gamma} J^s(\gamma) \tag{4.1.26}$$

where $J_n^+$ is the component of the bulk diffusion flux normal to the surface evaluated on it. For the chemical reaction we are considering in which only two species are involved in each reaction, the stoichiometric coefficients are $\nu_{kr} = -\delta_{k,r} + \delta_{k-1,r}$. Then, for the component $k$ the contribution of the reactions to its balance equation

can be expressed as

$$\sum_{k=1}^{n-1} \nu_{kr} J_r^s = -\frac{J_k^s - J_{k-1}^s}{k-(k-1)} \rightarrow -\frac{\partial}{\partial \gamma} J^s(\gamma) \tag{4.1.27}$$

which corresponds to the last term appearing in eq.(4.1.26). The surface Gibbs equation (4.1.17) is now

$$T\frac{d^s s^s}{dt} = -\int_{\gamma_i}^{\gamma_f} \mu^s(\gamma)\frac{d^s c^s(\gamma)}{dt} d\gamma \tag{4.1.28}$$

After substituting eq.(4.1.27) in eq.(4.1.28) one then obtains

$$\begin{aligned} \rho^s \frac{ds^s}{dt} &= \frac{1}{T}\int_{\gamma_i}^{\gamma_f} \mu^s(\gamma)\nabla \cdot \vec{J}^s(\gamma) d\gamma + \frac{1}{T}\int_{\gamma_i}^{\gamma_f} \mu^s(\gamma)\frac{\partial}{\partial \gamma} J^s(\gamma) d\gamma \\ &+\frac{1}{T}\mu^s(\gamma) J_n^+ \delta(\gamma - \gamma_i) = -\vec{\nabla}_{\|} \cdot \vec{J}_s^s - \frac{1}{T}\int_{\gamma_i}^{\gamma_f} \vec{J}^s(\gamma) \cdot \vec{\nabla}_{\|}\mu^s(\gamma) d\gamma \\ &-\frac{1}{T}\int_{\gamma_i}^{\gamma_f} J^s(\gamma)\partial_\gamma \mu^s(\gamma) d\gamma + \frac{1}{T}\mu^s(\gamma) J_n^+ \delta(\gamma - \gamma_i) \end{aligned} \tag{4.1.29}$$

in which we have used the fact that the total density $\rho^s$ does not depend on $\gamma$ and that $J^s(\gamma)$ vanishes at the extrema of the definition domain of $\gamma$ [12]. Moreover, we have used the expression of the entropy flux in terms of the diffusion fluxes eq.(4.1.19) in the continuum limit

$$\vec{J}_s^s \equiv -\frac{1}{T}\int_{\gamma_i}^{\gamma_f} \mu^s(\gamma)\vec{J}^s(\gamma) d\gamma \tag{4.1.30}$$

Despite the entropy balance equation is obtained as a global quantity in the internal space, eq.(4.1.17), we will assume that local equilibrium is satisfied also locally in the internal configuration space, on the basis that the introduction of such a continuum variable was related with the idea that configurational changes had to be

smooth. Then, we introduce both an entropy flux and entropy production local in the space of internal configurations

$$\rho^s \frac{ds^s}{dt} = \int_{\gamma_i}^{\gamma_f} \left\{ -\vec{\nabla}_{\|} \cdot \vec{J}_s^s(\gamma) - J_{sn}^+ \delta(\gamma - \gamma_i) + \sigma^s(\gamma) \right\} d\gamma \tag{4.1.31}$$

Comparing then the balance eq.(4.1.31) with Gibbs eq.(4.1.29), and using the idea that equilibrium holds locally in the space of configurations[2], as expressed in eq.(4.A.97 ), we can identify both a local surface entropy flux

$$\vec{J}_s^s(\gamma) = -\frac{1}{T} \mu^s(\gamma) \vec{J}^s(\gamma) \tag{4.1.32}$$

and a local surface entropy production

$$\begin{aligned} \sigma^s(\gamma) &= -\frac{1}{T} \vec{J}^s(\gamma) \cdot \nabla \mu^s(\gamma) - \frac{1}{T} J^s(\gamma) \frac{\partial}{\partial \gamma} \mu^s(\gamma) \\ &\quad -\frac{1}{T} J_n^+ \left[ \mu^+ - \mu^s(\gamma) \right] \delta(\gamma - \gamma_i) \geq 0 \end{aligned} \tag{4.1.33}$$

instead of eq.(4.1.21). Again, use of Curie's principle for isotropic system allows us to obtain the corresponding phenomenological equations in the internal space

$$\vec{J}^s(\gamma) = -\vec{\vec{L}} \cdot \nabla \mu^s(\gamma) \tag{4.1.34}$$

$$J^s(\gamma) = -L_{11}(\gamma) \frac{\partial}{\partial \gamma} \mu^s(\gamma) - L_{12}(\gamma) \left[ \mu^+ - \mu^s(\gamma) \right] \delta(\gamma - \gamma_i) \tag{4.1.35}$$

$$J_n^+ = \left( -L_{21}(\gamma) \frac{\partial}{\partial \gamma} \mu^s(\gamma) - L_{22}(\gamma) \left[ \mu^+ - \mu^s(\gamma) \right] \right) \delta(\gamma - \gamma_i) \tag{4.1.36}$$

instead of eqs.(4.1.22)-(4.1.24). The phenomenological coefficients $L_{ij}$ may in general depend on the internal coordinate, and due to Onsager's symmetry principle, they satisfy the corresponding relations showed in the previous section.

[2]This is tantamount assuming that a local Gibbs relation in internal space can be formulated

Using the fact that $d\mu^s(\gamma) = \frac{\partial \mu^s(\gamma)}{\partial c^s(\gamma)} dc^s(\gamma)$ , we can write eq.(4.1.34) as the Fick's law at the interface

$$\vec{J}^s(\gamma) = -D^s(\gamma)\nabla c^s(\gamma) \tag{4.1.37}$$

where the diffusion coefficient is given by

$$D^s(\gamma) = L(\gamma)\frac{\partial \mu^s(\gamma)}{\partial c^s(\gamma)} \tag{4.1.38}$$

and, although it may, in general, depend on position and configuration, it is assumed to be constant, as usual[12].

Having obtained explicit expressions for the different fluxes, eqs.(4.1.34)-(4.1.36), we can rewrite the surface mass fraction balance equation (4.1.26) as

$$\begin{aligned} \rho^s \frac{dc^s(\gamma)}{dt} &= \nabla \cdot (D^s(\gamma)\nabla c^s(\gamma)) + \frac{\partial}{\partial \gamma} L_{11}(\gamma)\frac{\partial}{\partial \gamma}\mu^s(\gamma) \\ &\quad + \left[ L_{12}(\gamma)\frac{\partial}{\partial \gamma}\mu^s + (L_{22} + L_{12})(\mu^+ - \mu^s(\gamma)) \right] \delta(\gamma - \gamma_i) \end{aligned} \tag{4.1.39}$$

where Onsager's symmetry principle has been used. This equation describes the evolution of the surface concentration for an unspecified value of the internal coordinate $\gamma$, reflecting the fact that the variation in time of the $\gamma$-particle surface concentration is the result of three diffusion processes, namely, diffusion along the surface, diffusion through the internal configurational space, and mass exchange with the bulk. For an ideal system, one usually has a constant diffusion coefficient $D^s$, but we leave it yet as an unspecified function. Although with this formalism general balance equations are derived for the evolution of any internal variable, only the quantities corresponding to the minima of the attractive potential will be thermodynamically relevant.

### 4.1.3 Derivation of the kinetic adsorption equation

The results obtained in the previous section are quite general, in the sense that they can be applied even if the energy barrier is not too large. We have emphasized this feature because we are interested in the adsorption controlled by the surface energy potential. If the barrier is large, equilibrium between the bulk phase and the state at $\gamma_i$ will be achieved faster than any other equilibrium within the surface[5]. Then, we can set

$$\mu^+ = \mu^s(\gamma = \gamma_i) \tag{4.1.40}$$

which reduces the phenomenological equations (4.1.35)-(4.1.36) to

$$J^s(\gamma) = -L_{11}(\gamma)\frac{\partial}{\partial\gamma}\mu^s(\gamma) \tag{4.1.41}$$

$$J_n^+ = -L_{21}(\gamma)\frac{\partial}{\partial\gamma}\mu^s(\gamma)\delta(\gamma - \gamma_i) \tag{4.1.42}$$

Note that for $\gamma = \gamma_i$ these equations imply that the flux of mass from the bulk is proportional to the flux of mass disappearing from the state $\gamma = \gamma_i$ due to diffusion through the energy barrier. This can be intrepeted by saying that, once equilibrium between the bulk phase and the internal configuration in closer contact with it has been achieved, then the mass coming from the bulk is determined by the amount that disappears from this surface state diffusing to the more bounded state, closer to the solid surface.

In reaction-rate theory[9] [18], it is well-known that when diffusion takes place through a potential barrier large compared with $k_BT$, a quasistationary state is reached in which the flux becomes practically constant, its value being controlled by the dynamics of the system in the neighborhood of the potential maximum. This implies that, in our case, the diffusion flux through the energy barrier can be expressed as

$$J^s(\gamma, t) = J^s(t)\,[\theta(\gamma - 1) - \theta(\gamma - m)] \tag{4.1.43}$$

where, as we have already used, we take into account that the flux should vanish at the limits of the configurational space[12]. $J^s(t)$ is a reaction rate, showing that due to quasistationarity, mass is transported uniformly along the internal space. In this case, the phenomenological equations (4.1.41)-(4.1.42) show that the flux of mass coming from the bulk is proportional to the reaction rate, thus indicating that the mass diffusing through the energy barrier is supplied by the bulk, which is able to achieve equilibrium with the initial configuration at any time.

In this quasistationary situation, the diffusion equation at the surface, eq.(4.1.39), reduces to

$$\rho^s \frac{dc^s(\gamma)}{dt} = \nabla \cdot (D^s(\gamma)\nabla c^s(\gamma)) + J^s(t)\left[-\delta(\gamma-\gamma_i)+\delta(\gamma-\gamma_f)\right] + \frac{L_{21}}{L_{11}} J^s(t)\delta(\gamma-\gamma_i) \tag{4.1.44}$$

It is possible to obtain an explicit expression for $J^s(t)$ using the quasistationary property, and the fact that eq.(4.1.41) can be rewritten as

$$J^s = -L_{11}(\gamma)\frac{k_B T}{m}\exp\left(-\frac{m\mu^s(\gamma)}{k_B T}\right)\frac{\partial}{\partial\gamma}\exp\left(\frac{m\mu^s(\gamma)}{k_B T}\right) \tag{4.1.45}$$

where $m$ is the mass of the diffusing particles. After integration in $\gamma$, eq.(4.1.45) gives

$$J^s(t) = -\frac{\exp\left(\frac{m\mu^s(\gamma_f)}{k_B T}\right) - \exp\left(\frac{m\mu^s(\gamma_i)}{k_B T}\right)}{\int_{\gamma_i}^{\gamma_f} \frac{m\exp\left(\frac{m\mu^s(\gamma)}{k_B T}\right)}{L_{11}(\gamma)k_B T}d\gamma} \tag{4.1.46}$$

To proceed further, we should introduce an explicit expression for the chemical potential of the system in the interfacial region. In the bulk, and even in a fluid interface, one can assume that the binary mixture or suspension behaves as an ideal system. However, we have seen in the previous chapters that when a solid surface is considered, if particles are localized when adsorbing, due to large attractive potentials, then exclusion volume effects become important, which from a macroscopic point of

view implies that the system exhibits a non-ideal behavior. We will then express the chemical potential

$$\mu^s(\gamma) = \mu_0^s + \frac{k_B T}{m} \ln z(\gamma) + \frac{1}{m} U(\gamma) \tag{4.1.47}$$

where $\mu_0^s$ is a reference value, $z(\gamma)$ is an activity and $U(\gamma)$ the attractive potential energy per unit mass, which stands for the effective potential acting on the suspended particles characterized by a large maximum. Widom[19] studied the problem of sequentially adding spheres to a volume, forbidding fluctuations of the spheres around their positions. For this kinetic process, which is controlled by excluded volume effects, he argued that it was possible to define what he called a *non-equilibrium* chemical potential of the form (4.1.47) with the *non-equilibrium* activity satisfying

$$z = \frac{c^s}{\phi} \tag{4.1.48}$$

where $\phi$ is the function accounting for the excluded volume effects, which in his case coincided with the surface available function of RSA. We will assume that such an expression holds locally. For the time being, we do not need to specify the form of $\phi$. If we substitute eq.(4.1.48) in the expression for the flux, eq.(4.1.46), we arrive at

$$J^s(t) = -\exp\left(-\frac{m\mu_0^s}{k_B T}\right) \frac{\exp\left(\frac{m\mu^s(\gamma_f)}{k_B T}\right) - \exp\left(\frac{m\mu^+}{k_B T}\right)}{\int_{\gamma_i}^{\gamma_f} \frac{1}{D(\gamma)\phi(\gamma)} \exp\left(\frac{U(\gamma)}{k_B T}\right) d\gamma} \tag{4.1.49}$$

where $D(\gamma)$ is a kind diffusion coefficient associated to the diffusion through the potential barrier, and is given by, $D = Lk_B T/(mc^s)$. When $\phi$ is constant (ideal system), eq.(4.1.49) is equivalent to the reaction rate of a thermally activated process deduced by Kramers[9]. Moreover, we have used the equilibrium property eq.(4.1.40), introducing the bulk chemical potential. The bulk phase can be regarded as an ideal system, because the non-idealilities we are interested in are due to the exclusion effects peculiar of the interface, which implies that we can describe it by the chemical potential of an ideal system

$$\mu^+ = \mu_0^+ + \frac{k_B T}{m} \ln c^+ \tag{4.1.50}$$

Substituting it in eq.(4.1.49) leads to

$$J^s(t) = -l\exp\left(\frac{U(\gamma_f)}{k_BT}\right)c^s(\gamma_f) + l\exp\left(\frac{m(\mu_0^+ - \mu_0^s)}{k_BT}\right)c^+\phi(\gamma_f) \tag{4.1.51}$$

where we have also used the fact that the value of the constant in the denominator of eq.(4.1.49) will be controlled by the behavior og the integrand around the maximum of the attractive potential $U(\gamma)$. Since, in principle, volume excluded effects will affect practically all the adsorbed phase at any configuration, we approximate the factor $\phi(\gamma)$ appearing in the integrand by its value in the more bounded state, $\phi(\gamma_f)$. We have defined the coefficient $l$ as,

$$l \equiv \frac{1}{\int_{\gamma_i}^{\gamma_f} \frac{\exp\left(\frac{U(\gamma)}{k_BT}\right)}{D(\gamma)}} \sim D(\gamma_m)\sqrt{\frac{\pi}{2U''}}\exp\left(-\frac{U(\gamma_m)}{k_BT}\right) \tag{4.1.52}$$

which, as been approximated by Laplace's method using the fact that the integral is dominated by the region around the maximum of $U(\gamma)$, with $\gamma_m$ being the value of the internal variable at which the potential has its maximum, and $U''$ means the second derivative of the potential $U$ evaluated at that position. Since the system is non-ideal, $l$ will in general depend on the surface concentration, while for an ideal system, $l$ is constant [12].

In order to compare our results with previous ones, it is convenient to rewrite the expression for the mass rate across the barrier, eq.(4.1.51), as

$$J^s(t) = -k_dc^s(\gamma_f) + k_ac^+\phi(\gamma_f) \tag{4.1.53}$$

where we have introduced the adsorption and desorption constants

$$k_a = l\exp\left(\frac{-U(\gamma_m) + m(\mu_0^+ - \mu_0^s)}{k_BT}\right) \tag{4.1.54}$$

$$k_d = l\exp\left(-\frac{U(\gamma_m) - U(\gamma_f)}{k_BT}\right) \tag{4.1.55}$$

and, according to eq.(4.1.52), the common prefactor is given by

$$\hat{l} \sim D(\gamma_m)\sqrt{\frac{\pi}{2U''}} \tag{4.1.56}$$

The desorption and adsorption coefficients, $k_d$ and $k_a$, have the form of Arrhenius laws, characteristic of the activated processes. Analogous expressions for the adsorption rates, and the adsorption and desorption constants, have been obtained by Laidler *et al.*[7] using the absoulte activation rate theory to the adsorption of ideal systems, and by Baret[4] for an ideal gas. In both cases, they were able to give the prefactors of the exponentials of the adsorption and desorption constants a molecular interpretation since they use equilibrium statistical mechanics theories.

Once we have determined the adsorption rate, we can derive the appropriate mass balance equation of the adsorbed phase, using eq.(4.1.44). Looking at the different values of $\gamma$, one sees that the more bounded state $\gamma_f$ behaves different from the rest, since it receives the mass coming from the bulk, after having diffused through the different intermediate surface states through the barrier,

$$\rho^s \frac{d^s c^s}{dt} = \nabla \cdot (D^s(\gamma)\nabla c^s(\gamma)) \qquad , \gamma \neq \gamma_f \tag{4.1.57}$$

$$\rho^s \frac{d^s c^s}{dt} = \nabla \cdot (D^s(\gamma)\nabla c^s(\gamma)) + J^s \quad , \gamma = \gamma_f \tag{4.1.58}$$

If surface diffusion can be neglected, then the concentration is constant in all the surface states except in the one corresponding to the minimum of the potential energy, where the mass fraction increases according to the flux of mass which arrives after crossing the energy barrier. This behavior corresponds to the one expected in a quasistationary regime. However, as already pointed out before, only the mass fractions corresponding to minima of the energy barrier will have thermodynamic relevance. In this sense, two different situations can be found, as shown in fig.4.1b). When only one minimum is present, then only the balance equation for $\gamma = \gamma_f$ will be relevant, indicating that there exists a unique adsorbed state bounded to the surface. If the potential exhibits a secondary minimum, then two adsorbed states will coexist on the surface. Besides the one corresponding to $\gamma = \gamma_f$, the existence of a secondary

minimum produces a second adsorbed state at $\gamma = \gamma_i$, which is less bounded to the surface, and which attains a faster diffusion-like equilibrium with the bulk phase.

If surface diffusion can be also neglected in the more bounded state, then its mass balance equation reads

$$\rho^s \frac{d^s c^s(\gamma_f)}{dt} = k_a c^+ \phi(c^s(\gamma_f)) - k_d c^s(\gamma_f) \tag{4.1.59}$$

which has the form of a local generalized Langmuir equation , similar to the one discused in eq.(2), proposed by some authors to describe the irreversible adsorption of large particles[20]. At low coverages, the function $\phi$, can always be linearized[19], leading to

$$\rho^s \frac{d^s c^s(\gamma_f)}{dt} = k_a c^+ (1 - \alpha c^s(\gamma_f)) - k_d c^s(\gamma_f) \tag{4.1.60}$$

which is the local Langmuir adsorption equation[21] (see eq.(1), introduced at the beginning of the century to describe the adsorption of hydrogen on platinum.

Therefore, we have shown that local generalized Langmuir adsorption equations can be obtained generally if the transport from the bulk to the interface is controlled by an energy barrier. The validity of these results will obviously depend on the validity of the basic assumption of non-equilibrium thermodynamics, namely, local equilibrium in the internal space. Since it is a phenomenological theory, it cannot assess up to whichh point such an assumption will hold, although from the formal point of view, eq.(4.1.59) has the correct functional dependence for the whole kinetic adsorption process.

The right hand side of eq.(4.1.59) gives the incoming flux of particles. Therefore, this equation can be regarded as the boundary condition needed to solve the bulk concentration evolution equation. Solving the ensemble of differential equation gives then the evolution of the concentration on the surface as well as the diffusive profiles appearing the bulk as a consequence of the adsorption kinetics. Varoqui *et al*[25] have studied the low coverage regime, when the Langmuir equation eq.(4.1.60) applies. In fact, if $\phi = 1$ so that excluded effects are neglected, the Langmuir equation becomes a

first order chemical reaction. As we have discussed in chapter 3, this sort of boundary conditions have been obtained from the study of the bulk transport equations[22][24]. Even, higher order chemical reaction-like boundary conditions have been proposed phenomenologically[23], but without clarifying its origin.

Up to know we have considered the situation in which adsorption is controlled by an energy barrier. However, there exist situations in which adsorption is controlled by simple diffusion[4][5] (see fig.3.1a). In this case, adsorption kinetics is qualitatively different from the one described so far. If we apply the formalism developed before to this case in which no localized energy barriers are present, the corresponding mass balance equations are

$$\frac{d^+c^+}{dt} = D^+\nabla^2 c^+ \tag{4.1.61}$$

$$\frac{d^s c^s}{dt} = \nabla\cdot(L_1\nabla\mu^s) + J_n^+ \tag{4.1.62}$$

$$J_n^+ = L_2\left(\mu^+ - \mu^s\right) \tag{4.1.63}$$

where $L_1$ and $L_2$ are the corresponding Onsager coefficients, and the appropriate expression for the chemical potentials have to be supplemented. Again, eq.(4.1.63) is the boundary condition for the bulk diffusion eq.(4.1.62), and in order to know it, the evolution equation for the interfacial density, eq.(4.1.62) has also to be solved[13][14].

In the previous chapters we have considered adsorption processes in the absence of localized potentials. Then, eqs.(4.1.61)-(4.1.63) constitute the thermodynamic description of their interfacial dynamics. In order to arrive at explicit expressions, however, a specific expression for the chemical potential has to be formulated. A diferent situation is found if one is interested on the kinetics of the global surface.

Jacobs[27] proposed an approximated diffusion equation for a region with varying cross section in which the geometrical constraints appeared as an entropic contribution, and Zwangig[28][29], later on, considered in more detail the problem of diffusion along a tube with a varying cross section. Starting from the three dimensional diffusion equation, he showed that averaging in the plane normal to the axis of the tube leads to an effective one-dimensional diffusion equation for the averaged density in

which, to first approximation, the geometrical constraints appear as if the diffusion takes place in the presence of an entropic potential.

In the adsorption dynamics we have considered in the previous chapters there exist no surface energy potentials, but as the particles arrive at the surface, the geometric constraints determine the rate of arrival of particles at later times. Therefore, if the dynamics of the global surface is studied, it seems reasonable that we can consider that diffusion of the averaged density of particles to the surface takes place in the presence of a certain entropic potential, which takes into account the specific way in which adsorbed particles exclude certain regions for the arrival of further ones. For the effective one-dimensional diffusing system, we can then consider that the system is described by a chemical potential of the form

$$\mu^s(\gamma) = \mu_0^s + \frac{k_B T}{m} \ln c^s(\gamma) - \frac{k_B T}{m} \ln \phi(\gamma) \tag{4.1.64}$$

instead of eq.(4.1.47). The last term represents the entropic potential. If the entropy barrier is large compared to $k_B T$, the formalism developed for the energy controlled adsorption can be used. In fact, one arrives at the same formal equations for the flux across the barrier, that is

$$J^s(t) = -\hat{k}_a c^s(\gamma_f) + \hat{k}_d c^+ \phi \tag{4.1.65}$$

instead of eq.(4.1.53), and where now the adsorption and desorption constant have the form

$$\hat{k}_a = D(\gamma_f) \qquad , \qquad \hat{k}_d = D(\gamma_f) \exp\left(\frac{m\mu_0^+ - \mu_0^s}{k_B T}\right) \tag{4.1.66}$$

and we have assumed that the maximum of the entropic barrier is at the adsorbed state. We have again, assumed that the state at $\gamma_i$ is in equilibrium with the bulk, and that in that state the geometric constraints can be neglected. Therefore, generalized Langmuir equations can be seen to describe also the adsorption in the absence of surface energy potentials, although only for the dynamics of the global concentration. For RSA, an entropic potential for simple geometries has been calculated by Tarjus *et*

*al.*[32], and it exhibits the properties we have used to derive the previous equations. Up to now, it remains an open question the relationship between the entropic potential proposed in eq.(4.1.64), and the chemical potential which describes the system in a local description, and which is needed to solve the local dynamics, eqs.(4.1.61)-(4.1.63).

Recently, the activated-state-theory has been started to be applied to describe adsorption taking these entropic effects into account. However, up to now, only mean field approaches have been addressed[30].

From the experimental point of view, unless a detailed knowledge of the interfacial potentials is available, there is a priori no reason to prefer energy-controlled to diffusion-controlled adsorption.

Note that in order to derive the generalized Langmuir equation, it has been necessary to introduce an internal degree of freedom. If we have treated the diffusion through the barrier as an ordinary chemical reaction in the framework of non-equilibrium thermodynamics, identifying the reactants with the bulk phase in contact with the wall, and as products the adsorbed mass fraction, then we had arrived at a rate across the barrier linear in the chemical potentials, namely

$$J^s = L(\mu^s(\gamma_i) - \mu^s(\gamma_f)) \tag{4.1.67}$$

loosing the non-linear features of the adsorption process.

Finally, it is worth noting that we have considered during the whole section, that the diffusion through the energy barrier can be dealt with in the spirit of Kramer's work[9]. The validity of this assumption lies in the height of the energy barrier. If it is large compared with $k_B T$, the conclusions we have derived are correct. Otherwise, a more detailed analysis of the diffusion process in the surface should be undertaken. In this sense, for the adsorption on a liquid interface, where adsorbed surface phase can be regarded as ideal due to its mobility, Simonin *et al.*[26] have shown the range of validity of reaction rate theory in the adsorption processes depending on the profile of the energy barrier.

## 4.2 Fluctuating Hydrodynamics and Internal Degrees of Freedom

One of the advantages of formulating the adsorption dynamics in terms of a thermodynamic theory is that it provides a solid scheme which allows us to understand other features of the process. In particular, the dynamics of the fluctuations of the thermodynamic fields can be derived systematically from non-equilibrium thermodynamics along the ideas of fluctuating hydrodynamics[33].

In this section, we will study the fluctuation dynamics in the adsorbed layer when a steady state is reached. We will first show how to generalize fluctuating hydrodynamics when an internal degree of freedom is present, afterwards we will apply the result to formulate the evolution equations for the fluctuations of the adsorbed mass fractions, and finally we will illustrate these results studying the mass fraction fluctuation dynamics around a particular steady state.

### 4.2.1 Fluctuating hydrodynamics of a chemical reaction

As we have done when deducing the balance equations, we present the basic ideas of fluctuating hydrodynamics in the presence of an internal degree of freedom for the simpler case of a chemical reaction. In appendix4.A we summarize the essentials of non-equilibrium thermodynamics in the presence of an internal degree of freedom applied to a chemical reaction.

The basic idea is that, since local equilibrium has been assumed in the internal space, this space becomes the natural place where fluctuations should be introduced. According to fluctuating hydrodynamics, one splits up the dissipative currents into systematic and random contributions. In particular, the diffusion flux in the internal space reads

$$J(\gamma,t) = J^s(\gamma,t) + J^r(\gamma,t) \tag{4.2.68}$$

where the superscript $s$ refers to the systematic, and $r$ to the random contributions

to the total diffusing flux. The systematic part is given by eq.(4.A.107 ), while the random contribution constitutes a gaussian white noise stochastic process with zero mean and fluctuation-dissipation theorem given by[33]

$$\langle J^r(\gamma,t)J^r(\gamma',t')\rangle = 2k_B L(\gamma)\delta(\gamma-\gamma')\delta(t-t') \tag{4.2.69}$$

according to the fact that the diffusion in the configurational space is a linear process, and $L(\gamma)$ defined through eq.(4.A.104 ), is related to the diffusion constant by $L(\gamma) = Dc(\gamma)$. The value of $c(\gamma)$ corresponds to the mass fraction of constituents evaluated at the steady state which serves as a reference state to study fluctuations.

If we insert eq.(4.1.3) in the mass balance equation (4.A.101 ), and use the expression for the systematic contribution, eq.(4.A.107 ), we can write down the corresponding stochastic differential equation which describes the whole behavior of the density in the internal space

$$\begin{aligned}\frac{\partial c(\gamma)}{\partial t} &= -\frac{\partial}{\partial\gamma}J^s(\gamma,t) - \frac{\partial}{\partial\gamma}J^r(\gamma,t) = \frac{\partial}{\partial\gamma}\left[D\exp\left(-\frac{U(\gamma)}{k_BT}\right)\frac{\partial}{\partial\gamma}\exp\left(\frac{m\mu(\gamma)}{k_BT}\right)\right] \\ &\quad -\frac{\partial}{\partial\gamma}J^r(\gamma,t)\end{aligned} \tag{4.2.70}$$

Note that, since the diffusion coefficient has been assumed constant, (4.2.70) is a linear stochastic differential equation for $c(\gamma)$.

We have already seen that if a large energy barrier exists, the diffusion reaches a quasistationary state almost immediately. If fluctuations are present, we can correspondingly express the total diffusing flux as being homogeneous. If we split it into the systematic and random contributions, this fact allows us to write it as

$$J = k_B l\left[1-\exp\left(\frac{A}{k_BT}\right)\right] + J^r(t) \tag{4.2.71}$$

with $A$ being the affinity, and $l$ has been defined in eq.(4.A.109 ). Moreover, we have

introduced the quasistationary random flux, which satisfies

$$J^r(t) = \frac{1}{\int_{\gamma_i}^{\gamma_f} \exp\left(\frac{U}{k_B T}\right) d\gamma} \int_{\gamma_i}^{\gamma_f} \exp\left(\frac{U}{k_B T}\right) J^r(\gamma, t) d\gamma \tag{4.2.72}$$

which indicates that the global flux is controlled by the evolution of the system around the energy barrier, as could be expected in the quasistationary regime. The stochastic properties of $J^r(t)$ follows from those of $J^r(\gamma, t)$. In fact, we can derive the corresponding generalized fluctuation-dissipation theorem in the quasistationary regime, by using the expression for the quasistationary random flux, eq.(4.2.72), and the fluctuation-dissipation theorem in the configurational space, eq.(4.2.69),

$$< J^r(t) J^r(t') >= \frac{2 k_B D}{\left[\int_{\gamma_i}^{\gamma_f} \exp\left(\frac{U}{k_B T}\right)\right]^2} \int_{\gamma_i}^{\gamma_f} \exp\left(\frac{U}{k_B T}\right) c(\gamma)\, d\gamma \tag{4.2.73}$$

where we have used the relation between the diffusion coefficient and the phenomenological coefficient $L$, which depends on $\gamma$. Since the quasistationary regime is achieved, the density profile is that given by the Boltzmann distribution at the right and left of the energy maximum. We can then write the generalized fluctuation-dissipation theorem as

$$\begin{aligned} \langle J^r(t) J^r(t') \rangle \;=\; & \frac{2}{\int_1^2 \exp\left(\frac{U}{k_B T}\right) d\gamma} \left[ k_f c(\gamma_i, t) \int_{\gamma_i}^{\gamma_m} \exp\left(\frac{U}{k_B T}\right) d\gamma \right. \\ & \left. + k_b c(\gamma_f, t) \int_{\gamma_m}^{\gamma_f} \exp\left(\frac{U}{k_B T}\right) d\gamma \right] \delta(t - t') \end{aligned} \tag{4.2.74}$$

where $c(\gamma_i, t)$ is the mass fraction at the left minimum of the potential, and $c(\gamma_f, t)$ at the right minimum. Moreover, we have introduced the forward, $k_f$, and backward, $k_b$, rate constants, related to the diffusion constant through

$$k_f \;=\; \frac{D e^{\frac{U(\gamma_i)}{k_B T}}}{\int_{\gamma_i}^{\gamma_f} \exp\left(\frac{U(\gamma)}{k_B T}\right) d\gamma} \tag{4.2.75}$$

$$k_b = \frac{D \exp\left(\frac{U(\gamma_f)}{k_B T}\right)}{\int_{\gamma_i}^{\gamma_f} \exp\left(\frac{U(\gamma)}{k_B T}\right) d\gamma} \tag{4.2.76}$$

Since the energy barrier is very high, the integrals appearing in the generalized fluctuation-dissipation theorem, eq.(4.2.74) can be computed using Laplace's method. One can then show that the three are proportional, which leads to

$$\langle J^r(t) J^r(t') \rangle = (k_f c(\gamma_i) + k_b c(\gamma_f)) \delta(t - t') \tag{4.2.77}$$

If the stationary state is an equilibrium state, then detailed balance is satisfied, and one has $k_f c(\gamma_i)^{eq} = k_b c(\gamma_f)^{eq} = k_B l$[12]. Consequently, (4.2.77) becomes

$$\langle J^r(t) J^r(t') \rangle = 2 k_B l \delta(t - t') \tag{4.2.78}$$

which corresponds to the fluctuation-dissipation theorem consistent with the linear law eq.(4.A.99 ).

We have to relate now the concentration of activated complex at the minima with the concentrations of reactants and products, which are the physical quantities of interest. For an unimolecular reaction, both quantites coincide, as noted in appendix4.A. At the end of that appendix, we also derive the law of mass action for a general reaction, $\sum_{i=1}^{k} \nu_i B_i \rightleftharpoons \sum_{i=1}^{j} \nu_i' C_i$. According to the relationships between the mass fractions in the internal space, and those of reactants and products (see eq.(4.A.111 )), the generalised fluctuation-dissipation theorem is

$$< J^r(t) J^r(t') > = \left( k_f \prod_{i=1}^{k} n_{B_i}^{\nu_i} + k_b \prod_{I=1}^{j} n_{C_i}^{\nu_i'} \right) \delta(t - t') \tag{4.2.79}$$

which coincides with the corresponding result obtained by Keizer[34]obtained using a statistical-mechanical theory. Note that, according to the basic scheme of fluctuating hydrodynamics[33], the densities of reactants and products appearing in eq.(4.2.79) correspond to the values of the concentrations at the reference state around which fluctuations have to be computed. This is equivalent to consider that linearization

of the fluctuation dynamics around such reference state has been performed. Generalization to non-linear fluctuations should be carried out with care[35]. Finally, let us mention that the more general situation of having a set of coupled unimolecular chemical reactions can be also derived within the same formalism[36].

### 4.2.2 Fluctuating hydrodynamics of the adsorbing interface

The same scheme of the previous section introduced to deal with fluctuations in a chemical reaction can be applied to study fluctuations in the adsorbing interface, due to the analogy between both processes. As we have done when deriving the adsorbing mass flux, we will have to generalize the formalism of the previous subsection, because now the activated process is restricted to the interface, and there will exist more fluctuating fluxes. We will then follow the standard scheme of fluctuating hydrodynamics in the presence of an interface[13] to derive the appropriate fluctuation-dissipation theorems corresponding to the fluctuating interfacial fluxes. In the absence of fluctuations, we have seen that in the bulk phase the usual balance equations are obtained. Correspondingly, fluctuations do not differ from those known for unbounded systems. At the interface, we have to consider three diffusion fluxes, namely the usual surface diffusion flux, the flux of mass along the energy barrier, and the normal component of the bulk mass flux in contact with the interface. As Bedeaux *et al.*[13] proved, the interfacial fluctuation fluxes satisfy fluctuation-dissipation theorems equivalent to the ones obtained for bulk phases. Then, we apply the same expressions in the internal space, which is now confined to the interfacial region, which allows us to write

$$< \vec{J}_s^r(\vec{r},\gamma,t)\vec{J}_s^r(\vec{r}',\gamma',t') > = 2k_B\vec{\vec{L}}\delta(\vec{r}-\vec{r}')\delta(t-t')\delta(\gamma-\gamma') \quad (4.2.80)$$

$$< J_n^{+r}(\vec{r},\gamma,t)\vec{J}_n^{+r}(\vec{r}',\gamma',t') > = 2k_B L_{22}\delta(\vec{r}-\vec{r}')\delta(t-t')\delta(\gamma-\gamma') \quad (4.2.81)$$

$$< J_n^{+r}(\vec{r},\gamma,t)J^r(\vec{r}',\gamma',t') > = 2k_B L_{21}\delta(\vec{r}-\vec{r}')\delta(t-t')\delta(\gamma-\gamma') \quad (4.2.82)$$

$$< J^r(\vec{r},\gamma,t)J^r(\vec{r}',\gamma',t') > = 2k_B L_{11}\delta(\vec{r}-\vec{r}')\delta(t-t')\delta(\gamma-\gamma') \quad (4.2.83)$$

where use has been made of the fact that fluxes of the same tensorial character are coupled, according to Curie's principle. Moreover, Onsager symmetry principle has

been used in eq.(4.2.82). Note that the delta correlation in $\gamma$ is obtained due to the special chemical reaction process which is considered to model the crossing of the energy barrier, which has led to a local coupling in internal space[3]. As usual, the fluctuation-dissipation theorem can be rewritten in terms of the diffusion coefficients, which allows to make explicit the dependence on $\gamma$ and $\vec{r}$, since the diffusion coefficients can be considered constants. It is important to remember that two diffusion coefficients exist at the interface; the usual surface diffusion coefficient, and the diffusion coefficient associated to the activated process.

In the quasistationary regime, we know that the fluctuations of the flux across the energy barrier become uniform, and that, according to the results of the previous section, its stochastic properties are defined by their second moment, which is the equivalent of eq.(4.2.77),

$$< J^r(\vec{r},t)J^r(\vec{r}',t' >= (k_a c^+ + k_d c^s)\delta(\vec{r}-\vec{r}')\delta(t-t') \tag{4.2.84}$$

and if two adsorbed states are present at the interface, instead of $c^+$ the corresponding mass fraction should be inserted. Once the stochastic properties of the random fluxes have been determined, we can study the dynamics of the mass fraction fluctuations, which are driven by the fluctuating fluxes. When considering the thermodynamically relevant adsorbed states, the approperiate values of $\gamma$ have to be evaluated in eqs.4.2.80)-(4.2.82).

### 4.2.3 Fluctuations around Adsorption Steady States

Let us now analyze the case in which there exist a single adsorbed state. The balance equation for the global fluctuating mass fraction will then read

$$\frac{dc^s}{dt} = D\nabla^2 c^s + k_a c^+ \phi(c^s) - k_d c^s + \nabla \cdot \vec{J}_s^r + J^r \tag{4.2.85}$$

[3]This correlation can be derived along the same lines used in the previous section to derive the law of mass action, starting from $k$ coupled chemical reactions, and letting $k$ become a continuous variable at the end

where we have used eq.(4.1.58), assumed that diffusion is allowed, and decomposed the total fluxes in their deterministic and fluctuating parts. Eq.(4.2.85) constitutes a Langevin equation for the fluctuating concentration $c^s$, in which the properties of the fluctuation fluxes is determined by eqs.(4.2.80) and (4.2.83). It is worth pointing out that eq.(4.2.85) will enable us to study the fluctuation dynamics to linear order on the deviation to the reference steady state, because the properties of the random fluxes have also been determined up to that order.

The steady states are the solutions of the equation

$$D\nabla^2 c^s + k_a c^+ \phi(c^s) - k_d c^s = 0 \tag{4.2.86}$$

and the specific solution will be fixed by the initial and boundary conditions corresponding to the process to be considered. The adsorption process we have been describing is characterized by an initially empty surface which is progressively filled with particles arriving from an homogeneous suspension. Then, it is reasonable to consider an homogeneous steady state as a good reference to study fluctuation dynamics. Such a steady state is the solution of

$$\bar{c}^s = \frac{k_a}{k_d} \bar{c}^+ \phi(\bar{c}^s) \tag{4.2.87}$$

where the quatities $\bar{c}^s$ their values in the steady state. The specific value of $\bar{c}^s$ will depend on the expression for the function $\phi$. The equation for the dynamics of the fluctuations around this homogeneous steady state can be obtained, linearizing around such a state, consistently with the way in which the random fluxes have been determined, leading to

$$\frac{d\delta c^s}{dt} = D\nabla^2 \delta c^s + k_a \bar{c}^+ \frac{\partial \phi}{\partial c^s}|_{\bar{c}^s} \delta c^s + k_a \phi(\bar{c}^s) \delta c^+ - k_d \delta c^s + J^r + \nabla \cdot \vec{T}_s^r \tag{4.2.88}$$

where we have decomposed the total mass fraction into its steady and random contributions, $c^s = \bar{c}^s + \delta c^s$, and we have use the fact that $\bar{c}^s$ satisfies eq.4.2.86). Note that the fluctuation in the adsorbed state depend also on the bulk mass fluctuations

in contact with the substrate. Since eq.(4.2.88) is linear in the fluctuations, it can be solved. In particular, if we transform both space and time to Fourier space, it gives

$$\delta c^s = \frac{k_a \phi(c^s)}{-i\omega + D^s k^2 + \tilde{l}} \delta c^+ + \frac{J^r}{-i\omega + D^s k^2 + \tilde{l}} - \frac{i\vec{k} \cdot \vec{J}_s^r}{-i\omega + D^s k^2 + \tilde{l}} \tag{4.2.89}$$

where we have introduced the new characeristic time scale $\tilde{l}^{-1}$ defined as $\tilde{l} = -k_a \frac{\partial \phi}{\partial c^s} + k_d$, and $k$ and $\omega$ refer to the two-dimensional vector in spatial reciprocal space and frequency space, respectively. $i$ is the imaginary unity. This new time scale is associated to the exchange of mass between the surface and the bulk phase, indicating that, although the interface is a bidimensional system, it is coupled to the bulk phese, and can dissipate energy through mass exchange with it.

In order to find an expression for the correlations of the interface mass fluctuations, we should know the dynamics of the correlations of the bulk concentration fluctuations in contact with the interface. As we have pointed out in the revious subsection, they satisfy the usual fluctuation dynamics for a diffusive process in an unbounded fluid, and will be decoupled from the interfacial fluctuating quantities. Then, the correlations have the form,

$$\begin{aligned} < \delta c^s(\vec{k},\omega) \delta c^s(\vec{k}',\omega') > = & \frac{(k_a \phi(\bar{c}^s))^2 < \delta c^+(\vec{k},\omega) \delta c^+(\vec{k},\omega) >}{(-i\omega + D^s k^2 + \tilde{l})(-i\omega' + D^s k'^2 + \tilde{l})} + \\ & \frac{< J^r(\vec{k},\omega) J^r(\vec{k},\omega) >}{(-i\omega + D^s k^2 + \tilde{l})(-i\omega' + D^s k'^2 + \tilde{l})} - \\ & \frac{\vec{k} \cdot < \vec{J}_s^r(\vec{k},\omega) \vec{J}_s^r(\vec{k},\omega) > \cdot \vec{k}'}{(-i\omega + D^s k^2 + \tilde{l})(-i\omega' + D^s k'^2 + \tilde{l})} \end{aligned} \tag{4.2.90}$$

The correlations for the surface fluxes are obtained from eqs.(4.2.80) and (4.2.82). For the surface diffusion flux we will also use the fact that the phenomenological coefficient can be written as $\vec{\vec{L}} = D^s c^s \vec{\vec{I}}$, and that we are considering only the thermodynamically relevant adsorbed state. The correlations for the bulk mass fraction are the ones corresponding to a diffusive unbounded system. We should simply take

care that we are interested in the fluctuations in contact with the wall. Hence,

$$< \delta c^+ \delta c^+ >= \int_{-\infty}^{\infty} \frac{D^+ \bar{c}^+}{\omega^2 + (D^+(x^2+k^2))^2} dx \delta(\vec{k}+\vec{k}')\, \delta(\omega+\omega') \qquad (4.2.91)$$

Subsituting the expressions for the corresponding correlation functions in eq.(4.2.90), we arrive at

$$< \delta c^s(\vec{k},\omega)\delta c^s(\vec{k}',\omega') >= \left\{ \frac{(k_a\phi(\bar{c}^s))^2 2D^+\bar{c}^+}{(\omega^2+(D^s k^2+\tilde{l})^2)} \int_{-\infty}^{\infty} \frac{1}{\omega^2+(d^2+(x^2+k^2))^2} dx + \right.$$
$$\left. + \frac{k_a \bar{c}^+ k_d \bar{c}^s}{(\omega^2+D^s k^2+\tilde{l})^2} - \frac{k^2 2D^s \bar{c}^s}{\omega^2+(D^s k^2+\tilde{l})^2} \right\} \delta(\vec{k}+\vec{k}')\delta(\omega+\omega') \qquad (4.2.92)$$

which give the general expression for the density correlation functions in the adsorbed state. We will now study in more detail the behavior of this correlation function, in the particular case of the equal time, or stationary, correlations. After integration in frequency, one arrives at the simpler expression,

$$< \delta c^s(\vec{k},t)\delta c^s(\vec{k}',t) > \;=\; (k_a\bar{c}^+ + k_d\bar{c}^s - D^s\bar{c}^s\hat{l})\frac{\pi}{D^s k^2+\hat{l}} + \frac{2\pi D^s \bar{c}^s}{D^s} \qquad (4.2.93)$$

in which the coupling with the bulk phase disappears. Transforming back to real space, one has

$$\begin{aligned} < \delta c^s(x,t)\delta c^s(x',t) > &= \bar{c}^s\delta(x-x') \\ &+ (k_a\bar{c}^+ + k_d\bar{c}^s - D^s\bar{c}^s\hat{l})\frac{\pi}{D^s\hat{l}} e^{-|x-x'|\sqrt{\frac{\hat{l}}{D^s}}} \qquad (4.2.94) \\ < \delta c^s(\vec{r},t)\delta c^s(\vec{r}',t) > &= \bar{c}^s\delta(\vec{r}-\vec{r}') \\ &+ (k_a\bar{c}^+ + k_d\bar{c}^s - D^s\bar{c}^s\hat{l})\frac{\pi}{2D^s\hat{l}} K_0\left(-|\vec{r}-\vec{r}'|\sqrt{\frac{\hat{l}}{D^s}}\right) \qquad (4.2.95) \end{aligned}$$

for a one dimensional and a two dimensional substrate, respectively, and where $K_0$ is the second order modified Bessel function.

The static correlation function for an unbounded system in equilibrium exhibits a delta function behavior. We can see that now, due to the mass exchange with the bulk, an slower decay of the correlation functions is observed. This decay is given by the characteristic length scale, $\sqrt{D^s/\hat{l}}$, which considers the mass transport from the bulk to the surface, relative to the transport in the surface. The fluctuation dynamics in a steady state is qualitatively different from the one obtained during the adsorption filling of the substrate. In that case, diffusion can be neglected,and a faster decay of the correlations is observed[37].

## 4.3 Discussion

In this chapter we have developed a thermodynamic theory to describe the adsorption process at a macroscopic level. The basic assumption in the formulation of such a theory has been to consider that the transport near the wall is controlled by an energy barrier. Then, in order to account for the non-linearities inherent to the transport, we have introduced an internal degree of freedom at the wall, which takes into account the diffusion process along the enrgy barrier. Following the spirit of non-equilibrium thermodynamics, local equilibrium is assumed to hold in the internal space, associated to this new internal variable. In this way, we have been able to derive an expression for the flux rate of particles arriving at the adsorbed state. In the absence of an energy barrier, the adsorption is controlled by diffusion, and the non-ideal character of the sysem is introduced through the appropriate interfacial chemical potential. If the dynamics of the total coverage is considered, we have also shown that an equivalent expression for the rate of particles to the one obtained when an energy barrier is present can be obtained, because an entropy barrier can be developed as a result of the geometric constraints that the incoming particles have to fullfill due to the previously adsorbed ones. Again, it is necessary to assume that the arrival at the surface is controlled by this entropic barrier. Therefore, the usual generalized Langmuir equations which are obtained in the kinetic adsoprtion models for the global coverage, can be obtained from a thermodynamic formalism.

The relationship between the global description, and the local balance equations for these systems where the transport is controlled by entropic bariers, remains unclear so far.

The formulation of the adsorption in terms of a thermodynamic theory, has allowed us to obtain the fluctuation-dissipation theorems for the different fluxes which appear at the adsorbing surface. Again, the formalism in the presence of an internal degree of freedom has been developed, and the results have been applied for adsorption. Finally, we have considered the mass fluctuation dynamics of an adsorbed phase around a homogeneous steady state. The mass exchange with the bulk has introduced a new length scale when surface diffusion is present, leading to a slower decay of the correlations with respect to diffusing equilibrium systems.

# Appendices

## 4.A Internal Degrees of Freedom in Non-Equilibrium Thermodynamics

It is well-known that the second law of thermodynamics states that[12]

$$\int_V \sigma(S) d\delta V \geq 0 \qquad (4.A.96)$$

where $\sigma(S)$ is the entropy production per unit of time and volume of a macroscopic volume $\delta V$, being $V$ the total volume of the system. However, non-equilibrium thermodynamics is based on the assumption that not only eq.(4.A.96 ) holds, but that at every subvolume the entropy production is positive, that is

$$\sigma(S) \geq 0 \qquad (4.A.97)$$

Therefore, a precise definition of the space in which the thermodynamic processes take place becomes also of crucial importance. Hence, if the particles which constitute

the system posses some internal degree of freedom, they should be introduced in the description of the system, as is the case of a system made of dipoles where the their orientation with respect with a reference axis is relevant when an external field is applied.

A chemical reaction constitutes another example where an additional degree of freedom should be introduced. For simplicity's sake, let us consider the unimolecular reaction $1 \longrightarrow 2$, 1 being the reactant and 2 the product. In the standard description of chemical reaction within non-equilibrium thermodynamics, one considers a homogeneous process, which leads to an entropy production of the form

$$\sigma = -\frac{JA}{T} \tag{4.A.98}$$

with $A = \mu_2 - \mu_1$ the affinity, $\mu_1$ and $\mu_2$ the chemical potentials of the reactant and product respectively, $J$ the flux of mass, and $T$ the temperature. Since the reaction takes place in all the volume, eq.(4.A.98 ) is an homogeneous relation, which leads to a linear relationship between the flux and the affinity,

$$J = -l\frac{A}{T} \tag{4.A.99}$$

$l$ being a phenomenological coefficient. However, it is well known that, except very close to equilibrium, the relation between the flux and the affinity is non-linear, being defined through the law of mass action[12]. In this case, the additional degree of freedom is not related to additional degrees associated with either molecules of the reactant or product. Rather, one should realize that in a reaction, the molecules of reactant should form an activated complex, which pass through a series of energy states until reaching the product molecules. A more detailed description of the reaction at the thermodynamic level would then be to introduce an additional variable which would characterize the state of evolution along this "energy" space[15].

In general, let us assume that we have a closed uniform system, characterized by its density $\rho(y)$ which depends on a certain internal variable $y$ which can take an infinite sequence of values. For constant energy and volume, the total differential of

the entropy per unit mass, $\delta s$ is given by

$$\delta s = -\frac{1}{\rho_{tot} T} \int \mu(y) \delta\rho(y) dy \qquad (4.A.100)$$

where $\mu(y)$ is the chemical potential per unit mass for configuration $y$, and $\rho_{tot}$ the total density. As expected, at equilibrium the chemical potential is constant. Assuming that the density is conserved in this internal space, we can write

$$\frac{\partial\rho(y)}{\partial t} = -\frac{\partial J(y)}{\partial y} \qquad (4.A.101)$$

which defines the flux in the space of the internal coordinate $J(y)$. Using eq.(4.A.101 ) in eq.(4.A.100 ), we can derive the corresponding expression for the entropy production of this system, which gives

$$\sigma = -\frac{1}{\rho_{tot} T} \int J(y) \frac{\partial\mu(y)}{\partial y} dy \geq 0 \qquad (4.A.102)$$

leading, in general, to phenomenological relations for the thermodynamic forces and fluxes of the form

$$J(y) = -\int L(y, y') \frac{\partial\mu(y')}{\partial y'} dy' \qquad (4.A.103)$$

As indicated at the beginnig of this appendix, however, non-equilibrium thermodynamics assumes that not only the global entropy production should be positive, but that at each point it should be positive defined. In this case, this assumption indicates that the internal coordinate changes in a continuous way, and therefore finite changes at a time are forbidden. In this case, by demanding that he integrand of eq.(4.A.102 ) be positive, one obtains, instead of relations like eq.(4.A.104 ),

$$J(y) = -L(y) \frac{\partial\mu(y)}{\partial y} \qquad (4.A.104)$$

indicating that the flux now does not depend on the whole distribution along the internal variable. At this point, once supplied the appropriate expression for the chemical potential in this internal space from equilibrium thermodynamics, one can deduce the corresponding expression for the flux and also, after inserting it in eq.(4.A.101 ) gives the corresponding evolution equation for the density, once the appropriate initial and boundary conditions are prescribed. For, example, for an ideal system

$$\mu(y) = \frac{kT}{m} \ln \rho(y) + \frac{U(y)}{m} \qquad (4.A.105\ )$$

where $U(y)$ stands for a potential which affect the motion of the internal degree of freedom, and $m$ is the mass of the system. When substituted in eq.(4.A.104 ) leads to

$$J(y) = D\frac{\partial \rho(y)}{\partial \gamma} + \rho(y) b U(y) \qquad (4.A.106\ )$$

with $D = L(y)kT/(m\rho(y))$ a diffusion coefficient, which can be considered constant as usual, and $b = L/(\rho m)$ a mobility coefficient. Note the similarity of eq.(4.A.106 ) with the expression of the flux for a diffusing system in the presence of an external field. In general, by choosing the appropriate density and internal variable, this formalism has been applied to study the diffusion of dipoles on an external field and in a shear flow[10][12], and has been also applied to obtain the Fokker-Planck equation for the case of Brownian motion in velocity space[12] and for diffusion in a thermal gradient[16].

### The chemical reaction

In the case of a chemical reaction, $U(y)$ represents the energy of the activated complex, which has a maximum in the internal space and two minima, corresponding to the reactant and product states. As the maximum is usually quite pronounced, one usually arrives at a quasistationary state, in which the flux of mass is constant in all the space and is controlled by the behavior of the system at the maximum. We use

the fact that eq.(4.A.104 ) as

$$J(y) = -kTD\exp\left(-\frac{U(y)}{kT}\right)\frac{\partial}{\partial y}\exp\left(\frac{m\mu(y)}{kT}\right) \tag{4.A.107}$$

and since $J$ is constant, after integrating along the internal space, gives

$$J = -\frac{D}{\int_{y_i}^{y_f}\exp\left(\frac{U(y)}{kT}\right)dy}\left[e^{\frac{m\mu_2}{kT}} - e^{\frac{m\mu_1}{kT}}\right] \tag{4.A.108}$$

where $y_i$ and $y_f$ correspond to the limits of the domain where $y$ is defined, and which coincides with the values at which the density is at the initial and final stage of the reaction. For unimolecular reactions, the activated complex is formed by one molecule of the reactant. Therefore, in this case the density of the activated complex at the initial and final states coincide with the density of the reactants and products, respectively. By defining the constant $l$ as

$$l \equiv \frac{\frac{m}{k}D\exp\left(\frac{m\mu_1}{kT}\right)}{\int_{y_i}^{y_f}\exp\left(\frac{U(y)}{kT}\right)dy} \tag{4.A.109}$$

one arrives at

$$J = \frac{k}{m}l\left[1 - \exp\left(\frac{mA}{kT}\right)\right] \tag{4.A.110}$$

which constitutes the law of mass action, a nonlinear relation between $J$ and $A$. Therefore, although the entropy production can be expressed as a bilinear form in $J$ and $A$, a non-linear relation between them can be derived in the appropriate regime.

Although we have derived the law of mass action for an unimolecular reaction, it is possible to the derive the corresponding law of mass action for a general reaction $\sum_{i=1}^{k}\nu_i B_i \rightleftharpoons \sum_{i=1}^{j}\nu_i' C_i$. In this case, the same technique used for the unimolecular reaction can be applied to study the rate of reaction. Now, the reaction starts when the appropriate number of molecules of reactants, according to their stoichiometry,

meet together to form the activated complex. Once they meet, they start to diffuse in the configuration space, passing through the activated state, until they reach the second minimum in configuration space, corresponding to the products. Then, as before, the internal space is carachterized by an internal continuous variable, diffusing through a potential which has a maximum and two minima. Therefore, eq.(4.A.108 ) is still applicable. The only difference with the unimolecular reaction is that now, the mass concentration of the activated complex is not equal to the mass concentration of reactant, because $\nu_i$ molecules of $B_i$ should meet together to form the activated complex. Then,

$$c(\gamma_i) = \prod_{i=1}^{k} n_{B_i}^{\nu_i} \quad , c(\gamma_f) = \prod_{i=1}^{j} n_{C_i}^{\nu_i'} \tag{4.A.111}$$

where $n_{B_i}$ is the mass fraction of reactant $B_i$ and $n_{C_i}$ is the mass fraction of product $C_i$. Therefore, the law of mass action eq.(4.A.110 ) is correct if these relations are appropriately introduced.

Note that by the use of the internal degrees of freedom, we are able to derive the kinetic equation for the ensemble of reactants, and the one corresponding to the ensemble of products. Finally, it is worth pointing out that, by choosing an internal degree of freedom indicating the state of advance of the activated complex, one finds that the appropriate thermodynamic force is the derivative of the chemical potential defined in this space, instead of the affinity, as is obtained in usual non-equilibrium thermodynamics.

## 4.B BAM Thermodynamic Formalism for Interfaces

In this appendix we will show the basic principles underlying the formulation of non-equilibrium thermodynamics of surfaces introduced by Bedeaux, Albano and Mazur[2][13] (BAM). The objective of such formalism is to derive the appropriate balance equations for the different relevant physical magnitudes both in the bulk phases and in the interfacial region, as well as to provide the appropiate boundary conditions relating the bulk fields at the interface with the interfacial magnitudes.

Consider a physical system composed of two coexisting phases, separated by a moving surface of discontinuity. The presence of a surface does not mean that the discontinuity is sharp, nor that it can located with absolute precision. It is taken to identify the nonhomogeneous region which separates the two bulk phases, and which has a width of the order of the bulk correlation length. The thermodynamic level of description describes the dynamics of the system such that the details of what happens on length scales smaller than the bulk correlation length are negligible. In the bulk phase this implies that one may replace the molecular density by a continuous field obtained after averaging over cells with a diameter of the order of the bulk correlation length. The surface of discontinuity is a two dimensional layer of cells in which the variables change rapidly in one direction over a distance of the order of the bulk correlation length from the value in one phase to the value in the other, but which change slowly in the other two directions. We now choose a time-dependent dividing surface in this two dimensional layer of cells such its radii of curvature are large compared to the bulk correlation length. The uncertainties in the location of this surface lead to differences in the physical magnitudes of the order of the bulk correlation length if the system can be assumed to be in local equilibrium.

In order to describe the time-dependent evolution of the dividing surface, a set of time-dependent orthogonal curvilinear coordinates, $\xi_i(\vec{r},t)$, $i=1,2,3$, is chosen, such that the location of the dividing surface is given by

$$\xi_1(\vec{r},t)=0 \qquad \text{(4.B.112 )}$$

The dynamic properties of the system are described using balance equations for the thermodynamic quantities. For one of such quantities $d(\vec{r},t)$, we will then write

$$\frac{\partial}{\partial t}d(\vec{r},t)+\nabla\cdot\vec{J}_d(\vec{r},t)=\sigma_d(\vec{r},t) \qquad \text{(4.B.113 )}$$

where $\vec{J}_d(\vec{r},t)$ is the current of $d$, and $\sigma_d(\vec{r},t)$ stands for the production of $d$ in the system. All the quantities introduced, will behave smoothly in the bulk phases, and will exhibit large deviations from the expected bulk values in the interfacial region. BAM's procedure consists of assigning all the deviation of the magnitudes in the

interface with respect to the bulk values to the surface of discontinuity. Therefore, such quantities can be written as

$$d(\vec{r},t) = d^-(\vec{r},t)\Theta^-(\vec{r},t) + d^+(\vec{r},t)\Theta^+(\vec{r},t) + d^s(\vec{r},t)\delta^s(\vec{r},t) \quad (4.B.114)$$

$$\vec{J}_d(\vec{r},t) = \vec{J}_d^-(\vec{r},t)\Theta^-(\vec{r},t) + \vec{J}_d^+(\vec{r},t)\Theta^+(\vec{r},t) + \vec{J}_d^s(\vec{r},t)\delta^s(\vec{r},t) \quad (4.B.115)$$

$$\sigma_d(\vec{r},t) = \sigma_d^-(\vec{r},t)\Theta^-(\vec{r},t) + \sigma_d^+(\vec{r},t)\Theta^+(\vec{r},t) + \sigma_d^s(\vec{r},t)\delta^s(\vec{r},t) \quad (4.B.116)$$

with $\Theta^-$ and $\Theta^+$ being the characteristic functions of the two bulk phases (characterized by the superscript + and -), which are 1 in one phase and 0 in the other. These characteristic functions can be expressed in terms of the Heaviside function,

$$\Theta^{\pm}(\vec{r},t) = \theta(\pm\xi_1(\vec{r},t)) \quad (4.B.117)$$

and, correspondingly, $\delta^s$ is the surface delta function,

$$\delta^s(\vec{r},t) = |\nabla\xi_1(\vec{r},t)|\delta(\xi_1(\vec{r},t)) \quad (4.B.118)$$

Note that, according to this formulation, the surface quantities do not depend on $\xi_1$, and then, their derivatives normal to the surface are zero. If one proceeds to introduce expressions (4.B.114 )-(4.B.116 ) in the balance equation (4.B.113 ), one obtains

$$\left[\frac{\partial}{\partial t}d^-(\vec{r},t) + \nabla\cdot\vec{J}_d^-(\vec{r},t) - \sigma_d^-(\vec{r},t)\right]\Theta^-(\vec{r},t) + \left[\frac{\partial}{\partial t}d^+(\vec{r},t) + \right.$$
$$\left.\nabla\cdot\vec{J}_d^+(\vec{r},t) - \sigma_d^+(\vec{r},t)\right]\Theta^+(\vec{r},t) + \left[\frac{\partial}{\partial t}d^s(\vec{r},t) + \nabla\cdot\vec{J}_d^s(\vec{r},t) - \sigma_d^s(\vec{r},t)\right.$$
$$\left.+J_{d,n}^+(\vec{r},t) - J_{d,n}^-(\vec{r},t) - w_n^s(\vec{r},t)(d^+(\vec{r},t) - d^-(\vec{r},t))\right]\delta^s(\vec{r},t) +$$
$$\left[J_{d,n}^s(\vec{r},t) - w_n^s(\vec{r},t)d^s(\vec{r},t)\right]\vec{n}(\vec{r},t)\cdot\nabla\delta^s(\vec{r},t) = 0 \quad (4.B.119)$$

where properties of the derivatives of the distributions have been applied[13]. The subscript $n$ indicates the normal component to the diving surface, $\vec{n}(\vec{r},t)$ being its

normal vector, and the normal components of the bulk phases which appear in the third term are evaluated at contact with the dividing surfaceand the velocity field of the dividing surface. In the previous expression, $\vec{w}(\vec{\xi})$ is the velocity of the curvilinear coordinates

$$\vec{w}(\vec{\xi}) = \frac{\partial}{\partial t}\vec{r}(\vec{\xi}, t) \qquad (4.B.120)$$

and the velocity field $\vec{w}^s(\xi_2, \xi_3, t)$ can be expressed in terms of this velocity field through $\vec{w}^s(\xi_2, \xi_3, t) = \vec{w}(\xi_1 = 0, \xi_2, \xi_3, t)$. There is a freedom to choose the curvilinear coordinates which define the interface, and we have considered that the velocity of the interface equals its barycentric velocity, i.e. $\vec{w}^s = \vec{v}^s$. Since the four distributions appearing in eq.(4.B.119 ) are independent[2], then it splits in four equations. The first two tems give

$$\frac{\partial}{\partial t} d^{\pm} + \nabla \cdot \vec{J}_d^{\pm} = \sigma_d^{\pm} \quad \pm\xi(\vec{r}, t) > 0 \qquad (4.B.121)$$

which describe the balance in the bulk phases. They have the same expression as for unbounded systems[12]. The third term describes the balance equation for the excess density

$$\frac{\partial}{\partial t} d^s + \nabla \cdot \vec{J}_d^s + J_{d,n,-} - w_n^s d_- = \sigma_d^s \qquad , \qquad \xi_1(\vec{r}, t = 0) \qquad (4.B.122)$$

The subscript $-$ means that the difference of the bulk values of the corresponding quantity at both sides of the dividing surface is taken. In this surface balance equation, one can see that, besides the usual terms, a contribution due to flow from the bulk appears, as well as a second new contribution standing for the fact that during its motion, the interface should "push" the field at one side, and the space left behind it should be "occupied" with the field coming from the bulk. Finally, the fourth term in eq.(4.B.119 ) gives

$$J_{d,n}^s - w_n^s d^s = 0 \qquad (4.B.123)$$

expressing that the surface flux is parallel to the interface in a comoving frame, as could be expected.

This procedure is then applied to all the thermodynamic fields of the particular system, e.g. density, momentum and energy for a two phase simple fluid. In the text, we work out in more detail the case of mass fraction field in a mixture.

In order to formulate a thermodynamic theory, we have to deduce also the balance equations for the entropy in the different phases. They give

$$\rho^{\pm}\frac{d}{dt}s^{\pm} = -\nabla\cdot\vec{J}^{\pm}+\sigma^{\pm} \qquad (4.B.124)$$

$$\rho^{s}\frac{d}{dt}s^{s} = -\nabla\cdot\vec{J}^{s}-\vec{n}\cdot\left[(\vec{v}-\vec{v}^{s})\rho(s-s^{s})+\vec{J}\right]_{-}+\sigma^{s} \qquad (4.B.125)$$

The first equation gives the usual entropy balance equation, showing that the balance equations for the bulk phases look like the ones obtained for unbounded phases[12]. The subscript $s$ which should appear in the flux and production term to indicate that they are the entropy flux and production is dropped to avoid confusion with the superscript $s$ labelling the excess contributions. According to the principles of non-equilibrium thermodynamics, one knows that the entropy production is locally positive defined,

$$\sigma^{\pm}\geq 0 \quad , \quad \sigma^{s}\geq 0 \qquad (4.B.126)$$

In standard non-equilibrium thermodynamics[12], in order to derive an explicit expression for the entropy production, one uses the fact that from thermodynamics, the entropy of a system in equilibrium is a well-defined function of the thermodynamic variables which define macroscopically the state of the system, and that its total differential is given by the Gibbs relation. Gibbs showed that this is also the case for a system with two phases separated by an interface[17]. Then for an $n$- mixture of simple fluids, it is determined by specifying, for example, the internal energy, $u$, the specific volume, $v$, and the mass fractions, $c_k$. The Gibbs relations corresponding to the bulk and surface phases are then written as

$$T^{\pm} ds^{\pm} = du^{\pm} + p^{\pm} dv^{\pm} - \sum_{k=1}^{n} \mu^{\pm} dc_k^{\pm} \qquad (4.B.127)$$

$$T^{s} ds^{s} = du^{s} - \gamma dv^{s} - \sum_{k=1}^{n} \mu^{s} dc_k^{s} \qquad (4.B.128)$$

where $T$ are the temperatures, and $\mu$ the chemical potentials in the different phases, $p$ is the pressure, and $\gamma$ the surface tension. The basic idea of non-equilibrium thermodynamics is that even if the system is not in global equilibrium, Gibbs relations are locally satisfied. BAM assumes that Gibbs relations apply both for the bulk and the interface. Again, this assumption restricts the description to situations where the change of variables is small over distances of the order of the bulk correlation length. Then, the rate of change of the entropy will be given by

$$T^{\pm} \frac{d}{dt} s^{\pm} = \frac{d}{dt} u^{\pm} + p^{\pm} \frac{d}{dt} v^{\pm} - \sum_{k=1}^{n} \mu^{\pm} \frac{d}{dt} c_k^{\pm} \qquad (4.B.129)$$

$$T^{s} \frac{d}{dt} s^{s} = \frac{d}{dt} u^{s} - \gamma \frac{d}{dt} v^{s} - \sum_{k=1}^{n} \mu^{s} \frac{d}{dt} c_k^{s} \qquad (4.B.130)$$

for the local thermodynamic fields. Comparing eqs.(4.B.129 ) and (4.B.130 ), which are given by equlibrium thermodynamics, with the balance equations (4.B.124 )-(4.B.125 ), and after insertion of the balance equation for $u$, $v$, and $c_k$ obtained from the general eqs.(4.B.121 )-(4.B.122 ), lead to expressions for the entropy fluxes and entropy productions both in the bulk and interface phases. Regarding the internal energy, one should take into account that the balance equation should be written for the total energy of the system, which is composed by a kinetic, potential and internal part, and the first two contributions should be substracted. The kinetic contribution is deduced once the balance equation for the momentum has been obtained. The potential part can be constructed taking into account that it derives from conservative forces.

Once the entropy production is known, using Curie's principle after identifying the thermodynamic fluxes and forces, it is possible to derive linear relations between

them. From the bulk term one derives the usual constitutive equations for the fluxes (Fick's law, Fourier law, etc.). The surface entropy production couple more terms because, due to the brekdown of the translational symmetry, not only surface fluxes and forces appear, but also normal components of bulk fluxes evaluated at the interface. These terms have a different tensorial character at the interface that in the bulk phase, allowing for couplings which are forbidden in the bulk. Some of the relations obtained are surface constitutive relations, giving the equivalent of Fick's or Fourier law, whereas the remaining ones are the boundary conditions for the bulk fields at the interface.

Let us consider the surface entropy production for an $n-$mixture in which $r$ chemical reactions take place, but in the absence of external fields, if the fluid is at rest, and the temperature is homogeneous. Then, the interfacial entropy production has the form[13]

$$\sigma^s = -\sum_{k=1}^{n-1} \vec{J}_k^s \cdot \nabla \left( \frac{\mu_k^s - \mu_n^s}{T} \right) - \frac{1}{T} \sum_{j=1}^{r} J_j^s A_j^s - \frac{1}{T} \sum_{k=1}^{n} [J_{k,n}(\mu_k - \mu_k^s)]_- \quad \text{(4.B.131 )}$$

and using Curie's principle one obtains the linear phenomenological relations

$$\vec{J}_i^s = \sum_{k=1}^{n-1} \vec{\vec{L}}_{ik}^s \cdot \nabla \left( \frac{\mu_k^s - \mu_n^s}{T} \right) \quad \text{(4.B.132 )}$$

$$J_i^s = -\frac{1}{T} \sum_{j=1}^{r} R_{ij}^s A_j^s - \frac{1}{T} \sum_{k=1}^{n-1} R_{ik+}^s (\mu_k^s - \mu_N^s) \quad \text{(4.B.133 )}$$

$$J_{i,n,+} = -\frac{1}{T} \sum_{j=1}^{r} R_{i-,j}^s A_j^s - \frac{1}{T} \sum_{k=1}^{n-1} L_{i-,k+}^s (\mu_k^s - \mu_k^n) \quad \text{(4.B.134 )}$$

$$J_{i,n,-} = -\frac{1}{T} \sum_{j=1}^{r} R_{i+,j}^s A_j^s - \frac{1}{T} \sum_{k=1}^{n-1} L_{i+,k+}^s (\mu_k^s - \mu_k^n) \quad \text{(4.B.135 )}$$

The first equation is the equivalent of Fick's law for a mixture at the interface, and expreses the fact that there exist $n-1$ independent diffusion fluxes in an $n-$component

mixture. The second one is the linearized version of the law of mass action, but one can see that an additional term appears, associated to the fact that incorporation of mass to the surface may affect the chemical reaction. Similarily, eqs.(4.B.134 ) and (4.B.135 ) constitute boundary conditions for the normal components of the bulk mass fluxes, which depend on the difference of chemical potential between the bulk and the surface, but which is also affected by the rate at which surface mass appears or disappears due to surface chemical reactions. Note that, since mass diffusion is a vectorial process, while chemical reactions are scalar ones, in the bulk there is no coupling between such processes.

# References


[1] H. Brenner and L.G. Leal, J. Coll. Int. Sci. **62**, 238 (*1971*).

[2] D. Bedeaux, A. M. Albano and P. Mazur, Physica **82A**, 438 (*1976*).

[3] A.M. Albano, D. Bedeaux and J. Vlieger, Physica **99A**, 293 (*1979*).

[4] J.F. Baret, J. Chim. Phys. **65**, 895 (*1968*).

[5] A.F.H. Ward and L. Tordai, J. Chem. Phys **14**, 453 (*1946*).

[6] G.E. Kimball, J. Chem. Phys. **6**, 447 (*1938*).

[7] K.J. Laidler, S. Glasstone and H. Eyring, J. Chem. Phys. **8**, 659 (*1940*).

[8] M. Shapiro, H. Brenner and D.C. Guell, J. Coll. Int. Sci. **136**, 552 (*1990*).

[9] H.A. Kramers, Physica **7**, 284 (*1944*).

[10] I. Prigogine and P. Mazur, Physica **19**, 241 (*1953*).

[11] J. Frenkel, *Kinetic Theory of Liquids*, Oxford, Clarendon Press *1946*, chap. 7

[12] S.R. de Groot and P. Mazur, *Non- Equilibrium Thermodynamics*, Dover Publications, Inc., New York, *1984*

[13] D. Bedeaux, Advances in Chemical Physics **64**, 47 (*1986*).

[14] J. Kovak, Physica **A86**, 1 (*1977*); Physica **A107**, 280 (*1981*).

[15] H. Eyring and E.M. Eyring, *Modern Chemical Kinetics*, Reinhold Publishing Co., New York, *1963*; H. Eyring, J. Chem. Phys. **3**, 107 (*1935*).

[16] A. Pérez-Madrid, M. Rubí and P. Mazur, Physica **A212**, 231 (*1995*).

[17] J.W. Gibbs, *Collected Works*, 2 vols., Dover, New York *1961*.

[18] P. Hänggi, P. Talkner and M. Borkovec, Rev. Mod. Physiscs **62**, 251 (*1990*).

[19] B. Widom, J. Chem. Phys. **44**, 3888, (*1966*).

[20] P.Schaaf and J. Talbot, J. Chem. Phys. **91**, 4401 (*1989*).

[21] I. Langmuir, J. Amer. Chem. Soc. **38**, 221 (*1916*); **39**, 1848 (*1917*).

[22] E. Ruckenstein and D.C. Prieve, J. Chem. Soc. Faraday II **69**, 1522 (*1972*).

[23] P.L. Chambré and A. Acrivos, J. Appl. Phys. **27**, 1322 (*1956*).

[24] T.G.M. Van de Ven, *Colloidal Hydrodynamics*, Academic Press, London *1989*.

[25] R. Varoqui and E. Pefferkorn, J. Coll.Int.Sci. **109**, 520 (*1986*).

[26] J.P. Simonin and M. Moreau, Mol. Phys. **70**, 265 (*1990*).

[27] M.H. Jacobs, *Diffusion Processes*, Springer, New York *1967*.

[28] H.-X. Zhou and R. Zwanzig, J. Chem. Phys. **94**, 6147 (*1991*).

[29] R. Zwanzig, J. Phys. Chem. **96**, 3926 (*1992*).

[30] I.G. Pitt, R.G. Gilbert and K.R. Ryan, J. Chem. Phys. **102**, 3461 (*1995*).

[31] P. Schaaf, A. Johner and J. Talbot, Phys. Rev. Lett. **66**, 1603 (*1991*).

[32] G. Tarjus and P. Viot, Phys. Rev. Lett. **68**, 2354 (*1992*).

[33] L.D. Landau and E.M. Lifschitz, *Fluid Mechanics*, Pergamon Press, Oxford (*1959*).

[34] J. Keizer, *Statistical Thermodynamics of Nonequilibrium Processes*, Springer Verlag, New York, (*1987*).

[35] W. van Saarlos, D. Bedeaux and P.Mazur, Physica A **110**, 147 (*1982*).

[36] I. Pagonabarraga, A. Pérez-Madrid and J.M. Rubí, preprint.

[37] B. Bonnier, D. Boyer and P. Viot, J. Phys. A **27**, 3671 (*1994*).

# Conclusions and Perspectives

In this thesis we have studied the influence of transport mechanisms on the adsorption kinetics of colloidal suspensions, as well as in the distribution of colloidal particles in the adsorbed layer. Adsorption of colloidal particles is controlled by the geometric exclusion effects at the surface originated by the finite size of the particles and by the irreversible character of the adsorption in these systems, and is also influenced by the specific transport mechanisms which determine the arrival of the colloids from the bulk to the interface. Our main objective has been to elucidate the effects of each contribution, as well as their relative importance and mutual influence in some specific situations.

After a first chapter in which we have introduced the basic kinetic models which have been proposed in the literature to take into account the surface exclusion effects, in the second chapter we have studied the adsorption in the presence of an external field parallel to the substrate. Our objective has been to study how surface exclusion effects are sensitive to the imposed external conditions upon which adsorption takes place, showing that they do not arise from purely geometric constrains, as had been already pointed out in BM. Therefore, instead of describing carefully the actual transport process, we have modified conveniently the usual kinetic models. Then, the external field we introduce can model either an external field parallel to the substrate or an adsorption from a fluid subject to a shear. The basic feature of this new model is that it introduces a new minimum length at which two particles can approach once on the substrate, and the kinetics becomes asymetric in the sense that this minimum distance depends on the side at which the incoming particle adsorbs.

We have observed a decrease of the jamming limit in the strength of this imposed force, and also a tendency to form more locally ordered aggregates when the force increases. A model using RSA rules has been solved exactly in 1-D, and a second one using BM rules has also been introduced. In this last model, new adsorption mechanisms are induced by the external field: a particle may roll over a number of preadsorbed spheres before being adsorbed or rejected. This new mechanism implis that adsorption in a 1-D substrate becomes non-local in the sense that the incoming particle can interact with many disks. The pair distribution function exhibits a richer structure than in standard BM, in which a number of delta functions appear, related to the different minimum distances at which particles can be found. If the exclusion distance is a multiple of the diameter, then a resonance is observed, and a higly locally ordered substrate is formed. The generalization of the previous models to the more realistic 2-D model is under study. While the RSA generalization is standard, new rolling situations are met in BM. However, similar features can be expected to hold. The inclusion of desorption in these adsorption models with shear is also of relevance, because it is now that an imposed shear favors desorption. In this case, it would be interested to elucidate how surface exclusion effects are modified.

In chapter 3 we have studied the effect of the transport on the adsorption of colloidal particles at high Péclet number in the presence of a gravity field, when their diffusion can be neglected. As a new mechanism with respect to previous studies, we have incorporated the hydrodynamic interactions (HI) existing between the incoming particle and the adsorbed ones due to the fact that the particles are suspended in a fluid. We have shown that the basic effect of HI is to introduce an effective repulsive interaction between the incoming particle and the preadsorbed ones. Some analytic results obtained in very simplified conditions have helped us to understand how HI show up, computer simulations of the adsorption have been carried out to study the general adsorption process. Simulations of BM have also been performed, in order to compare the results. We have studied both the 1-D and 2-D models. On the first case, which is simpler to deal with due to its simpler geometry, we have seen that, although the global quantities obtained with HI do not differ quantitatively from the ones obtained for BM, as for example the coverage as a function of time, the jamming limit, or the available fraction of the line, the local structure differs significantly from the one obtained with BM. The pair correlation function is characterized in both models

by having a series of peaks due to the rolling of incoming spheres over preadsorbed ones. The behavior after the peaks, however, is different, showing a slower decay with HI, indicating that because of the effective repulsion that they introduce larger gaps between the spheres are prefered. In 2-D we have shown that the effective repulsion introduced by HI favor the formation of elongated triplets on the surface where BM would predict an isotropic cluster. The radial distribution function again differs from the BM one behind the peaks due to the same reason explained in the 1-D case. In this model, we have compared with experimental results on the adsorption of mellamine particles. The curves obtained with HI agrees better with the experimental ones than those obtained with BM, explaining therefore some of the discrepancies observed when comparing with BM. In particular, the slower decay behind the first peak can be thought to be due to the effect of HI. This has served to show that BM, which was thought to be a good model to describe the adsorption of heavy colloidal particles, is restricted to situations where inertial effects dominate the transport to the wall. A more detailed study of the structure of the adsorbed layer is in progress. It will help us to elucidate the statistical importance of the elongated clusters that we have observed in our simulations, and also a more clear kinetics of the cluster evoultion will be obtained. Experimental results for the adsorptioon of systems ranging from RSA to BM are starting to be obtained. We also plan to generalize our simulation to finite Péclet number in order to understand new experimental situations. It is also of interest the inclusion of HI in a fluid subject to a shear. This study would help to elucidate the competition between interactions and excluded effects, which have been addressed in chapter 2.

Finally, in chapter 4 we have developed a thermodynamic theory of the adsorption process. We have focused our analysis on the situation in which adsorption is controlled by a surface energy barrier. This is more realistic for the adsorption of small particles. In this case, the transport to the interface is controlled by the diffuison through the energy barrier. In order to describe it properly, we have introduced an additional internal variable for the thermodynamic fields at the surface. The surface exclusion effects within this description are introduced considering that the system at the surface is not ideal. In this way we have derived a local generalized Langmuir equation for the evolution of the surface concentration. If the adsorption is not controlled by an energy barrier, as is the case in the kinetic models, then

the local thermodynamic description is different. We have shown how it is possible to obtain global generalized Langmuir equation which describe the evolution of the global surface concentration, using the fact that entropical barriers appear for the incoming particles. The relationship between this global descritpion and the local one in this case, however, remains as one of the open questions to be answered. The thermodynamic formulation allows to introduce in a systematic way the study of the fluctuations around steady states. We have shown how to deduce the corresponding fluctuation-dissipation theorem when an internal degree of freedom is introduced, and we have applied the results to study the density correlation function to a simple adsorption model with diffusion.

We can conclude that there exists a close interplay between the transport mechanisms whihch control the arrival of colloids to the surface, and the exclusion volume produced by the immobile particles. Moreover, new transport phenomena induce new adsorption kinetics, which influence both the rate of arrival of particles and the distribution of the colloids on the substrate. Therefore the physical properties of the interface will depend on the transport mechanisms.